The role of oxidative stress, subclinical inflammation and protein O-GlcNAcylation in diabetes mellitus, ischemia-reperfusion and chronic kidney disease

Ph.D. thesis

Boglárka Laczy M.D.

Mentors:
István Wittmann M.D., Ph.D.
John C. Chatham D. Phil.

Head of the Doctoral (Ph.D.) Program:
Judit Nagy M.D., D.Sc.

Head of the Doctoral (Ph.D.) School:
Sámuel Komoly M.D., D.Sc.

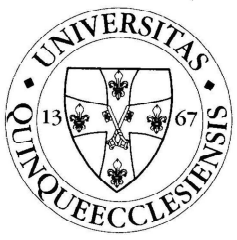

University of Pécs, School of Medicine
2nd Department of Internal Medicine and Nephrological Center, Pécs

University of Alabama at Birmingham, School of Medicine
Division of Cardiovascular Disease, Birmingham, Alabama, US

Pécs, 2011

TABLE OF CONTENTS

Abbreviations 2.

Introduction 3.

Aims 15.

Methods and Results 17.

1. **Oxidative stress and endothelial dysfunction: *In vitro* experiments on the cigarette smoke induced alterations in endothelial cells.** 17.

2. **Oxidative stress and cardiac dysfunction: *Ex vivo* experiments on the role of protein O-GlcNAcylation in mediating cardioprotection against ischemia-reperfusion injury in the isolated perfused rat heart.** 28.

3. **Investigations on the role of increased HBP flux and protein O-GlcNAcylation, micro-inflammatory state and oxidative stress as contributing factors to the pathogenesis of diabetes-related complications and chronic kidney disease.** 54.

   3.1. ***Ex vivo* experiments on the effects of increased HBP flux and protein O-GlcNAcylation on the regulation of cardiac metabolism.** 54.

   3.2. ***Clinical study* to investigate effectiveness of the anti-inflammatory pentoxifylline and pentosan polysulfate combination therapy on diabetic neuropathy and albuminuria in type 2 diabetic patients.** 62.

   3.3. ***Clinical study* to investigate erythropoietin resistance and the effects of the anti-inflammatory acetylsalicylic acid on anemia correction in type 2 diabetes mellitus and chronic kidney disease.** 68.

Discussion 74.

Theses 97.

References 99.

Publications related to the thesis 103.

Acknowledgements 105.

ABBREVIATIONS

ACC: acetyl-CoA carboxylase
ACE-I: angiotensin converting enzyme inhibitor
ACO2: aconitase 2
AGE: advanced glycation end products
AMPK: AMP-activated protein kinase
ARB: angiotensin receptor blocker
ASA: acetylsalicylic acid
ATP: adenosine triphosphate
BMI: body mass index
BSA: bovine serum albumin
CA-N: cardiovascular autonomic neuropathy
cGMP: cyclic guanosine monophosphate
CKD: chronic kidney disease
CRP: C-reactive protein
CSB: cigarette smoke buffer
cTnI: cardiac troponin I
DAPI: 4',6 diamidino-2-phenylindole
EDP: end-diastolic pressure
eNOS: endothelial nitric oxide synthase
EPO: erythropoietin
ERK: extracellular-signal regulated kinase
FAT: fatty acid translocase/transporter; CD36
GAPDH: glyceraldehyde-3-phosphate dehydrogenase
GFAT: glutamine: fructose-6-phosphate amidotransferase
GFR: glomerular filtration rate
GlcNAc: β-N-acetylglucosamine
GP: glycogen phosphorylase
GSH: reduced glutathione
H_2O_2: hydrogen peroxide
HBP: hexosamine biosynthesis pathway
HIF: hypoxia-inducible transcription factor
HPLC: high performance liquid chromatography
HSP: heat shock protein
ICAM: intercellular adhesion molecule
IL: interleukine
I/R: ischemia-reperfusion
IRS: insulin receptor substrate
KHB: Krebs-Henseleit bicarbonate
LDH: lactate dehydrogenase
LVDP: left ventricular developed pressure
MALDI-TOF/MS: matrix-assisted laser desorption/ionization- time of flight/ Mass Spectrometry
MAPK: mitogen activated protein kinase
NADP: nicotinamide adenine dinucleotide phosphate
NAG-thiazoline: 1,2 dideoxy-2`-methyl-α-D-glucopyranoso(2,1-d)-Δ2`-thiazoline
NMR: nuclear magnetic resonance
NO: nitric oxide
OGA: β-N-acetylglycosidase; O-GlcNAcase
O-GlcNAc: O-linked β-N-acetylglucosamine
OGT: O-GlcNAc transferase
PAGE: polyacrylamide gel electrophoresis
PAI-1: plasminogen activator inhibitor-1
PCA: perchloric acid
PF: pentoxifylline
PI3-K: phosphatidylinositol 3-kinase
PKA: cAMP-dependent protein kinase
PKB: protein kinase B/Akt
PKC: protein kinase C
PPS: pentosan polysulfate
PUGNAc: O-(2-acetamido-2-deoxy-d-glucopyranosylidene)amino-N-phenylcarbamate)
RAS: renin-angiotensin system
ROS: reactive oxygen species
RPP: rate pressure product
Ser/Thr: serine/threonine
SHR: sponatneous hypertensive rat
STZ: streptozotocin
T2DM: type 2 diabetes mellitus
TCA: tricarboxylic acid
TGF: transforming growth factor
TNF: tumor necrosis factor
UDP-GlcNAc: uridine diphospho-N-acetyl-glucosamine
UDP-HexNAc: uridine diphospho-N-acetyl-hexosamine
VCAM: vascular cell adhesion molecule
VEGF: vascular endothelial growth factor
Vinc: vinculin
ZDF: zucker diabetic fatty

INTRODUCTION

Endothelial dysfunction involves several damaging mechanisms to the vessel wall, the most important of which is the decreased endothelium-dependent vasodilation due to reduced nitric oxide (NO) availability (68). Impaired endothelial function is the major hallmark of several macrovascular diseases associated with accelerated atherosclerosis, including ischemic heart disease, hypertension, diabetes mellitus, and chronic kidney disease (CKD). In addition, microvascular endothelial dysfunction is closely associated with and could contribute to insulin resistance and microalbuminuria (68, 110). NO is synthesized by three isoforms of the nitric oxide synthase (NOS) enzyme, of which endothelial NOS (eNOS) is constitutively expressed in the vascular endothelium (3). Endothelial NO plays a pivotal role in the maintenance of vascular homeostasis; by regulating vascular tone and hemodynamics (i.e. anti-hypertensive), by inhibiting the platelet aggregation (i.e. anti-thrombogenic), leukocyte adhesion and vascular smooth muscle cell proliferation (i.e. anti-inflammatory, anti-atherogenic) (68). NO leads to vascular relaxation via activation of soluble guanylate cyclase and subsequent elevation of cyclic guanosine monophosphate (cGMP) in vascular smooth muscle cells (3).

Endothelial NO bioavailability depends on both transcriptional and posttranscriptional activation of eNOS, and the increased antioxidant defense capacity by reducing the ROS (reactive oxygen species)-induced inactivation of NO (3). The posttranslational modification of eNOS is relatively complex involving the regulation by cofactors and substrates, dimer formation, subcellular targeting, protein-protein interactions, O-GlcNAc (O-linked β-N-acetylglucosamine) modification, and multisite phosphorylations (3, 37). The regulation of eNOS activity via phosphorylations at Ser(1177) and Thr(495) has been well-described; for example, Ser(1177) site is rapidly phosphorylated in response to different stimuli, including fluid shear stress (12), VEGF and insulin (36), hydrogen peroxide (122), red wine polyphenols (89), or bradykinin (6) leading to increased eNOS activity and NO production. Conversely, Thr(495) residue,

located in the calmodulin-binding sequence, is known as the negative regulatory site and its phosphorylation decreases eNOS activity (43, 77).

Cigarette smoking associated with sustained endothelial dysfunction is an important risk factor in the progression of both macro- and microangiopathy of vascular diseases (68, 81, 110). Cigarette smoke contains a large amount of ROS (112), free radicals, prooxidants, and aldehydes, all of which are highly toxic to endothelial cells (82, 144). Cigarette smoke exposure induces oxidative stress and consequences of increased ROS overload are deleterious to the targeted vascular-endothelial cells. ROS could interfere with critical cellular and protein functions e.g., by oxidizing SH-containing proteins, by inducing morphological abnormalities (87), impaired VEGF-induced cell migration and tube formation (82), or DNA damage and apoptosis (22). In addition to increased levels of exogenous ROS (e.g. superoxide, hydrogen peroxide, hydroxyl radical, and peroxynitrite) from the cigarette mainstream smoke, ROS could arise secondary from endogenous sources, including uncoupled eNOS, NAD(P)H oxidase, xanthine oxidase, or the mitochondrial electron transport chain (7, 82, 137).

All these mechanisms lead to endothelial dysfunction characterized by decreased endothelium-dependent vasodilation related to a reduced NO production or availability (95). In addition, cigarette smoke results in decreased endothelium-dependent vasodilation in both macrovascular (e.g. pulmonary arteries, coronaries) and microvascular beds (e.g. kidney) (81). We earlier showed that cigarette smoke dose-dependently decreased the agonist-induced calcium signaling and cGMP production in porcine aortic endothelial cells (78), whereas reduced glutathione (GSH) protected the cells against the cigarette smoke induced damaging effects (87). Wagner at al. (126) showed that cigarette smoke caused a dose-dependent degradation of certain proteins in intact endothelial cells, and an unidentified protein at the molecular weight of dimer eNOS (270 kDa) disappeared. While we and others demonstrated that cigarette smoke causes endothelial dysfunction by disturbing the integrity of eNOS-NO-cGMP pathway at different levels; the effects on eNOS posttranslational modifications and the role of responsible protein kinases are unknown.

Diabetes mellitus has become an increasing health burden in both developed and developing countries and its prevalence is predicted to further increase affecting

globally 366 million people by 2030 (132). Type 2 diabetes (T2DM) is characterized by insulin resistance, hyperglycemia, and dyslipidemia. Chronic hyperglycemia is a major contributing factor to the increased risk for microangiopathy associated with diabetes (1), and there are additional causes of increased risk for both micro- and macrovascular diseases, such as smoking, hypertension, dyslipidemia, or obesity. All of these factors create a state of constant and progressive injure to the vascular wall, manifested by low-grade inflammatory processes (110).

In the development of diabetic vascular complications, the adverse effects of hyperglycemia have been attributed to four major mechanisms, including increased polyol pathway flux, increased advanced glycation end-product (AGE) formation, increased protein kinase C (PKC) activity, and increased flux through the hexosamine biosynthesis pathway (HBP) and increased O-GlcNAc levels (16). It has been suggested that hyperglycemia induces increased metabolic substrate input into the mitochondria, and the subsequent superoxide overproduction inhibits GAPDH (glyceraldehyde-3-phosphate dehydrogenase), thereby decreasing glycolytic flux and increasing the accumulation of glycolytic intermediates thus their entry into these alternative pathways (16). Therefore, one common final mechanism underlying the diabetes-associated vascular complications could be related to increased oxidative stress and ROS generation.

Increased oxidative stress and chronic inflammation in diabetes, particularly in T2DM, are important factors in the pathogenesis of microangiopathy. This notion is supported by reports indicating that increased inflammatory activity is closely related to the onset and progression of both cardiac autonomic dysfunction and urinary albumin excretion (49, 113), the surrogate symptoms of diabetic neuropathy and nephropathy, respectively. Characteristically, adverse effects of increased pro-inflammatory cytokines (e.g. TNF-α, IL-6), growth factors, adhesion molecules (e.g. ICAM-1, VCAM-1) have been linked to increased vascular permeability, altered vasoregulatory responses, increased leucocyte adhesion, and facilitated thrombus formation via increased pro-coagulant activity and decreased anti-coagulant pathways and/or fibrinolysis (110). Given that primary function of the microvascular vessels is to optimize nutrient and oxygen supply, functional abnormalities (e.g. altered vasomotor

tone) and structural damages (e.g. basal membrane thickening, increase in wall-to-lumen ratio or occlusion) could clearly contribute to tissue hypoxia and microvascular dysfunction such at the level of vasa nervorum or the glomeruli. In addition to adverse hemorheological features (e.g. hypercoagulability, hyperviscosity), the red blood cell microrheological changes (e.g. impaired deformability, reduced O_2-binding capacity, increased aggregation) have been also implicated in the pathogenesis of diabetic microangiopathy (80, 114, 139).

Diabetic neuropathy is a heterogeneous group of neuropathies resulting from impaired autonomic and/or peripheral nerve functions hence it can be presented with a wide range of clinical symptoms. The most common types are the chronic sensory-motor distal symmetric polyneuropathy and the cluster of autonomic neuropathies affecting multiple organ systems leading to substantial morbidity and negative impact on quality of life (14, 124). It is well-established that assessments of vibration perception and cardiovascular autonomic functions are simple and valuable tools for evaluating the severity of the two most progressive forms of neuropathies in diabetes, namely the peripheral sensory-, and the cardiovascular autonomic neuropathy (CA-N) (14, 125). Coppini et al. (32) in survival analysis of 794 diabetic patients during a 12-year interval demonstrated that peripheral sensory neuropathy diagnosed by reduced vibration threshold values was an independent predictor of increased mortality, indicating that this is an important, often overlooked marker for those at higher risk. Clinically the most important form of autonomic dysfunctions is the CA-N, which encompasses damage to the autonomic nerve fibers that innervate the heart and blood vessels, resulting in abnormalities in heart rate control and vascular dynamics (125). Prognosis of CA-N is poor; reviewed data of epidemiological studies showed that 5-year mortality rate from CA-N is 5-fold higher in diabetics with CA-N compared to those without (125). Major adverse symptoms of CA-N may involve resting tachycardia, exercise intolerance, intraoperative instability, or severe orthostatic hypotension; and CA-N is closely associated with increased risk for both silent myocardial ischemia and cardiovascular mortality (125).

Majority of patients with diabetic neuropathy requires an instant pharmacological treatment, often combinations of therapies, when they have painful symptoms.

Currently a large variety of drugs are available, however, these commonly used agents are often partially effective, even after long-term administration at relatively high doses, thus with financial expenses. For example, infusion therapy by the antioxidant alpha-lipoic acid (600 mg) improved vibration perception and reduced peripheral neuropathic pain after three weeks in patients with T2DM (145); however in the SYDNEY study there were no improvements neither in sensory nor in autonomic functions after a two-weeks infusion therapy (4); while its oral administration reduced CA-N symptoms (from 24.1% to 17.2%) after four months (146).

Diabetic nephropathy is the leading cause of end-stage renal disease due mainly to the increased prevalence of T2DM (107). Diabetic patients with overt nephropathy are known to have higher risk for cardiovascular morbidity and mortality; even before the development of end-stage kidney failure, the presence of microalbuminuria is associated with 2-4-fold higher risk for cardiovascular mortality (120). Moreover, progression of albuminuria within the normal range may be also deleterious (111). The major therapeutic aspects of diabetic nephropathy include tight glycemic control, optimal blood pressure control via renin-angiotensin system (RAS) inhibition, dyslipidemia control, and optimal anemia correction (135). In both secondary and tertiary prevention of diabetic kidney disease (i.e. the progression from micro- to macroalbuminuria, and the delay of progression to kidney failure), the ACE-I (angiotensin-converting enzyme-inhibitors) and/or ARB (angiotensin II receptor blockers) are efficiently used drugs (107, 135).

In face of multiple pathogenic factors and co-morbidities associated often with diabetic neuropathy and nephropathy, specific treatments are still not feasible. Recently, however a number of new promising drugs have gained interests that potentially could delay the progression of diabetic nephropathy, including anti-fibrotic agents (e.g. pentoxifylline) and glycosaminoglycans (e.g. pentosan polysulfate) (79, 123), although their potential benefits on symptomatic diabetic neuropathy have not been determined. ***Pentoxifylline (PF)***, a methyl-xanthine derivative has been widely used for treating peripheral arterial disease with a good safety profile. PF can substantially reduce claudication symptoms, thus it is effective in conditions associated with systemic atherosclerosis (e.g. diabetes mellitus, hypertension, hyperlipidemia,

smoking) (42). Pro-circulatory effects of PF on blood flow have attributed to its beneficial rheological actions; it reduces blood/plasma viscosity and fibrinogen levels, inhibits platelet aggregation (40), and it also improves red blood cell deformability and inhibits their aggregation via its phosphodiesterase activity (85). PF also possesses significant anti-inflammatory and antioxidant effects by decreasing the level of pro-inflammatory cytokines and oxidative stress markers (97, 136). Moreover, immunoregulatory effects of PF have been shown to afford renoprotection against various kidney injuries via the suppression of pro-inflammatory and pro-mitogenic mediators (e.g. TNF-α, Il-6, CRP, TGF-β), and this was shown *in vivo* experimental models of several kidney diseases, including diabetic nephropathy (52) as well as in human clinical studies in both diabetic and non-diabetic kidney disease (41, 101). Furthermore, human clinical trials have demonstrated that overall renoprotective effect of PF leads to a marked reduction in proteinuria when either administered alone or combined with ACE-I or ARB (79). ***Pentosan polysulfate (PPS)*** is a polymer of β-D-xylopyranose possessing a heparin-like activity, thus it exerts advantageous rheological and anti-atherogenic effects, such as the inhibition of leukocyte adhesion, attenuation of mesangial cell and vascular smooth muscle cell proliferation, inhibition of phagocyte activation, or the promotion of vasodilatory response via increasing NO and decreasing endothelin-1 release (128). PPS has been shown to decrease blood viscosity, fibrinogen levels, and to improve erythrocyte deformability. PPS has been also shown to exhibit anti-inflamamtory and renoprotective effects; it has been implicated in the inhibition of leucocyte arachidonic acid metabolism in humans (44). PPS prevented proteinuria, glomerular hypertension and hyperfiltration in rats after subtotal renal ablation (10), and it preserved renal autoregulation by reducing TGF-β levels and vascular smooth muscle cell proliferation at the afferent arteriole (51).

Anemia is acknowledged as a common complication of both T2DM and CKD (106). The pathogenic mechanisms underlying anemia in CKD are multiple; both extrarenal (e.g. deficiencies) and renal factors are involved, although one of the major causes is the lack of serum erythropoietin (EPO) due to the structural damage of EPO producing renal interstitial fibroblasts. This is supported by fact that hypoproliferative anemia in patients with CKD could be dose-dependently reversed by hormonal

substitution with recombinant human EPO. On the other hand, EPO resistance may also occur due to an increased acute-phase inflammation characteristic of CKD (75), thus the formation of red blood cells (i.e. erythropoiesis) is impaired even if endogenous EPO levels were normal. Additionally, increased oxidative stress in CKD could also lead to altered red blood cell morphology and function; typically, decreased membrane fluidity has been attributed to lipid peroxidation leading to their shortened life-time and early elimination from the circulation (48).

In diabetes, several putative mechanisms have been put forward to explain anemia, including impaired secretion or increased urinary loss of EPO, glycoxidation of both EPO and its receptor, osmotic/oxidative stress-induced early elimination of red blood cells, or autonomic sympathetic neuropathy (9, 116). Alternatively, it has been suggested that EPO resistance may be a consequence of chronic low-grade inflammation similarly to other hormone resistances (e.g. insulin, leptin, NO) observed in T2DM (110). Oberg et al. (92) showed that there were higher levels of oxidative stress and inflammatory markers (e.g. CRP, IL-6) in patients with stage 3-5 CKD compared to healthy individuals, and that there was a further increase in oxidative stress in patients with diabetes and hypercholesterinemia. This finding would predict that patients with diabetic nephropathy showing higher levels of pro-inflammatory and pro-oxidative states compared to CKD patients may have higher degree of EPO resistance; however, this has not been investigated.

In recent years, several erythropoiesis-stimulating drugs other than recombinant human EPO have been developed for anemia correction in patients with CKD, including two inhibitors of the hypoxia-inducible transcription factor (HIF-1) (35). ROS are known to mediate intracellular signaling and transcriptional events through redox-sensitive pathways; one such example is the regulation of renal EPO production via HIF-1 and hydroxyl free radicals as the second messengers (60). Under normoxic conditions in oxygen-sensing cells, excess of hydroxyl free radicals bind to HIF-1α leading to its degradation, thus decreasing HIF dimer formation, and consequently EPO transcription is inhibited. In contrast, under hypoxia, there are low levels of hydroxyl free radicals, which inhibit HIF-1α from degradation leading to increased HIF dimer formation and EPO gene transcription (60). It is possible that increased ROS

production seen in patients with T2DM and CKD may critically alter the oxygen sensing regulatory mechanisms in EPO producing cells resulting in disturbed HIF-1 activation and suppressed EPO synthesis. If so, a potent anti-inflammatory and free radical scavenger would be beneficial in regulating EPO production by preventing HIF-1α from degradation, thus up-regulating EPO gene transcription and protein secretion. It is well-described that acetylsalicylic acid (ASA), a potent hydroxyl free radical scavenger, possesses significant anti-inflammatory effects by irreversibly inhibiting cyclooxygenase. Therefore, it is conceivable that ASA may have advantageous impact on the synthesis and actions of EPO, thereby it potentially could improve anemia in patients with T2DM and CKD.

Cardiovascular complications are the leading cause of excess premature morbidity and mortality in diabetic patients (133). While late onset complications of diabetes can be attributed to macro- and microvascular disease, accumulating evidence demonstrates that diabetes also leads to functional and structural abnormalities at the level of cardiomyocyte (e.g. diabetic cardiomyopathy), independent of vascular defects, thereby increasing the risk for ventricular dysfunction and heart failure (13). The mechanisms underlying cardiomyocyte dysfunction in diabetes are multiple; and as with the vascular dysfunction, the hyperglycemia-induced activation of alternative pathways (i.e. activation of polyol pathway; AGEs; PKC) and oxidative stress (13) as well as altered cardiac metabolism undoubtedly contribute to the pathogenesis of diabetic cardiomyopathy (5).

Experimental and clinical studies showed that insulin resistant and diabetic state lead to maladaptive metabolism in the heart, typically, a switch to excessive fatty acid oxidation and suppressed glucose metabolism at several points (e.g. impaired glucose uptake, glycolysis, pyruvate oxidation, lactate uptake) (118). The consequences of altered cardiac substrate utilization in diabetes have been linked to perturbations in Ca^{2+}-regulation, contraction-relaxation mechanics, and cardiomyocyte growth leading to impaired contractility, hypertrophy, fibrosis, or apoptosis (5). Our current understanding on cardiac metabolic regulation is primarily based on substrate availability and the effects of hormones, particularly insulin, on phosphorylation of key regulatory proteins including IRS1/2 (insulin receptor substrate) and AMPK (AMP-

activated protein kinase) (53, 118). However, there may be alternative protein targets and important mechanisms involved in regulating cardiac metabolism.

Protein O-GlcNAcylation, the posttranslational modification of proteins by O-GlcNAc is increasingly recognized as a novel signal transduction mechanism regulating diverse cellular functions (19, 66, 142).

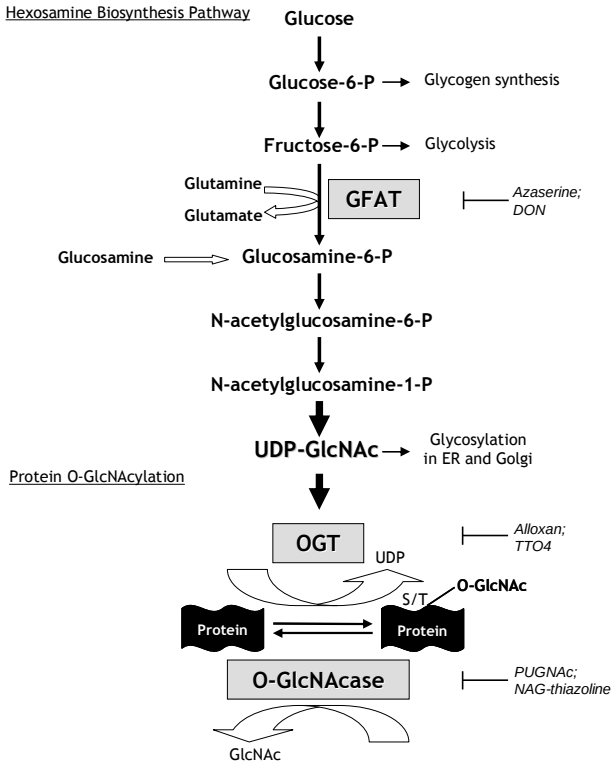

The Hexosamine Biosynthesis Pathway and Protein O-GlcNAcylation

Briefly, the activity of OGT is sensitive to the intracellular concentration of its obligatory substrate, UDP-GlcNAc (uridine diphospho-N-acetyl-glucosamine), which is the end-product of the HBP. Flux through the HBP and thus the synthesis of UDP-GlcNAc is regulated in large part by the metabolism of glucose. Glucose entry into the HBP is regulated by GFAT (L-glutamine-D-fructose 6-phosphate amidotransferase), which converts fructose-6-phosphate to glucosamine-6-phosphate with glutamine as the amine donor and it can be inhibited by glutamine analogs (DON: 6-diazo-5-oxo-L-norleucine; Azaserine: O-diazoacetyl-L-serine). Exogenously given glucosamine, which enters cells via the glucose transporter system and is phosphorylated to glucosamine-6-phosphate by hexokinase, thus bypassing the rate-limiting enzyme GFAT it rapidly increases UDP-GlcNAc levels, thus the O-GlcNAcylation of proteins. O-GlcNAcylation of proteins can be blocked by inhibiting OGT with the uridine analog Alloxan or with TTO4 (2[(4-chlorophenyl)imino] tetrahydro-4-oxo-3 (2-tricyclo[3.3.1.13.7]dec-1-ylethel)); whereas it can be rapidly increased by inhibiting O-GlcNAcase with PUGNAc (O-(2-acetamido-2-deoxy-d-glucopyranosylidene)amino-N-phenylcarbamate) or with NAG-thiazoline derivatives (e.g. NAG-Bt: 1,2 dideoxy-2`-propyl-α-D-glucopyranoso-(2,1-d)-Δ2`-thiazoline; NAG-Ae: 1,2 dideoxy-2`-ethylamino-α-D-glucopyranoso-(2,1-d)-Δ2`-thiazoline)(66).

In contrast to classical protein glycosylation in the endoplasmic reticulum (ER) and Golgi, characterized by stable and complex elongated oligosaccharide structures, protein O-GlcNAcylation is a ubiquitous and dynamic process involving the reversible addition of a single O-GlcNAc moiety to Ser/Thr residues of nuclear and cytosolic proteins, analogous to phosphorylation (56). This process is regulated by the activities of two key enzymes, O-GlcNAc transferase (OGT), which catalyzes the addition of O-GlcNAc, and β-N-acetylglucosaminidase (O-GlcNAcase, OGA), which catalyzes its removal (56).

Sustained activation of the HBP and O-GlcNAcylation has been linked to the etiology of glucose toxicity and insulin resistance the major hallmarks of diabetes (18, 31). Increased O-GlcNAc levels were shown in human carotid atherosclerotic plaques from T2DM patients (39), as well as in the glomeruli and tubuli of kidney samples from T2DM patients with nephropathy (34). The nutrient excess via the HBP and increased protein O-GlcNAcylation has been also implicated in the pathogenesis of the diabetic vascular-endothelial dysfunction associated with increased oxidative stress and inflammation (66). For example, increased O-GlcNAc has been associated with decreased Akt/eNOS activity in endothelial cells (37, 39); in mesangial cells it has been linked to increased expression of TGF-β (62), a major factor in the progression of diabetic nephropathy.

In the heart, increased protein O-GlcNAcylation has been linked to cardiomyocyte dysfunction in experimental models of both T1DM and T2DM. Pang et al. (94) found that short-term STZ/Streptozotocin/-induced diabetes blunted the inotropic response of the heart to the α-adrenergic agonist phenylephrine and this could be partially abrogated by pre-treatment with azaserine (GFAT inhibitor). Hu et al. (59) showed that after prolonged STZ-induced diabetes, mice hearts exhibited impaired Ca^{2+}-handling and contractile dysfunction together with increased OGT expression and O-GlcNAc levels, both of which could be reversed by increased OGA expression. Fülöp at al. (45) showed that in ZDF/Zucker Diabetic Fatty/-rats the transition from normoglycemia to hyperglycemia has been associated with increased UDP-GlcNAc and O-GlcNAc levels in conjunction with impaired Ca^{2+}-transient decay and cardiomyocyte relaxation. In addition, glucosamine, which rapidly increases the flux through the HBP and O-

GlcNAc levels, has been also shown to mimic some of the diabetes-induced changes on cardiomyocyte function, such as abnormalities in excitation-contraction coupling (100) and prolonged Ca^{2+}-transient decay (25). Recently, McClain et al. (73) demonstrated that glucosamine treatment of 3T3L1 adipocytes resulted in increased protein O-GlcNAcylation and increased palmitate oxidation via activation of AMPK and ACC (acetyl-CoA carboxylase), similar to the metabolic changes seen in the diabetic heart. Therefore, it is conceivable that activation of HBP and protein O-GlcNAcylation may also have a role in regulating cardiac metabolism.

While chronic elevation of the HBP flux and protein O-GlcNAcylation has been typically perceived as detrimental (18, 31), accumulating evidence shows that acute activation of pathways leading to increased protein O-GlcNAcylation exerts protective effects in the cardiovascular system (66). Zachara et al. (143) demonstrated in multiple cell lines that acute increases O-GlcNAc resulted in protection against different lethal stresses and that inhibition of this response decreased cell survival; whereas its augmentation increased cellular stress tolerance. They first provided the concept that protein O-GlcNAcylation represents an internal stress-activated response which potentially could confer a survival advantage.

Following this observation several groups demonstrated that ***acute augmentation of protein O-GlcNAcylation*** mediates protection against a wide range of injuries in different experimental settings, including heat stress, vascular endoluminal injury, trauma-hemorrhage, and ischemia-reperfusion (I/R) injury in the heart (66). Consistently, Chatham et al. (46, 70) showed that acute increases in the HBP flux by glucosamine in the perfused heart resulted in improved functional recovery and decreased tissue injury following reperfusion. Liu et al. (69) demonstrated that acute increases in O-GlcNAc by inhibiting OGA with PUGNAc also increased tolerance of the perfused heart to I/R injury. Pre-ischemic treatment with PUGNAc reduced myocardial infarct size *in vivo* after I/R in mice (64). However, glucosamine can be metabolized through a number of other pathways in addition to its conversion to UDP-GlcNAc and is effective at only higher concentrations (117), thus it could have effects independent of increasing O-GlcNAcylation. On the other hand, PUGNAc, which has been widely used to inhibit OGA, is known to inhibit other glycoside hydrolases (e.g.

lysosomal β-hexosaminidases), thereby affecting glycoconjugates in addition to O-GlcNAc (50). Thus, the lack of specificity and other off-target effects of glucosamine and PUGNAc may give rise to disparate physiological actions, thereby limiting their value and potential clinical applications. Recently, Vocadlo et al. (74) have developed novel OGA inhibitors, the NAG-thiazolines, which have markedly higher selectivity for OGA. Fore example, NAG-Bt showed ~1500-fold greater specificity toward OGA than PUGNAc, whereas NAG-Ae is more potent (~30-fold) than NAG-Bt (50). NAG-Bt has been shown to successfully increase O-GlcNAc in isolated cardiomyocytes (23); however, neither NAG-Bt nor NAG-Ae has been tested to determine their efficacy against I/R injury at the whole organ level.

Despite a growing body of reports showing overall changes in cardiac O-GlcNAc in response to pathological stresses, subcellular distribution of O-GlcNAc in the intact adult heart or how it is affected by ischemia and I/R is not known. Protein O-GlcNAcylation is a key regulator of many biological processes, including nuclear transport, translation and transcription, signal transduction, cytoskeletal reorganization, proteasomal degradation and apoptosis (56), all of which potentially could mediate protection in the heart against ischemia and reperfusion. Several putative mechanisms have been advanced to explain ischemic cardioprotection with increased O-GlcNAcylation; it has been attributed to increased synthesis of HSP40 and HSP70 (64, 143), increased p38 phosphorylation (46), the inhibition of mitochondrial permeability transition pore formation and Ca^{2+}-overload (64). On the other hand, O-GlcNAc signaling likely involves intracellular targets which may contribute to myocardial preservation during ischemia and reperfusion. However, there are scarce data on those specific cardiac proteins that are targeted by O-GlcNAc during ischemia and/or reperfusion. Progress in this area has been restricted because of limitations in tools necessary for the identification of O-GlcNAc targets (141).

AIMS

1. Oxidative stress and endothelial dysfunction: *In vitro* experiments on the cigarette smoke induced alterations in endothelial cells.

1.1. Assess the acute effects of cigarette smoke on eNOS phosphorylations, eNOS dimerization, and PKB/Akt activation

1.2. Examine whether reduced glutathione prevented the cigarette smoke induced changes in eNOS phosphorylations and its dimer formation

1.3. Determine the effects of protein kinase pathways on the cigarette smoke induced changes in eNOS phosphorylations using selective PKA, PI3-K/PKB and PKC inhibitors

1.4. Determine whether the isoform specific PKCβII-inhibitor, ruboxistaurin had a role in preventing the cigarette smoke induced changes in eNOS phosphorylations

2. Oxidative stress and cardiac dysfunction: *Ex vivo* experiments on the role of protein O-GlcNAcylation in mediating cardioprotection against ischemia-reperfusion injury in the isolated perfused rat heart.

2.1. Verify that acute increases of protein O-GlcNAcylation by selectively inhibiting OGA at the time of reperfusion attenuated ischemia-reperfusion injury in the heart

2.2. Determine the effects of ischemia, ischemia-reperfusion and selective OGA inhibitor treatment on the distribution of O-GlcNAc-modified proteins in cardiac tissue

2.3. Determine whether selective OGA inhibitor treatment prevented the changes in cardiac structural integrity and Z-line proteins following ischemia and ischemia-reperfusion

2.4. Determine the effects of ischemia, ischemia-reperfusion and selective OGA inhibitor treatment on specific cardiac proteins targeted by O-GlcNAc modification

3. Investigations on the role of increased HBP flux and protein O-GlcNAcylation, micro-inflammatory state and oxidative stress as contributing factors to the pathogenesis of diabetes-related complications and chronic kidney disease.

3.1. *Ex vivo* experiments on the effects of increased HBP flux and protein O-GlcNAcylation on the regulation of cardiac metabolism.

3.1.1. Determine whether acute activation of the HBP and O-GlcNAcylation with glucosamine resulted in alterations in cardiac energy and substrate utilization, similar to those seen in the diabetic heart

3.1.2. Assess whether activation of AMPK, ACC or increased FAT/Fatty acid transporter/CD36 levels was responsible for the altered cardiac metabolism

3.1.3. Determine whether increases in FAT/CD36 levels could be a direct result of O-GlcNAc modification

3.2. *Clinical study* to investigate effectiveness of the anti-inflammatory pentoxifylline and pentosan polysulfate combination therapy on diabetic neuropathy and albuminuria in type 2 diabetic patients.

3.2.1. Determine whether pentoxifylline and pentosan polysulfate improved cardiovascular autonomic and peripheral sensory neuropathy in type 2 diabetic patients

3.2.2. Determine whether pentoxifylline and pentosan polysulfate reduced urinary albumin excretion in type 2 diabetic patients

3.3. *Clinical study* to investigate erythropoietin resistance and the effects of the anti-inflammatory acetylsalicylic acid on anemia correction in type 2 diabetes mellitus and chronic kidney disease.

3.3.1. In a cross-section study to determine the presence of erythropoietin resistance in the background of anemia in patients with type 2 diabetes mellitus and/or chronic kidney disease

3.3.2. In an intervention study to determine the effects of the anti-inflammatory acetylsalicylic acid on serum erythropoietin levels and whether it ameliorated anemia in a subgroup of patients with type 2 diabetes mellitus and chronic kidney disease

METHODS AND RESULTS

1. Oxidative stress and endothelial dysfunction: *In vitro* experiments on the cigarette smoke induced alterations in endothelial cells.

Smoking associated with sustained endothelial dysfunction is one of the major cardiovascular risk factors and it often complicates the progression of other vascular diseases, such as diabetes mellitus, CKD. In the vascular endothelium cigarette smoke leads to oxidative stress via enhanced ROS generation. An early consequence of endothelial dysfunction is decreased endothelium-dependent vasodilation and reduced NO availability, typically through decreased eNOS activity. It is well-recognized that in response to different stimuli, phosphorylation at Ser(1177) leads to eNOS activation, whereas at Thr(495) it decreases eNOS activity. Our objectives were to determine the acute effects of cigarette smoke on eNOS phosphorylations and its dimer formation; and whether GSH prevented the cigarette smoke induced changes to eNOS modifications; as well as the role of protein kinase pathways in mediating the cigarette smoke induced changes in eNOS phosphorylations.

Materials and methods:

Materials: All chemicals and reagents were purchased from Sigma (Budapest, Hungary) unless otherwise noted.

Cell culture: Primary mouse endothelioma cell line was used (LGC Promochem, UK). Endothelial cells were cultured in 75 cm^2 flasks in Dulbecco's Modified Eagle Medium (Gibco, Hungary) containing 10% fetal bovine serum and 2% mixture of penicillin-streptomycin at 37ºC and 5% CO_2. Cultures from 3 to 10 passages at 90-100% confluence were used for all experiments. Prior to experiments cells were serum deprived for overnight in medium containing 4.5 g/L glucose, L-glutamine, pyruvate.

Preparation of cigarette smoke buffer (CSB): Commercial cigarettes with filter (Camel®; R.J. Reynolds Tobacco, US; ≤10 mg of tar) were smoked by a tube-driven apparatus into Krebs-Henseleit bicarbonate (KHB) buffer [pH: 7.4, (in mM): NaCl 118.0, KCl 4.7, $CaCl_2$ 2.5, KH_2PO_4 1.2, $MgSO_4$ 1.2, $NaHCO_3$ 25.0, and glucose 5.5] as

previously described (87). Briefly, burning cigarette was smoked for 5 min under hood by a constant vacuum of -5 cmH_2O through the side tube of Erhlenmeyer bottle whilst smoke was driven into 5 mL KHB buffer via the other tube at the top the bottle. This protocol corresponded to exposure of cigarette smoke in humans; as one cigarette takes ~5 min to smoke which interacts with ~5 mL of lining fluid in the lung epithelial cells. The resultant stock CSB was diluted to 5 - 50% in the dose-dependent experiments; and cells were incubated with CSB for 5 - 30 min in the time-dependent experiments.

Cell lysis and treatments: Confluent monolayers of cells were washed with KHB buffer to remove medium, and were incubated with either KHB buffer (Control) or CSB at 37ºC. Cells were preincubated with reduced glutathione (GSH; 5 mM; 15 min) in the series of antioxidant experiments. To examine the effects of protein kinase pathways, the following inhibitors were used: 1) selective cAMP-dependent protein kinase (PKA) inhibitor (H-89; 10 μM); 2) selective phosphatidylinositol 3-kinase (PI3-K)/PKB inhibitor (LY-294002; 100 μM); 3) selective protein kinase C (PKC) inhibitor (Ro-318425; 1 μM); and 4) isoform specific PKCβII-inhibitor (Ruboxistaurin; LY-379196; 30 nM; Eli Lilly, US). Cells were harvested in modified RIPA buffer containing (in M) Tris (pH: 7.4) 1.0, EDTA 0.5, EGTA 0.2, dithiothreitol (DTT) 0.1, 1.15 (v/v)% Triton-X and phosphatase/protein kinase inhibitors [5-5 mg/mL phenylmethanesulfonyl fluoride (PMSF), leupeptin, aprotinin, 100 mM sodium orthovanadate (Na_3VO_4)]. Cells were scraped off and lyzed for 30 min on ice, then stored at − 80ºC for further analyses.

Immunoblot analysis: After sonication lysates were centrifuged (15,000 g, 10 min, at 4ºC) and protein concentration of the supernatant was determined by Bradford assay using BSA as the standard (BioRad). Proteins were solubilized in Laemmli buffer (2X), boiled for 5 min and resolved by SDS-PAGE, then blotted on nitrocellulose membrane (Amersham-Biotech, Hungary). To detect dimer eNOS levels, samples were not denatured (i.e. not boiled) and temperature was maintained at 4ºC during SDS-PAGE (low-temperature PAGE) and transfer processes. The blots were blocked in nonfat dry milk, then probed with the following monoclonal antibodies (1:1000): anti-phospho-Thr(495)-eNOS, anti-eNOS (BD Pharmingen, Hungary), anti-phospho-Ser(1177)-eNOS, phospho-Ser(473)-Akt, and anti-Akt (Cell Signaling, Hungary). After incubation

with appropriate horseradish peroxidase (HRP)-conjugated secondary antibodies (1:2000), blots were washed and visualized by enhanced chemiluminescent method (ECL; Pierce, Hungary). Blots were reprobed for total eNOS and total Akt levels after stripping. Scion Image for Windows Software was used for densitometric analyses.

Statistical analysis: Statistical significance was evaluated by one-way analysis of variance (ANOVA) followed by Dunnett`s posthoc test, and unpaired t-test for data where appropriate using SPSS 10.0 (SPSS Inc). Jonckheere-Terpstra test was used evaluate concentration- and time-dependent effects of CSB. Results are expressed as means ± SE, and $p < 0.05$ was defined as statistically significant.

Results:

1.1. Acute effects of cigarette smoke on eNOS phosphorylations and PKB/Akt phosphorylation

Cigarette smoke augmented eNOS phosphorylation at both Ser(1177) and Thr(495) sites: In contrast with the concept of a reciprocal phosphorylation-dephosphorylation reaction between the Ser(1177) and Thr(495) residues (55, 77), we found that CSB treatment increased both phosho-Ser(1177) eNOS and phospho-Thr(495) eNOS levels in a concentration-dependent (*Fig. 1A*) and time-dependent (*Fig. 1B*) manner. Maximal response to CSB generally occurred at 50% CSB after 30 min treatment. CSB treatments had no effect on total eNOS protein levels. After CSB treatment, phospho-Thr(495) eNOS levels were considerably higher at all concentration and time points compared to phospho-Ser(1177) eNOS levels (*Figs. 1A, B*), suggesting that eNOS activity is decreased in response to CSB. Increased eNOS phosphorylations at both Ser(1177) and Thr(495) residues also suggest that there may be independent upstream mechanisms regulating these phosphorylation sites in response to CSB.

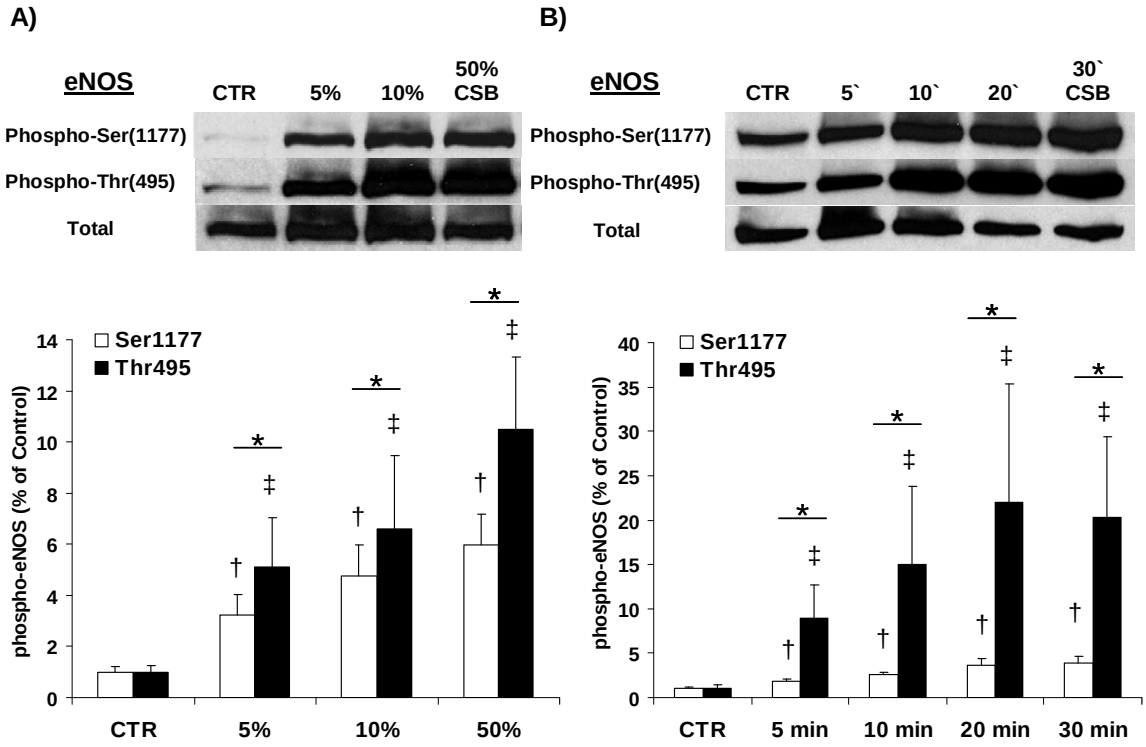

Figure 1. *Representative immunoblots and densitometric analyses demonstrate A) concentration-dependent and B) time-dependent increases of both phospho-Ser(1177) and phospho-Thr(495) eNOS levels compared to untreated controls (CTR) in endothelial cells after cigarette smoke buffer (CSB) treatment. Endothelial cells were A) subjected to increasing concentrations of CSB (5%, 10%, 50%; 30 min); or B) incubated with 50% CSB for 5, 10, 20, 30 min. After CSB treatment, phospho-Thr(495) eNOS levels were higher compared to phospho-Ser(1177) eNOS levels at each A) concentration and B) time point (* p<0.05; unpaired t-test).*
† p<0.05 phospho-Ser(1177) eNOS vs. Control; ‡ p<0.05 phospho-Thr(495) eNOS vs. Control (one-way ANOVA; Dunnett); [n=4-4]

Cigarette smoke inhibited PKB/Akt phosphorylation at Ser(473) site: We subsequently examined whether phosphorylation of PKB/Akt, which can directly phosphorylate eNOS at Ser(1177) in response to a variety of stimuli (47), was also increased after CSB treatment as seen with phospho-Ser(1177) eNOS levels. Under basal conditions, PKB/Akt was phosphorylated at Ser(473) in CSB-untreated, control cells. We found that CSB markedly decreased phospho-Ser(473) Akt levels in a concentration-dependent (*Fig. 2A*) and time-dependent (*Fig. 2B*) manner. CSB-induced inactivation of PKB/Akt suggests that it unlikely had downstream effects activating eNOS at Ser(1177) in response to CSB.

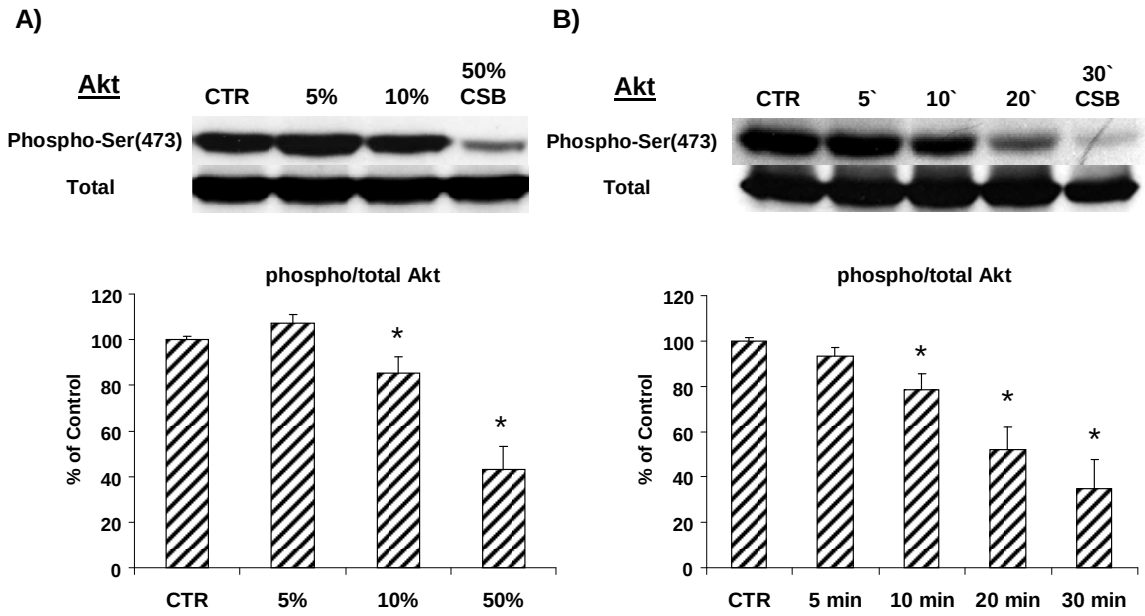

Figure 2. *Cigarette smoke buffer (CSB) significantly reduced PKB/Akt phosphorylation at Ser(473) site in A) concentration-dependent and B) time-dependent manner. Endothelial cells were treated with A) increasing concentrations of CSB (5%, 10%, 50%; 30 min) or B) with 50% CSB for 5, 10, 20, or 30 min. The maximal effect of CSB inactivating PKB/Akt was after 30 min treatment with 50% CSB.*
** p<0.05 vs. Control (one-way ANOVA; Dunnett); [n=5-5]*

1.2. Effects of reduced glutathione on the cigarette smoke induced changes in eNOS phosphorylations and eNOS dimer formation

Reduced glutathione prevented the cigarette smoke induced increases in phospho-Ser(1177) and phospho-Thr(495) eNOS levels: Cigarette smoke containing more than 4700 chemical compounds, including several free radicals and oxidants rapidly initiates oxidative damage (112). We earlier showed in endothelial cells that inhibitory effects of the water-soluble gas phase CSB on cGMP production appeared to be independent from superoxide, hydroxyl free radical or lipid peroxidation, but were rather related to aldehydes and could be diminished with GSH (78). Here we also used GSH as a potent aldehyde and free radical scavenger to study whether it could prevent the CSB-induced oxidant stress to eNOS modifications. GSH markedly attenuated the CSB-induced increases in both phospho-Ser(1177) eNOS (~20%) and phospho-Thr(495) eNOS levels (~45%) compared to GSH-untreated cells (*Fig. 3A*). GSH-induced reduction in eNOS phosphorylations was more

pronounced at Thr(495) than at Ser(1177) site (*Fig. 3B*). GSH treatment did not alter total eNOS levels.

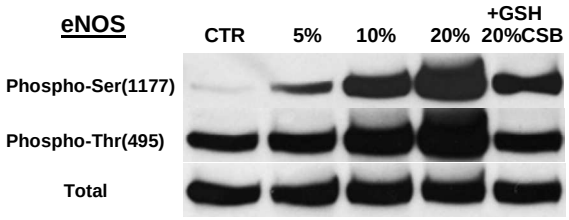

A)

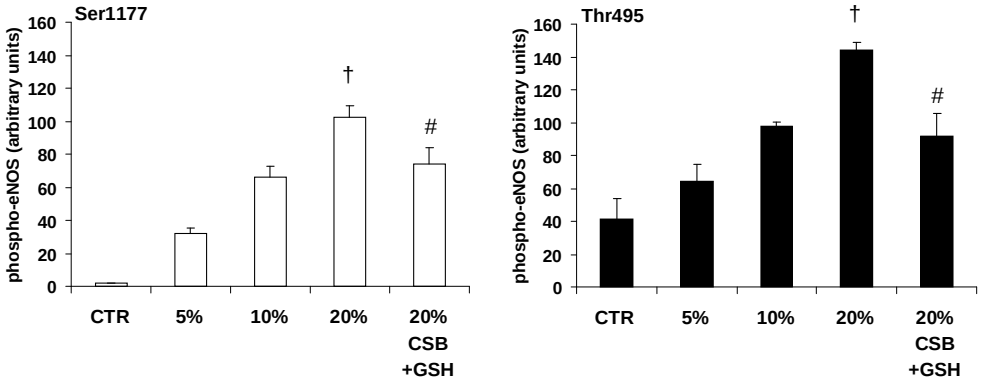

B)

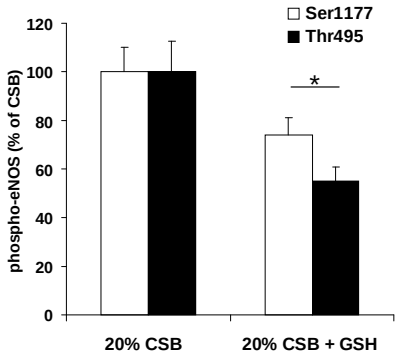

Figure 3. *A) Reduced glutathione (GSH) attenuated the cigarette smoke buffer (20% CSB; 30 min) induced increases in phospho-eNOS levels at both Ser(1177) and Thr(495) sites. B) Following CSB treatment, GSH decreased eNOS phosphorylation at Ser(1177) by 20%, and at Thr(495) by 45% compared to GSH-untreated cells. GSH caused a greater reduction in phospho-Thr(495) eNOS that of phospho-Ser(1177) eNOS levels (* p<0.05; unpaired t-test).*

† p<0.05 vs. Control (one-way ANOVA; Dunnett); # p<0.05 vs. 20% CSB (unpaired t-test); [n=4-4]

Reduced glutathione prevented the cigarette smoke induced disruption of eNOS dimers: It is accepted that homodimeric structure of eNOS is required for its catalytic activity, whereas the monomeric form is less active and it produces mainly superoxide free radical (108). We first assessed whether CSB alters the levels of dimer and monomer eNOS. We found that CSB significantly decreased eNOS dimerization in a concentration-dependent (*Fig. 4A*) and time-dependent (*Fig. 4B*) manner. CSB significantly reduced the ratio of dimer/monomer eNOS levels compared to CSB-untreated controls with greatest response at 50% CSB after 20 min treatment.

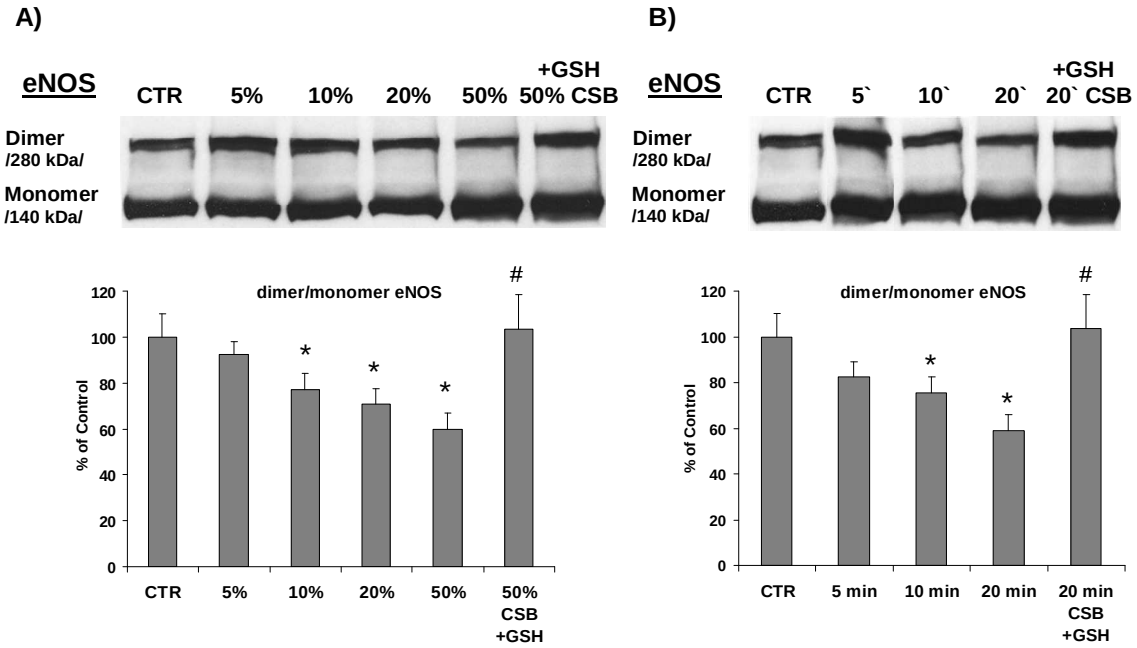

Figure 4. *Cigarette smoke buffer (CSB) significantly decreased the ratio of dimer/monomer eNOS levels in A) concentration-dependent and B) time-dependent manner, which was the lowest by 50% CSB, 20 min. Endothelial cells were treated with A) increasing concentrations of (CSB; 5%, 10%, 20%, 50%; 20 min) or B) with 50% CSB for 5, 10, 20 min. Reduced glutathione (GSH) treatment inhibited the CSB-induced disruption of eNOS dimers maintaining the normal dimer/monomer eNOS ratio similarly to that seen in CSB-untreated, control cells (NS: 50% CSB+GSH vs. CTR).*
** p<0.05 vs. Control (one-way ANOVA; Dunnett); # p<0.05 vs. 50% CSB (unpaired t-test); [n=7-7]*

GSH treatment markedly prevented the CSB-induced disruption of eNOS dimers (*Figs. 4A, B*). This was more apparent at the peak effect of CSB (50%, 20 min), at which GSH totally reversed the dissociation of homodimeric eNOS and the ratio of dimer/monomer eNOS remained comparable to that seen in CSB-untreated controls. Using the cell-premeable glutathione monoethyl ester (5 mM, Calbiochem) showed similar effects to those seen with GSH (data not shown). These results suggest that GSH might result in increased NO production by preventing the CSB-induced inactivating modifications of eNOS. The protective effects of GSH also suggest that CSB-induced changes in eNOS phosphorylations could be mediated by aldehydes, whereas eNOS dimerization could be preserved by eliminating the oxidative damage of key thiol groups within eNOS.

1.3. Effects of selective PKA, PI3-K/PKB and PKC inhibitors on the cigarette smoke induced changes in eNOS phosphorylations

PKC pathway blockade significantly altered the cigarette smoke induced changes in eNOS phosphorylations: Selective inhibitors of PKA (H-89), PI3-K/Akt (LY-294002), and PKC (Ro-318425) pathways were used to determine their roles in mediating the CSB-induced changes in eNOS phosphorylations. The Ser/Thr kinase PKA also plays a role in phosphorylating eNOS at Ser(1177) leading to increased enzyme activity and NO production (6, 12). After CSB treatment, however, we did not find significant effects with PKA inhibitor on eNOS phosphorylations at either site (*Figs. 5A, B, C*), suggesting that PKA is unlikely to be involved in mediating the changes in eNOS phosphorylations seen with CSB.

Consistent with the CSB-induced PKB/Akt inactivation (*Fig. 2*), selective PI3-K/Akt inhibitor promoted the CSB-induced eNOS phosphorylation at Ser(1177) (*Fig. 5A*). Although selective PI3-K/Akt inhibitor increased phospho-Thr(495) eNOS levels after CSB treatment, statistical analysis showed no difference when compared to the untreated controls (*Fig. 5B*). These results indicate that CSB-induced eNOS phosphorylations are stimulated independently of the PI3-K/Akt pathway.

PKC has a wide variety of actions in signal transduction, and it has been shown to regulate eNOS catalytic activity by phosphorylating eNOS at the inhibitory Thr(495) site (83). In response to CSB, we found that selective PKC inhibitor significantly decreased eNOS phosphorylation at Thr(495) site (*Fig. 5B*), and it also resulted in augmented phospho-Ser(1177) eNOS levels (*Fig. 5A*). This opposite change in decreased phospho-Thr(495) and increased phospho-Ser(1177) eNOS levels with selective PKC inhibitor treatment was statistically significant (*Fig. 5C*).

Selective PKC inhibitor decreased the cigarette smoke induced eNOS phosphorylations at Thr(495) in a concentration-dependent manner: Effects of partially selective PKC inhibitor (Ro-318425) on the suppression of CSB-induced eNOS phosphorylation at Thr(495) were also confirmed in concentration-dependent experiments (*Fig. 6*), where endothelial cells were subjected to 10%, 20%, and 50%

CSB for 20 min in the absence and presence of Ro-318425 (Ro) treatment. In CSB-untreated cells, Ro had no effect on eNOS phosphorylations at either site. However, we found that Ro significantly reduced the CSB-induced increases in phospho-Thr(495) eNOS levels at all concentrations (10%, 20% or 50% CSB) (*Fig. 6B*), and it increased phospho-Ser(1177) eNOS levels only after 50% CSB treatment (*Fig. 6A*).

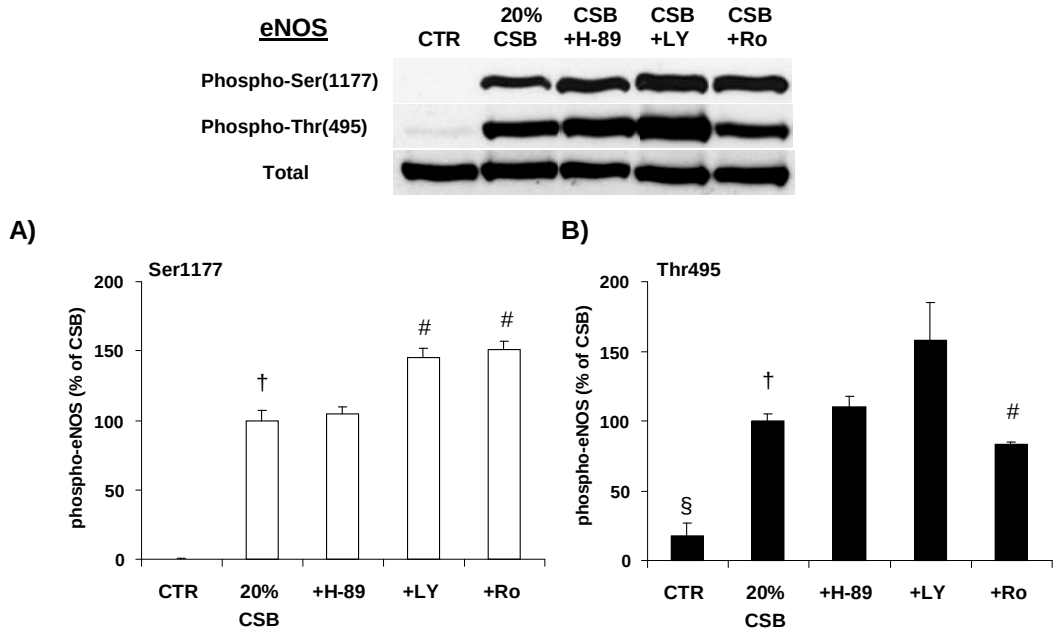

Figure 5. *Cigarette smoke buffer (CSB)-treated (20%, 20 min) endothelial cells were pre-treated with selective PKA inhibitor (H-89; 10 μM), selective PKB/PI3-K inhibitor (LY-294002; 100 μM), or selective PKC inhibitor (Ro-318425; 1 μM) for 30 min. In CSB-untreated controls, eNOS phosphorylations were higher at Thr(495) than at Ser(1177) (§ p<0.05; unpaired t-test). CSB significantly increased both A) phospho-Ser(1177) and B) phospho-Thr(495)-eNOS levels. A) Phosphorylation of eNOS at Ser(1177) was unaffected by H-89; conversely, it was increased with both LY and Ro treatments. B) Phosphorylation of eNOS at Thr(495) did not change with either H-89 or LY treatments; however, it was markedly suppressed by Ro treatment. C) The comparisons of Ser(1177) with Thr(495 phosphorylations demonstrate that addition of H-89 or LY resulted in similar changes at both sites, whereas Ro resulted in dissimilar changes leading to decreased phospho-Thr(495) and increased phospho-Ser(1177) eNOS levels (* p <0.001 Ser(1177) vs. Thr(495); unpaired t-test). Total eNOS protein level remained unchanged in all experiments. Data (means ± SE) are corrected for controls and total eNOS protein levels, and are expressed relative to the CSB effect without inhibitors.*
† p<0.05 vs. Control, # p<0.05 vs. 20% CSB (one-way ANOVA; Dunnett); [n=4]

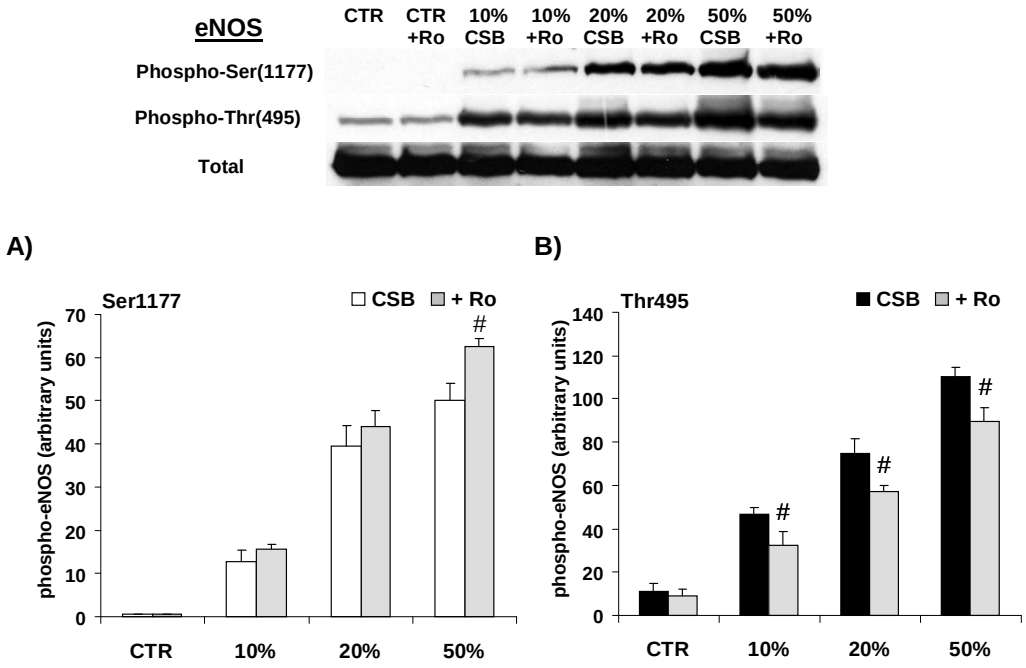

Figure 6. *Representative immunoblots demonstrate the phospho-Ser(1177) eNOS, phospho-Thr(495) eNOS and total eNOS protein levels in endothelial cells treated with increasing concentrations of cigarette smoke buffer (10%, 20%, 50% CSB; 20 min) in the absence and presence of selective PKC inhibitor (+ Ro-318425; 1 μM). A) Ro resulted in increased phosphorylations at Ser(1177) site only after 50% CSB treatment (# p <0.05 vs. CSB; unpaired t-test) B) Ro inhibited the CSB-induced Thr(495) phosphorylations at all CSB concentrations (# p <0.05 vs. CSB; unpaired t-test). Data (means ± SE) are corrected for controls and total eNOS protein levels. [n=3]*

1.4. Effects of the isoform specific PKCβII-inhibitor (ruboxistaurin) on the cigarette smoke induced changes in eNOS phosphorylations

Ruboxistaurin inhibited the cigarette smoke induced eNOS phosphorylations at Thr(495) in a concentration-dependent manner: The isoform specific, PKCßII-inhibitor (ruboxistaurin) has been previously shown to prevent vascular dysfunction by preserving endothelium-dependent vasodilation, in part by blocking the inhibitory PKC signaling to eNOS (8). We subsequently examined whether ruboxistaurin (Rub) could recapitulate the effects on the CBS-induced changes in eNOS phosphorylations seen with selective PKC inhibitior (Ro). As shown in *Fig. 7*, endothelial cells were treated with 10%, 20%, and 50% CSB for 20 min in the absence and presence of Rub. In CSB-untreated cells, Rub had no impact on eNOS phosphorylations at either site (*Fig. 7*). Rub significantly increased phospho-Ser(1177) eNOS levels, only after 50% CSB (*Fig. 7A*). In contrast, Rub markedly suppressed the CSB-induced increases in

phospho-Thr(495) levels regardless of CSB concentration (*Fig. 7B*). Moreover, Rub increased the ratio of phospho-Ser(1177)/phospho-Thr(495) eNOS levels in a concentration-dependent manner (*Fig. 7C*). These results indicate that PKC pathway, more importantly the PKCβII pathway has a role in mediating the CSB-induced changes in eNOS phosphorylations by rather increasing its inhibitory phosphorylation at Thr(495), than its activating phosphorylation at Ser(1177).

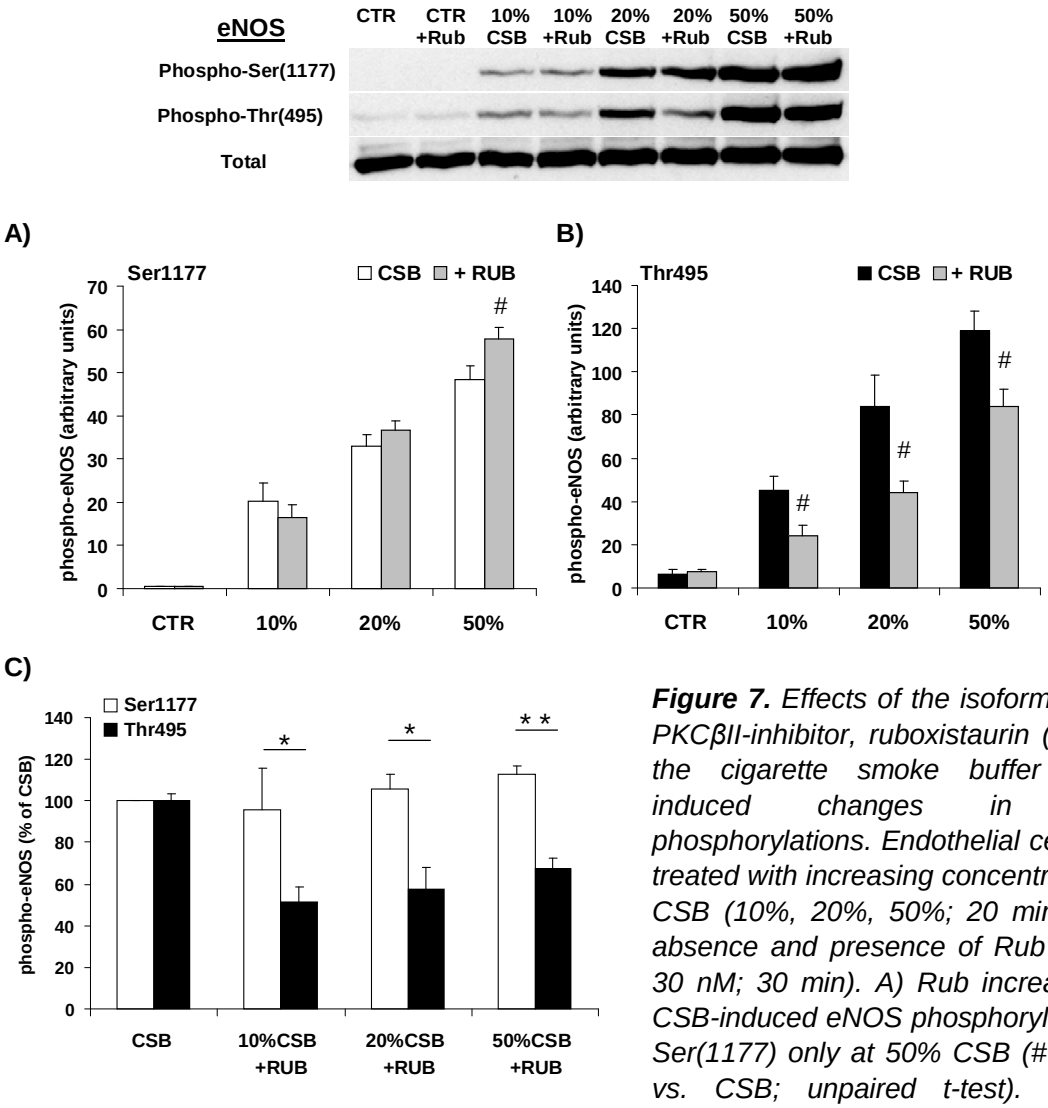

Figure 7. *Effects of the isoform specific PKCβII-inhibitor, ruboxistaurin (Rub) on the cigarette smoke buffer (CSB)-induced changes in eNOS phosphorylations. Endothelial cells were treated with increasing concentrations of CSB (10%, 20%, 50%; 20 min) in the absence and presence of Rub (+ Rub, 30 nM; 30 min). A) Rub increased the CSB-induced eNOS phosphorylations at Ser(1177) only at 50% CSB (# p <0.05 vs. CSB; unpaired t-test). B) Rub suppressed the CSB-induced Thr(495) phosphorylations at all CSB concentrations (# p <0.05 vs. CSB; unpaired t-test). C) Rub increased the ratio of phospho-Ser(1177)/phospho-Thr(495) eNOS levels in a concentration-dependent manner (10 % and 20 % CSB: * p<0.05 and 50% CSB: ** p<0.001 phospho-Ser(1177) vs. phospho-Thr(495); unpaired t-test). Data (means ± SE) are corrected for controls and total eNOS, and are expressed as % of the CSB effect without Rub. [n=6]*

2. Oxidative stress and cardiac dysfunction: *Ex vivo* experiments on the role of protein O-GlcNAcylation in mediating cardioprotection against ischemia-reperfusion injury in the isolated perfused rat heart.

Chronic activation of the HBP and resulting increases in protein O-GlcNAcylation have been implicated as a pathogenic contributor to glucose toxicity and insulin resistance, the major hallmarks of diabetes and its related vascular complications. Paradoxically, there is rapidly emerging evidence demonstrating that acute activation of these pathways affords protection against a wide range of injuries, including cardioprotection against I/R injury. Our primary goal was to verify that acute augmentation of O-GlcNAc with novel, highly selective OGA inhibitors protects the isolated perfused heart against I/R injury. We also purposed to determine the effects of ischemia, I/R, and OGA inhibitor treatment on the tissue distribution of O-GlcNAc in the heart, as well as specific cardiac proteins that are targeted by O-GlcNAc signaling in response to ischemia and/or reperfusion.

Materials and methods:

Materials: All chemicals and reagents were purchased from Sigma-Aldrich unless otherwise specified. The OGA inhibitors, NAG-Bt and NAG-Ae were kind gifts from Dr. David Vocadlo (Simon Fraser University, Burnaby, Canada).

Animals: Animal experiments were approved by the Institutional Animal Care and Use Committee at the University of Alabama at Birmingham and conformed to the Guide for the Care and Usage of Laboratory Animals published by the National Institutes of Health (NIH Publication No. 85-23, Revised 1996). Non-fasted, male Sprague-Dawley rats (Charles Rivers Laboratories) weighing 300-350 g were employed.

Heart perfusion: After anesthesia with intraperitoneal ketamine-hydrochloride injection (100 mg/kg; Vedco), rats were sacrificed by decapitation, and hearts were rapidly excised and arrested in ice-cold perfusion buffer. Isolated hearts were cannulated via the aorta for retrograde perfusion in a modified Langendorff model, as previously described (46, 69). The KHB perfusion buffer (pH 7.4) contained (in mM) NaCl 118, $NaHCO_3$ 25, KCl 4.8, KH_2PO_4 1.2, $MgSO_4$ 1.2, $CaCl_2$ 1.25, glucose 11.0, and

3% BSA (fatty acid free; Millipore) gassed with 95% O_2 and 5% CO_2. The solution was filtered through a 0.45 μM filter to remove contaminants. NAG-thiazolines were dissolved in the perfusion buffer immediately prior to use. Cardiac function was monitored via a fluid-filled balloon inserted into the left ventricle via the left atrium and connected to a TXD-310 pressure transducer, and was registered with a heart performance analyzer (HPA-410; Micro-Med). End-diastolic pressure (EDP) was set to 5 mmHg by adjusting balloon volume. Coronary flow was controlled by a perfusion pump and was adjusted to maintain a constant perfusion pressure of 75 mmHg. Myocardial temperature was maintained constant at ~37℃ throughout the experiments. Coronary flow was assessed by timed collections of right ventricle effluent and volume was measured. Hearts were allowed to beat spontaneously (non-paced) throughout the experiments. Coronary flow, heart rate, left ventricular developed pressure (LVDP = systolic pressure - EDP), maximum and minimum rate of left ventricular pressure development (± dP/dt) as the indexes of contraction and relaxation respectively, and rate-pressure product (RPP = LVDP x heart rate) were used to evaluate cardiac performance. Pressure signals were analyzed for ventricular tachycardia (VT; run of four or more consecutive ectopic beats) and/or fibrillation (VF; fast mechanical activity with barely discernible beat and minimal (<5 mmHg) LVDP) during reperfusion (61). At the end of reperfusion, hearts were either freeze-clamped into liquid nitrogen and stored at –80℃, or perfused with 4% paraformaldehyde and stored in 70% ethanol.

Experimental protocol: After 30 min equilibration, isolated hearts were randomly assigned to either a time-control, untreated normoxia group (Norm) or four ischemia-reperfusion (I/R) groups: 1) I/R, untreated (Control); 2) I/R, 50 μM NAG-Bt (NBt50); 3) I/R, 100 μM NAG-Bt (NBt100); 4) I/R, 50 μM NAG-Ae (NAe). In all I/R groups, hearts were subjected to 20 min global, no-flow ischemia followed by 60 min of reperfusion. In the treated I/R groups, hearts were perfused with NAG-thiazolines starting immediately at reperfusion and continued throughout the 60 min-reperfusion period. The starting concentration of NAG-Bt was chosen based on preliminary dose response studies which demonstrated an EC_{50} of ~30 μM for increasing O-GlcNAc in the normoxic heart

perfused with NAG-Bt for 60 min (data not shown). Due to limited availability of NAG-Ae at the time of these studies, we were able to examine only a single concentration; therefore, to enable direct comparison with NAG-Bt, 50 μM NAG-Ae was used. In the time-control groups, hearts were perfused for a total of 110 min under normoxic conditions. To determine whether inhibition of OGA alone had any effect on cardiac function, an additional group of hearts were perfused with NAG-Bt (50 μM) that was added 20 min after the initial 30 min equilibration period, and was present for the remaining 60 min of normoxic perfusion; thus the total perfusion time and exposure to NAG-Bt was the same as for the I/R treatment groups.

Cardiac troponin I release: As a marker of tissue injury, cardiac troponin I (cTnI) concentration was determined in pooled coronary effluents collected at 15, 30, 45 and 60 min of reperfusion using a high-sensitivity cTnI ELISA kit (Life Diagnostics).

Measurement of ATP and UDP-HexNAc levels: ATP levels were determined with HPLC from perchloric acid (PCA) extracted frozen heart tissue as previously described (46). Briefly, heart tissue (~70 mg) was precipitated in 1 mL 0.3 M PCA and centrifuged (15,000 g, 15 min, at 4℃). The supernatants were neutralized with trioctylamine:1,1,2-trichlorotrifluoroethane mixture (1:4 ratio), and were loaded onto Partisil 10 SAX anion-exchange column (Beckman), and then eluted with a linear salt (ammonium dihydrogen phosphate from 5 to 750 mM) and pH gradient (from pH 2.8 to 3.7). Concentrations were determined using ultraviolet detection (262 nm) after calibration with appropriate standards. This method also detects UDP-GlcNAc levels, however, it cannot separate completely UDP-GlcNAc from UDP-GalNAc (UDP-N-acetylgalactosamine) thus results are presented as the sum of UDP-GlcNAc and UDP-GalNAc (UDP-HexNAc; UDP-N-acetylhexosamine).

Protein identification with MALDI-TOF Mass Spectrometry: After the excision of Coomassie-stained (BioRad) gel plugs, samples were processed for mass spectrometry by enzymatic digestion with trypsin for 16 hrs at 37℃. Peptide solutions were extracted in formic acid and acetonitrile solution (1:1 ratio) for 30 min, then supernatants were collected and dried in Savant SpeedVac. Samples were resuspended in trifluoroacetic acid, then peptide mixtures were desalted using C^{18}

ZipTips (Millipore) prior to application to MALDI-TOF 96-well plate followed by the addition of α-cyano-4-hydroxycinnamic acid matrix (5 mg/mL; Acros). Spectra were analyzed using Voyager Explorer software, and peptide masses were submitted to MASCOT database for protein identifications. For protein identification studies additional series of perfusions were conducted; after 30 min stabilization, isolated hearts were randomly assigned to three groups: 1) Normoxia; hearts were perfused for further 10 min under normoxic conditions; 2) Ischemia; hearts were subjected to 10 min no-flow ischemia; 3) Reperfusion; hearts were subjected to 10 min no-flow ischemia followed by 60 min reperfusion.

Immunoblot analysis: Hearts were freeze-clamped and ground into tissue powder under liquid nitrogen. Pulverized heart tissue was homogenized in T-PER (Pierce) supplemented with 40 μM PUGNAc (Toronto Research Chemicals), 1 mM Na_3VO_4, 20 mM NaF, and 5% protease inhibitor cocktail (PIC), and lyzed for 60 min on ice. Whole tissue lysates were centrifuged (15,000 g, 15 min, 4℃), and protein concentration of the supernatant was assessed using BioRad Protein Assay Kit. Proteins were mixed with reducing loading buffer (5X; Pierce), boiled, and separated by SDS-PAGE, then transferred on polyvinylidene difluoride (PVDF) membrane (Millipore). Equal protein loading was confirmed by Ponceau-S staining and calsequestrin (Abcam) immunostaining. Blots were incubated with anti-O-GlcNAc (1:2,500; CTD110.6; Epitope Recognition and Immunodetection Facility, UAB), anti-Vinculin (1:4,000; CloneV284; Upstate), anti-phospho-Tyr(822) vinculin (1:1,000), anti-Desmin (1:4,000; Abcam), anti-OGT (1:2,000; DM-17, Sigma), anti-Aconitase 2 (1:4,000; Center, Abgent), anti-Glycogen phosphorylase (1:2,000; N20, Santa Cruz) antibodies in 1% casein-PBS blocking buffer (BioRad) for overnight at 4℃. After incubation with appropriate HRP-conjugated secondary antibodies for 60 min at room temperature, blots were washed with PBS and visualized with ECL kit (Pierce). Densitometric data were obtained using Scion Image for Windows software.

O-GlcNAc, desmin and vinculin immunofluorescence: At the end of the perfusion hearts were perfusion-fixed with 4% paraformaldehyde, stored in 70% ethanol until paraffin embedding, and sectioned at 5 μm before being mounted on slides,

deparaffinized in xylene, rehydrated in ethanol and blocked with 5% goat serum in 1% bovine serum for 60 min at room temperature. Sections were incubated with primary antibodies against O-GlcNAc (1:50, CTD110.6), desmin (1:300, Abcam), and vinculin (1:100, Abcam) diluted in 5% goat serum in 1% bovine serum overnight at 4℃; appropriate secondary antibodies conjugated to either Alexa Fluor 488 (green) or 594 (red) (Invitrogen) were used to visualize the specific proteins with 4',6 diamidino-2-phenylindole (DAPI) to identify nuclei (350 nm; blue). Image acquisition was performed on a Leica DM6000B epifluorescence microscope (Leica Microsystems) with a Hamamatsu ORCA ER cooled CCD camera and SimplePCI software (Compix Inc.). For the comparison of ischemia and I/R induced changes in O-GlcNAc, desmin, and vinculin tissue distribution, an additional series of perfusions were performed where hearts were subjected to 20 min ischemia (ISC) without reperfusion prior to fixation.

Immunoprecipitation: Cardiac tissue was homogenized to obtain whole tissue lysates, as described above. Pre-cleared tissue lysates containing equal amounts of protein (1000 µg) were mixed with 5-5 µg primary antibodies against vinculin, glycogen phosphorylase, aconitase 2, and OGT for overnight at 4℃. Immunocomplexes were pulled down by the addition of protein A/G agarose beads for 4hrs at 4ºC. Antigens were eluted from the beads with Laemmli buffer (2X) then samples were boiled and subjected to SDS-PAGE and blotting on PVDF membranes. Immunostaining and visualization were completed as described in western blot section. The specificity of anti-O-GlcNAc antibody was confirmed by a co-incubation with 10 mM β-N-acetylglucosamine (29).

Subcellular fractionation of heart tissue: Nuclear and cytoplasmic fractions were prepared with a commercially available kit of nuclear and cytoplasmic protein extraction reagents according to the manufacturer's instructions (Pierce). GAPDH and TATA-binding protein antibodies (Abcam) were used as purity controls. For preparation of the membrane compartment, heart tissue powder was lyzed in ice-cold homogenization buffer containing (in mM) Tris (pH: 7.4) 20.0, EDTA 5.0, sucrose 250, PMSF 1.0, and 2.5% PIC. Tissue homogenates were centrifuged (1,000 g, 10 min) to remove nuclei and debris, and supernatant was ultracentrifuged at 110,000 g for 75 min at 4ºC to pellet the crude membrane fraction (= sarcolemmal + microsomal

subfractions). The pellet was resuspended in solubilization buffer containing (in mM) Tris (pH: 7.4) 50.0, NaCl 100.0, LiCl 50.0, EDTA 5.0, and 0.5 (v/v)% Triton X-100, 0.05 (w/v)% SDS, 0.5 (w/v)% Na-deoxycholate using a glass homogenizer. After 30 min incubation on ice, the remaining insoluble material was collected by centrifugation (14,000 g, 10 min, 4ºC), and the supernatant (= particulate membrane fraction) was used. Pan-cadherin antibody (Abcam) was used as purity control. For the mitochondrial fractionation, frozen heart tissue powder was homogenized in mitochondrial isolation buffer containing (in mM) sucrose 70.0, mannitol 220.0, 3-(N-morpholino)propanesulfonic acid (MOPS) 5.0, EGTA 1.0 supplemented with 5 (v/v)% PIC and 0.2 (w/v)% BSA. Tissue homogenates were lyzed on ice for 5 min and centrifuged (750 g, 5 min, 4℃) to remove unlyzed cells and nuclei, and the supernatants were spun at 6,000 g for 10 min, at 4°C. The supernatants consisting of the cytosolic/microsomal subfractions (post-mitochondria) were saved for subsequent analyses. The resulting mitochondrial pellets were resuspended in the isolation buffer without BSA then centrifuged (6,000 g, 10 min, 4℃). The final pellets were resuspended in T-PER (Pierce), incubated on ice for 30 min, then centrifuged (2,500 g, 5 min, 4℃). COXIV and GAPDH (Abcam) antibodies were used as purity controls. The blots were immunostained and visualized as described above.

Aconitase enzyme activity assay: Frozen heart tissue powder was homogenized in buffer containing (in mM) Tris HCl (pH: 8.0) 100.0, 2% Triton-X 100, NaF 20.0, Na_3VO_4 1.0, and 2% PIC, then homogenates were spun (14,000 g, 15 min, 4℃) to remove debris. Equal amounts of protein (15 µg) were added to a mixture of reagents (in mg/mL) $MnCl_2$, 1.5, $NADP^+$ 7.6, isocitrate dehydrogenase (3 U/ml), Na-fluoroacetate 0.2, and Na-citrate 1.75. Aconitase activity was measured spectrophotometrically (340 nm) by the conversion of citrate to α-ketoglutarate coupled to the reduction of NADP.

Statistical analysis: All data are expressed as means ± SE. All examined variables showed normal distribution by Kolmogorov-Smirnov test. Statistical analyses were performed using two-way and one-way ANOVA followed by Bonferroni's posthoc test, Pearson's correlations, χ^2-test, and unpaired t-test for data as appropriate using Prism 4.0 (GraphPad Software Inc.). Statistically significant differences were defined as $p < 0.05$ and are indicated in the figure legends.

Results:

2.1. Effects of selective OGA inhibitor treatments at the time of reperfusion on functional recovery, tissue injury and protein O-GlcNAcylation following ischemia-reperfusion in the perfused rat heart

Baseline cardiac functions of ischemia-reperfusion groups: Baseline cardiac function was assessed after 30 min normoxic equilibration prior to 20 min zero-flow ischemia. There were no significant differences in pre-ischemic cardiac parameters between untreated I/R hearts (Control) and hearts treated with 50 µM NAG-Bt (NBt50), 100 µM NAG-Bt (NBt100) and 50 µM NAG-Ae (NAe) at the time of reperfusion (*Table 1*). Furthermore, in time-control normoxic perfusions (110 min) there was no significant difference in RPP between untreated hearts and those treated with 50 µM NAG-Bt for the same duration as the ischemic hearts (Norm: 19,621±2,285; +NBt: 20,688±1,311 mmHg/min), demonstrating that NAG-Bt alone has no effects on contractile function under normoxic conditions.

Table 1. Baseline cardiac functions (means ± SE) in control, untreated ischemia-reperfusion hearts; and hearts subsequently treated with NAG-thiazolines during reperfusion

Groups (N)	**Coronary Flow** (mL/min)	**Heart Rate** (beats/min)	**LVDP** (mmHg)	**+ dP/dt** (mmHg/s)	**- dP/dt** (mmHg/s)	**RPP** (mmHg/min)
Control (6)	10.1 ± 0.7	324 ± 13	96.6 ± 10.0	3,374 ± 174	2,166 ± 308	30,688 ± 1,725
NBt50 (7)	12.3 ± 0.9	323 ± 9	89.9 ± 9.9	3,451 ± 313	2,078 ± 253	28,905 ± 2,881
NBt100 (5)	13.2 ± 0.9	335 ± 18	83.6 ± 6.5	3,428 ± 259	1,966 ± 146	27,744 ± 1,610
NAe (3)	14.2 ± 1.0	359 ± 29	74.6 ± 5.5	3,930 ± 375	1,796 ± 125	27,029 ± 3,596

N, number of replicates/group; LVDP, left ventricular developed pressure; +dP/dt, maximum rate of change in left ventricular pressure; -dP/dt, minimum rate of change in left ventricular pressure; RPP, rate-pressure product (LVDP x heart rate);
[NS: one-way ANOVA, Bonferroni]

Ischemia-reperfusion significantly decreased cardiac functions and O-GlcNAc: Consistent with the model used, LVDP, ± dP/dt, and RPP markedly declined (~3-fold) in hearts subjected to 20 min global ischemia and 60 min reperfusion compared to the normoxic hearts perfused for the same duration (*Fig. 8A*). We also found that at the end of I/R there was a 50% loss of overall protein O-GlcNAcylation compared to time-

matched, normoxic hearts (*Fig. 8B*). The lack of significant protein degradation (i.e. unchanged calsequestrin levels) at the end of I/R suggests that lowered cardiac O-GlcNAc was secondary to other mechanisms during reperfusion, such as oxidative injury. Of note, UDP-HexNAc and ATP levels were markedly decreased parallel with increased tissue injury after I/R compared to the normoxic hearts (*Figs. 11A, B, C*).

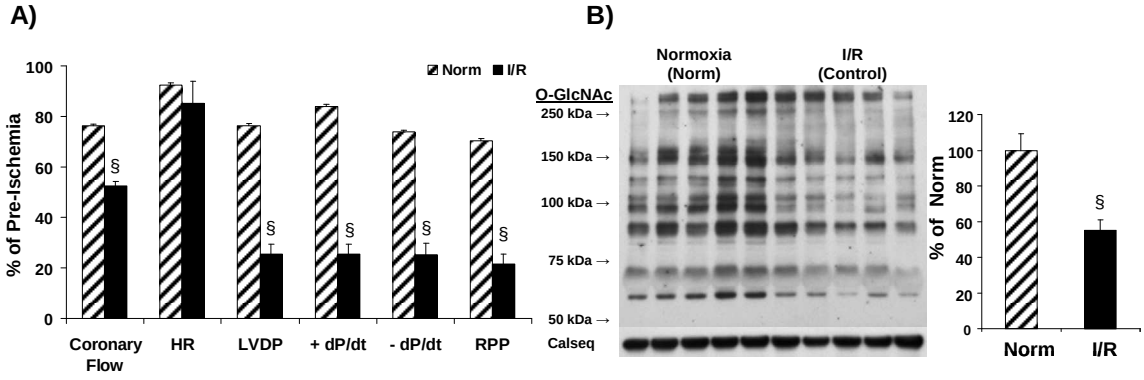

Figure 8. *Effect of ischemia-reperfusion on A) cardiac functions of coronary flow, heart rate (HR), left ventricular developed pressure (LVDP), positive and negative rates of left ventricular pressure change (± dP/dt), and rate pressure product (RPP); and B) the loss of cardiac O-GlcNAc in hearts subjected to 20 min no-flow ischemia followed by 60 min reperfusion (I/R; n=7) compared to the time-control normoxic hearts (Norm; n=5). Mean intensities of entire lanes are normalized to calsequestrin levels shown as protein loading control, and are relative to the normoxic group (§ p<0.05 vs. Norm; unpaired t-test).*

OGA inhibitors NAG-Bt and NAG-Ae significantly improved functional recovery following ischemia-reperfusion: As shown in *Fig. 9A*, during reperfusion NBt100 and NAe groups showed higher RPP values than the untreated Control group. Two-way repeated measurements of ANOVA indicated an overall significant treatment effect with both NAG-Bt and NAG-Ae compounds on RPP. Increased recovery of RPP was apparent as early as 5 min after reperfusion in the NAe group and this difference was maintained throughout reperfusion. Recoveries of LVDP and max dP/dt during reperfusion closely mirrored those seen with RPP (*Figs. 9B, C*). At the end of reperfusion RPP, LVDP, and ± dP/dt were all significantly higher in NBt100 and NAe groups compared to untreated controls (*Fig. 10*). In addition, RPP, LVDP, and ± dP/dt were all significantly higher in the NAe group compared to both NBt50 and NBt100

groups. There were no significant differences in either coronary flow or heart rate between any of the groups.

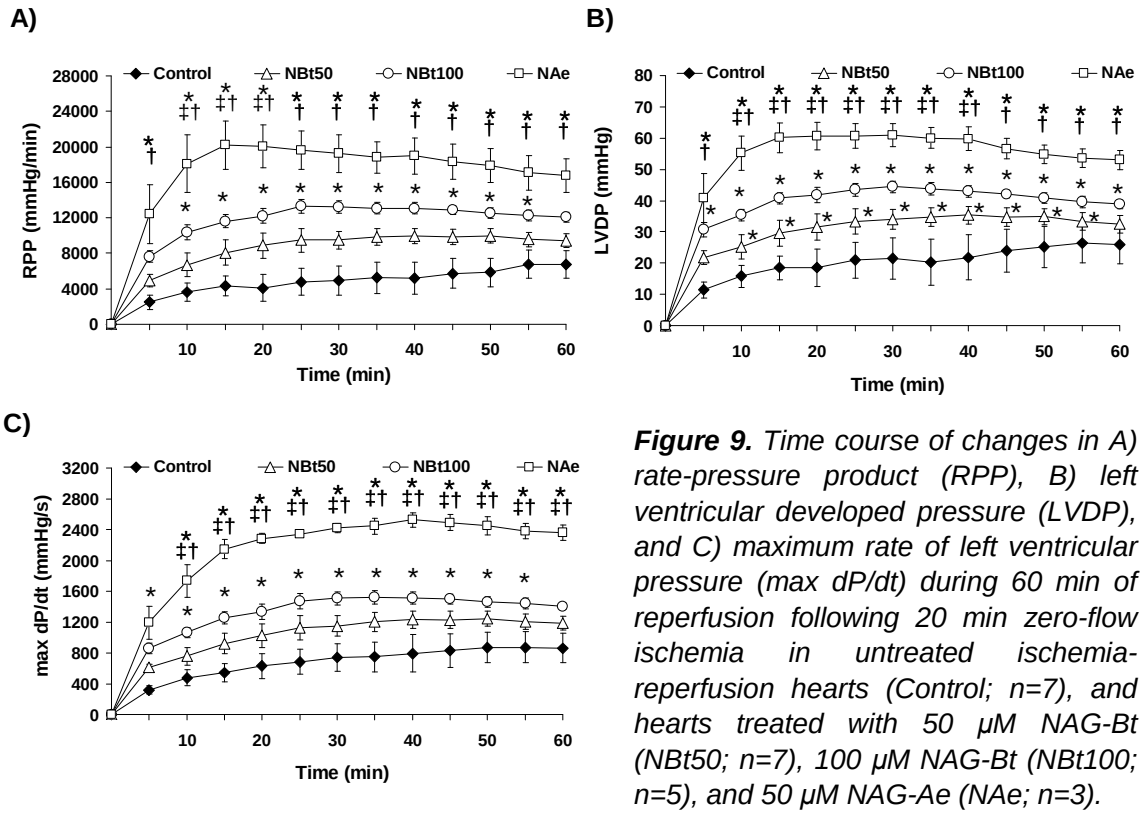

Figure 9. *Time course of changes in A) rate-pressure product (RPP), B) left ventricular developed pressure (LVDP), and C) maximum rate of left ventricular pressure (max dP/dt) during 60 min of reperfusion following 20 min zero-flow ischemia in untreated ischemia-reperfusion hearts (Control; n=7), and hearts treated with 50 µM NAG-Bt (NBt50; n=7), 100 µM NAG-Bt (NBt100; n=5), and 50 µM NAG-Ae (NAe; n=3).*

** p<0.05 vs. Control; † p<0.05 vs. NBt50; ‡ p<0.05 vs. NBt100 (two-way ANOVA; Bonferroni)*

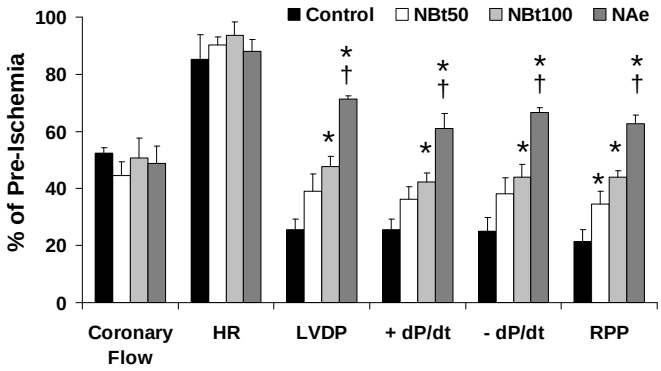

Figure 10. *Functional recoveries of coronary flow, heart rate (HR), left ventricular developed pressure (LVDP), positive and negative rates of left ventricular pressure change (± dP/dt), and rate pressure product (RPP) following 60 min reperfusion relative to the pre-ischemic values in untreated, ischemia-reperfusion hearts (Control; n=7) hearts, and hearts treated with 50 µM NAG-Bt (NBt50; n=7), 100 µM NAG-Bt (NBt100; n=5), and 50 µM NAG-Ae (NAe; n=3).*

** p<0.05 vs. Control; † p<0.05 vs. NBt50; ‡ p<0.05 vs. NBt100 (one-way ANOVA; Bonferroni)*

OGA inhibitors NAG-Bt and NAG-Ae significantly reduced tissue injury following ischemia-reperfusion with no effects on ATP and UDP-HexNAc levels: Indicative of reduced tissue injury, cTnI release during reperfusion was significantly lower in hearts from NBt100 and NAe groups compared to the untreated Control group, and was significantly lower in the NAe group compared to both NBt50 and NBt100 groups (*Fig. 11A*), similarly to the changes seen with improved functional recovery. In the time-control normoxic perfusions (110 min) basal cTnI release remained very low and was unaffected by NAG-Bt (Norm: 0.8 ± 0.1; +NBt: 0.8 ± 0.1 ng/mL).

ATP levels were significantly depressed in all I/R groups at the end of reperfusion compared to the time-matched Norm group after 110 min normoxic perfusions (*Fig. 11B*). Despite improved functional recovery and reduced tissue injury, there were no differences in ATP levels between any of the I/R groups regardless of treatments. Thus, increased functional recovery and reduction in tissue injury is clearly not a consequence of improved bioenergetic status.

UDP-GlcNAc, the essential sugar donor for O-GlcNAc synthesis is increased by the activation of the HBP. Following I/R, UDP-HexNAc levels were significantly reduced compared to the Norm group (*Fig. 11C*); however, there were no significant differences in UDP-HexNAc concentrations between any of the I/R groups regardless of treatments, demonstrating that inhibition of OGA during reperfusion had no upstream effects on precursors for O-GlcNAc synthesis.

In addition to improved contractile function, NAG-Bt and NAG-Ae during reperfusion significantly attenuated the arrhythmic activity. Ventricular premature beats could be observed in all hearts during the initial 10 min of reperfusion. Severe ventricular arrhythmias, VT and/or VF were seen in 86% of untreated control hearts; whereas the incidence of VT and/or VF was only 14% in the NBt50 group and was absent in both NBt100 and NAe groups ($p<0.05$; χ^2-test).

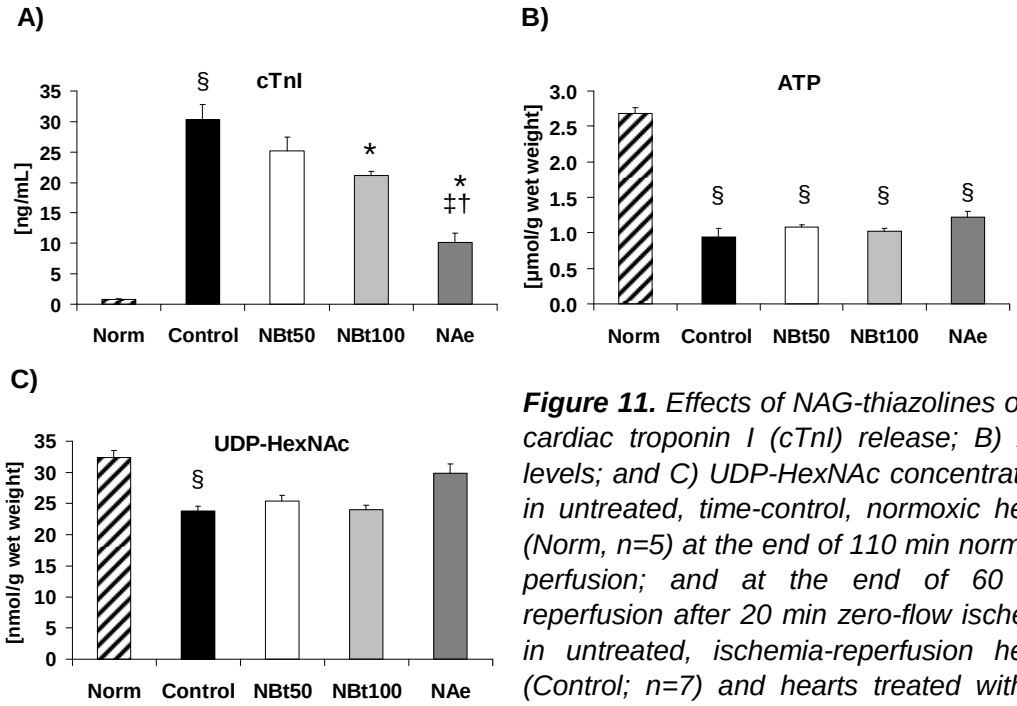

Figure 11. *Effects of NAG-thiazolines on A) cardiac troponin I (cTnI) release; B) ATP levels; and C) UDP-HexNAc concentrations in untreated, time-control, normoxic hearts (Norm, n=5) at the end of 110 min normoxic perfusion; and at the end of 60 min reperfusion after 20 min zero-flow ischemia in untreated, ischemia-reperfusion hearts (Control; n=7) and hearts treated with 50 µM NAG-Bt (NBt50; n=7), 100 µM NAG-Bt (NBt100; n=5), and 50 µM NAG-Ae (NAe; n=3).*

*§ p<0.05 vs. Norm; * p<0.05 vs. Control; † p<0.05 vs. NBt50; ‡ p<0.05 vs. NBt100 (one-way ANOVA; Bonferroni)*

OGA inhibitors NAG-Bt and NAG-Ae significantly increased cardiac O-GlcNAc levels following ischemia-reperfusion: Following I/R, overall O-GlcNAc levels were ~50% lower in the untreated Control group compared to the time-matched Norm group (*Figs. 8A, 12*); however, those were significantly higher in all treatment groups (NBt50, NBt100 and NAe) compared to the untreated Control group (*Fig. 12*). Cardiac O-GlcNAc was significantly higher in the NBt100 group compared to the NBt50 group, and NAe group exhibited significantly higher O-GlcNAc compared to both NBt50 and NBt100 groups.

Relationships between functional recovery, O-GlcNAc levels and tissue injury: We found significant correlations between overall O-GlcNAc and RPP (R^2 = 0.82; p<0.05; *Fig. 13A*), max dP/dt (R^2 = 0.77; p<0.05; *Fig. 13B*) and cTn (R^2 = 0.65; p<0.05; *Fig. 13C*). There was also significant relationship between RPP and cTnI (R^2 = 0.83; p<0.05; *Fig. 13D*). These data support the notion that treatments with OGA inhibitors

prevent the loss of O-GlcNAc that occurs on reperfusion, contributing to the improved functional recovery and decreased tissue injury.

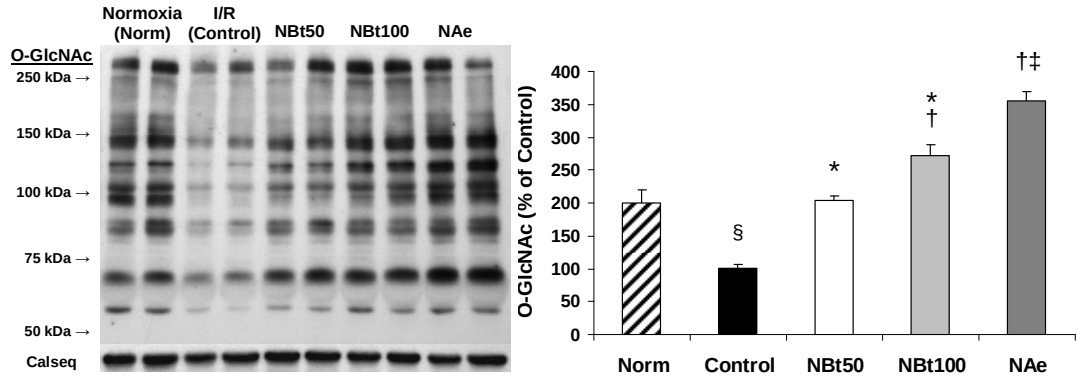

Figure 12. *Representative anti-O-GlcNAc (CTD110.6) immunoblot and densitometric results of protein-associated cardiac O-GlcNAc levels after time-control (110 min), normoxic perfusion (Norm); and after 20 min no-flow ischemia and 60 min reperfusion (I/R) in the absence (untreated, Control) and in the presence of 50 μM NAG-Bt (NBt50), 100 μM NAG-Bt (NBt100), and 50 μM NAG-Ae (NAe). Densitometric analyses were performed using original anti-O-GlcNAc immunoblots to compare all experimental groups (n=3-5 hearts/group). Mean intensities of entire lanes are normalized to calsequestrin shown as protein loading control, and are relative to the Control group.*
*§ p<0.05 vs. Norm; * p<0.001 vs. Control; † p<0.05 vs. NBt50; ‡ p<0.05 vs. NBt100 (one-way ANOVA; Bonferroni)*

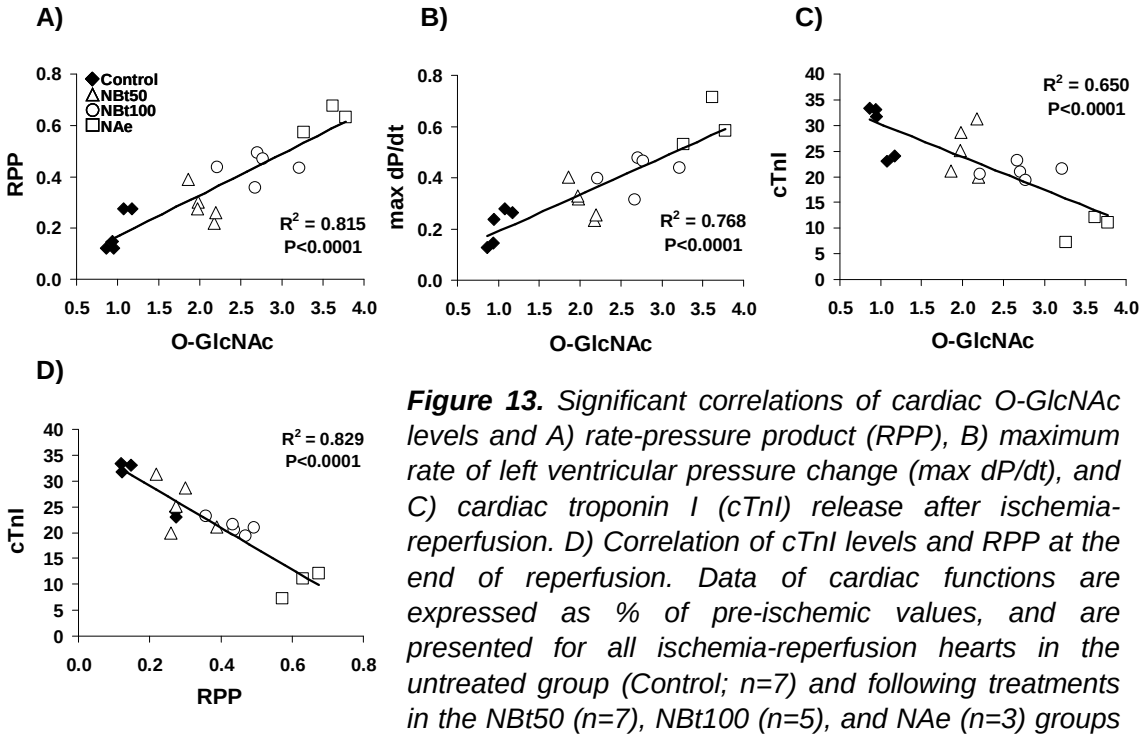

Figure 13. *Significant correlations of cardiac O-GlcNAc levels and A) rate-pressure product (RPP), B) maximum rate of left ventricular pressure change (max dP/dt), and C) cardiac troponin I (cTnI) release after ischemia-reperfusion. D) Correlation of cTnI levels and RPP at the end of reperfusion. Data of cardiac functions are expressed as % of pre-ischemic values, and are presented for all ischemia-reperfusion hearts in the untreated group (Control; n=7) and following treatments in the NBt50 (n=7), NBt100 (n=5), and NAe (n=3) groups (p<0.001; Pearson's correlation).*

2.2. Effects of ischemia, ischemia-reperfusion and selective OGA inhibitor treatments on subcellular O-GlcNAc distribution in cardiac tissue

OGA inhibitor NAG-Bt reduced the ischemia-reperfusion induced disruption of structural integrity, but did not prevent the loss of nuclear O-GlcNAcylation: While it is well-described that nuclear proteins are highly O-GlcNAcylated (56, 142), and changes in overall O-GlcNAc in cardiomyocytes have been demonstrated in response to different stresses, including I/R (66); the subcellular distribution of O-GlcNAc-modified proteins in the intact heart or how this is affected by ischemia and/or reperfusion is unknown. Consequently, we used immunohistochemistry to examine the effects of ischemia, I/R, and OGA inhibition on the cardiac distribution of protein O-GlcNAcylation (*Fig. 14*).

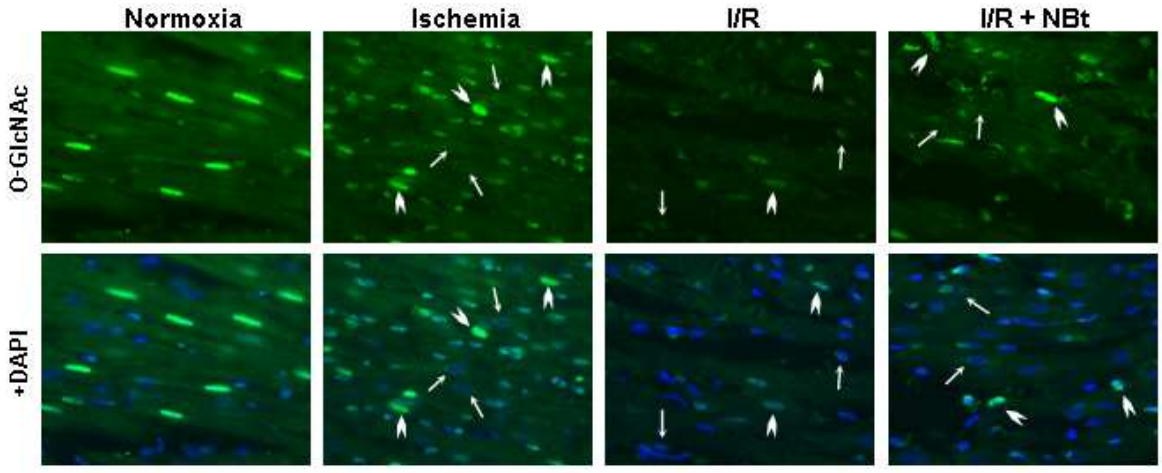

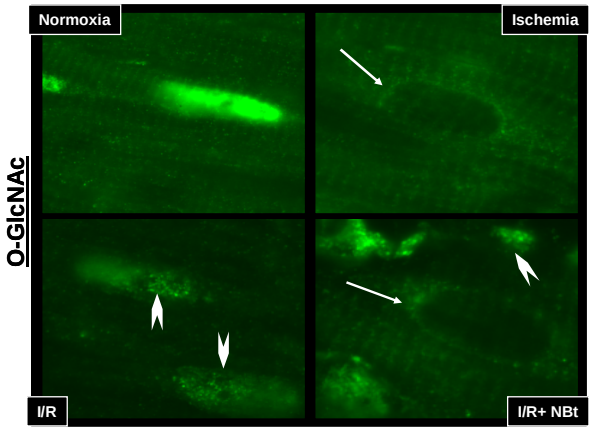

***Figure 14**. Immunohistochemistry of O-GlcNAc (green) and merged images with nuclei staining (blue; DAPI) of rat myocardium (upper panel) and nuclear O-GlcNAcylation (lower panel) after normoxic perfusions (Normoxia); after 20 min zero-flow ischemia (Ischemia); and after 60 min reperfusion with no treatment (I/R) or treatment with 50 µM NAG-Bt (I/R+NBt) at the time of reperfusion. In normoxic hearts (Normoxia), intensity of O-GlcNAc (green) staining is predominantly concentrated in the nuclei of cardiomyocytes. Note that ischemia and ischemia-reperfusion (I/R) lead to prominent changes in nuclear O-GlcNAc distribution with increased punctate (arrow heads) and perinuclear staining of otherwise O-GlcNAc negative nuclei (arrows).*

In normoxic hearts, O-GlcNAc staining was particularly intense within the nuclei of cardiomyocytes, consistent with other cell systems (2, 34, 102). Surprisingly, O-GlcNAc staining exhibited a clear cross-striated pattern through the cytoplasm consistent with Z-line structures in cardiomyocytes (*Fig. 14*).

Ischemia alone had a little effect on overall O-GlcNAc immunofluorescence and striated pattern remained relatively unchanged (*Fig. 14*). However, ischemia-induced changes in nuclear O-GlcNAc distribution were very striking with increased punctate staining and the appearance of O-GlcNAc negative nuclei with O-GlcNAc staining in the perinuclear region of cardiomyocytes (*Fig. 14*). O-GlcNAc negative nuclei with perinuclear staining were not seen in normoxic hearts.

After I/R, there was a marked loss of overall O-GlcNAc fluorescence in both nuclear and cytoplasmic compartments, consistent with decreased O-GlcNAc seen in the immunoblots (*Figs. 8, 12*). There was also a loss of striated structural integrity accompanied with the increased number of punctate and O-GlcNAc negative nuclei showing perinuclear staining (*Fig. 14*).

Administration of NAG-Bt during reperfusion (I/R+NBt) resulted in augmented O-GlcNAc fluorescence compared to that seen in untreated, reperfused hearts (I/R); also consistent with the O-GlcNAc immunoblot data (*Fig. 12*). In the NAG-Bt treated hearts, striated O-GlcNAc staining was preserved. However, nuclear O-GlcNAc staining remained low and the ischemia-induced punctate and perinuclear O-GlcNAc staining were still evident. Thus, while OGA inhibitor increased overall O-GlcNAc fluorescence and helped maintaining structural integrity, including the striated pattern of O-GlcNAc staining in the cytosol; it did not prevent the loss of nuclear O-GlcNAc which remained depressed (*Fig. 14*). Perfusion of normoxic hearts with NAG-Bt did not alter O-GlcNAc distribution in either the nucleus or cytoplasm (data not shown).

OGA inhibitors induced redistribution of O-GlcNAc and OGT was more enhanced in the cytosol following ischemia-reperfusion: We also examined the effects of NAG-thiazolines on the I/R-induced redistribution of O-GlcNAc and OGT by immunoblot analyses. At the end of reperfusion, there was ~50% loss of O-GlcNAc in both nuclear and cytosolic fractions (*Fig. 15A*). Consistent with immunohistochemistry,

50 μM NAG-Bt treatment had no significant effect on nuclear O-GlcNAc, although cytosolic O-GlcNAc levels were significantly increased. Higher concentrations of NAG-Bt (100 μM) and NAG-Ae (50 μM) increased both nuclear and cytosolic O-GlcNAc; however, their effects on nuclear O-GlcNAc levels were blunted compared to the cytosolic levels.

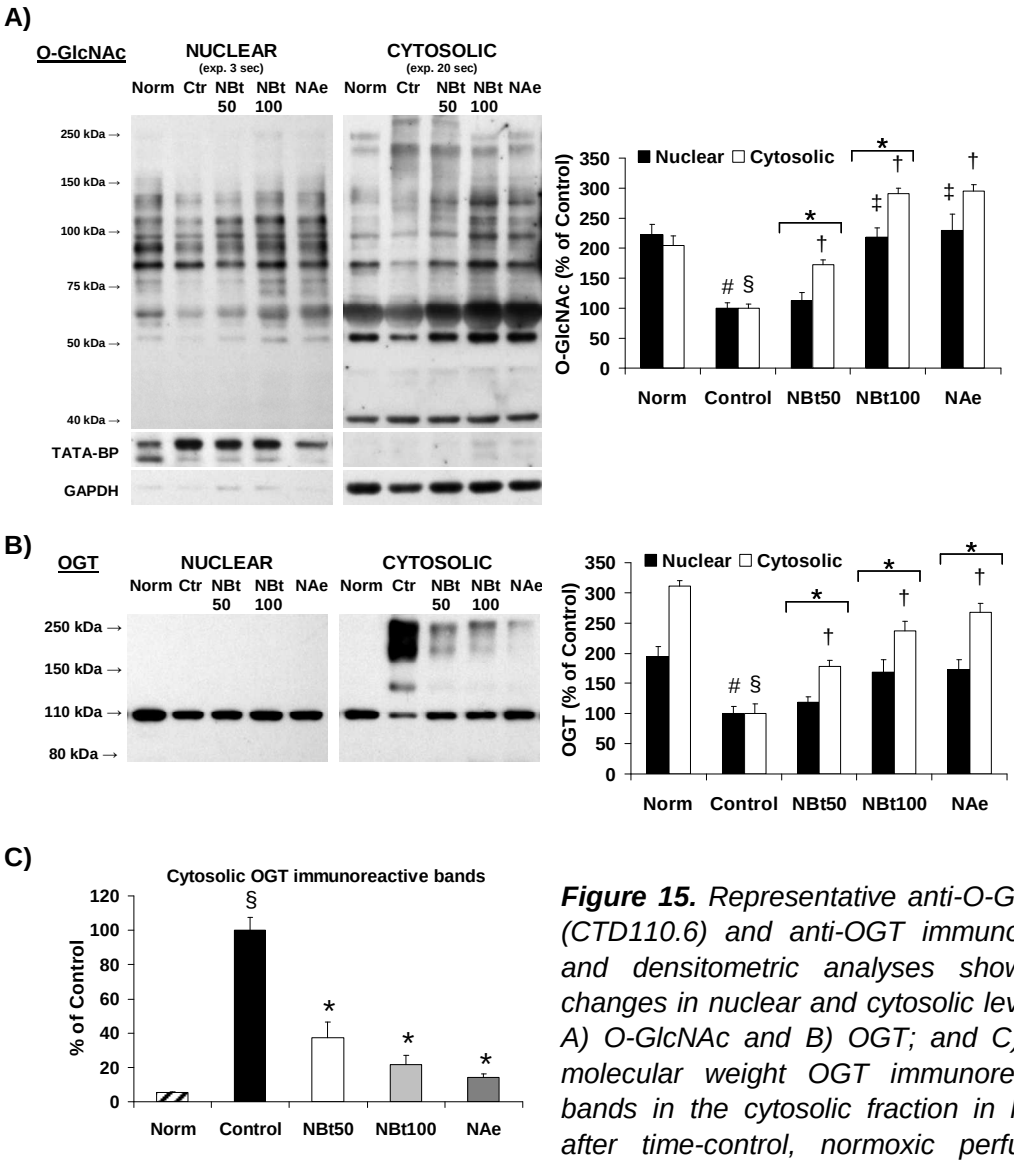

Figure 15. *Representative anti-O-GlcNAc (CTD110.6) and anti-OGT immunoblots, and densitometric analyses show the changes in nuclear and cytosolic levels of A) O-GlcNAc and B) OGT; and C) high molecular weight OGT immunoreactive bands in the cytosolic fraction in hearts after time-control, normoxic perfusions (Norm), and after ischemia-reperfusion in the untreated group (Control) and the treated NBt50, NBt100, NAe groups (n=3-4 hearts/group). TATA-binding protein and GAPDH are shown as purity controls.*
** p<0.05 Nuclear vs. Cytosolic (unpaired t-test)*
† p<0.05 vs. cytosolic Control; ‡ p<0.05 vs. nuclear Control; § p<0.05 vs. cytosolic Norm; # p<0.05 vs. nuclear Norm (one-way ANOVA; Bonferroni)

The loss of O-GlcNAc with I/R was associated with a marked loss of OGT in the nuclear, and in particular, the cytoplasmic fraction (*Fig. 15B*). Interestingly, while OGA

inhibitors attenuated the loss of OGT in the cytosolic fraction, there were no significant effects on nuclear OGT levels. In immunoblots of the nuclear fraction as well as the cytosolic fraction of the Norm group, OGT is apparent as a single band at ~110 kDa (*Fig. 15B*). Following I/R, however, intense OGT immunoreactive bands between 150-250 kDa could be observed in the cytosolic fraction (*Fig. 15B*). OGA inhibitors decreased the intensity of these high molecular weight bands and increased the band of the active OGT (110 kDa) (*Figs. 15B, C*). The absence of high molecular weight OGT bands in the nuclear fraction and their loss with OGA inhibitors suggests that these are OGT aggregates rather than non-specific staining.

2.3. Effects of ischemia, ischemia-reperfusion and selective OGA inhibitor treatments on structural integrity and cardiac Z-line proteins

Cardiac O-GlcNAc-modified proteins are enriched at Z-lines: As shown in *Fig. 14,* striated O-GlcNAc staining in the cytoplasm is localized to the Z-lines in normoxic hearts. Indeed, we found that the cross-striated O-GlcNAc staining is consistent with the patterns seen with desmin and vinculin (*Figs. 16, 17*), two cytoskeletal proteins associated with the Z-lines in cardiomyocytes (58, 65). Co-localization of O-GlcNAc at the Z-lines with desmin and vinculin was confirmed by analysis of changes in relative fluorescence intensity spatially across the cell (*Figs. 16A, B*).

The Z-line region is frequently viewed as playing primarily a passive mechanical role in force transmission; however, it is increasingly recognized that the Z-line is a critical component in regulating cardiomyocyte function by mediating the responses to hemodynamic and mechanical stresses via a number of signaling-related proteins localized at the Z-line (58, 96). The enrichment of O-GlcNAc-modified proteins at Z-lines suggests that cardioprotective effects associated with increased O-GlcNAcylation could be somewhat related to advantageous changes of the Z-line structures in response to I/R.

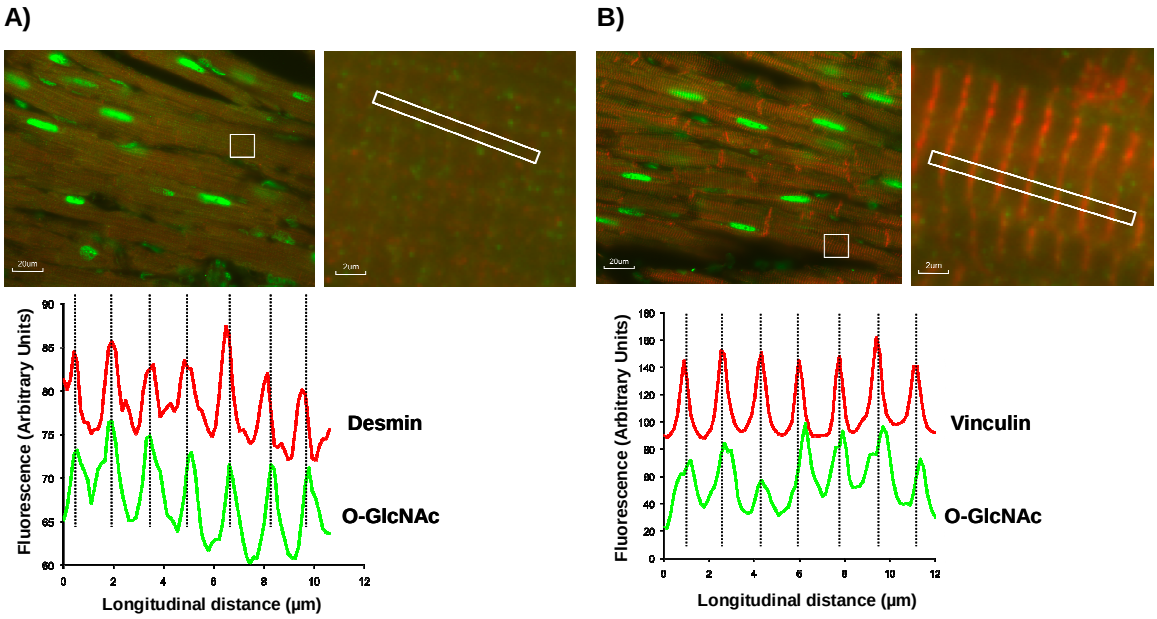

Figure 16. *Co-localization of O-GlcNAc with A) desmin and B) vinculin at the Z-lines in cardiomyocytes. Fluorescent images of normoxic hearts were taken simultaneously and merged. The same region of interest was chosen on both red (desmin or vinculin) and green (O-GlcNAc) images and the plot profiles of longitudinal sections (perpendicular to the Z-lines) were analyzed using ImageJ software. The plot profiles clearly demonstrate the coincidence of O-GlcNAc peaks with both desmin and vinculin signals.*

OGA inhibitors attenuated the ischemia-reperfusion induced changes of Z-line proteins: Although ischemia alone had a little effect on desmin and vinculin fluorescence; following I/R there was a loss of overall intensity in desmin fluorescence, and a loss of association with the Z-line showing reorganization into a longitudinal pattern (*Fig. 17A*). While the overall structural disruption was apparent, vinculin localization and intensity remained relatively unchanged following I/R (*Fig. 17B*). We found that OGA inhibition substantially attenuated the disruption of myocardial structure and helped to maintain the striated pattern of both desmin and vinculin and their co-localization with O-GlcNAc (*Figs. 17A, B*).

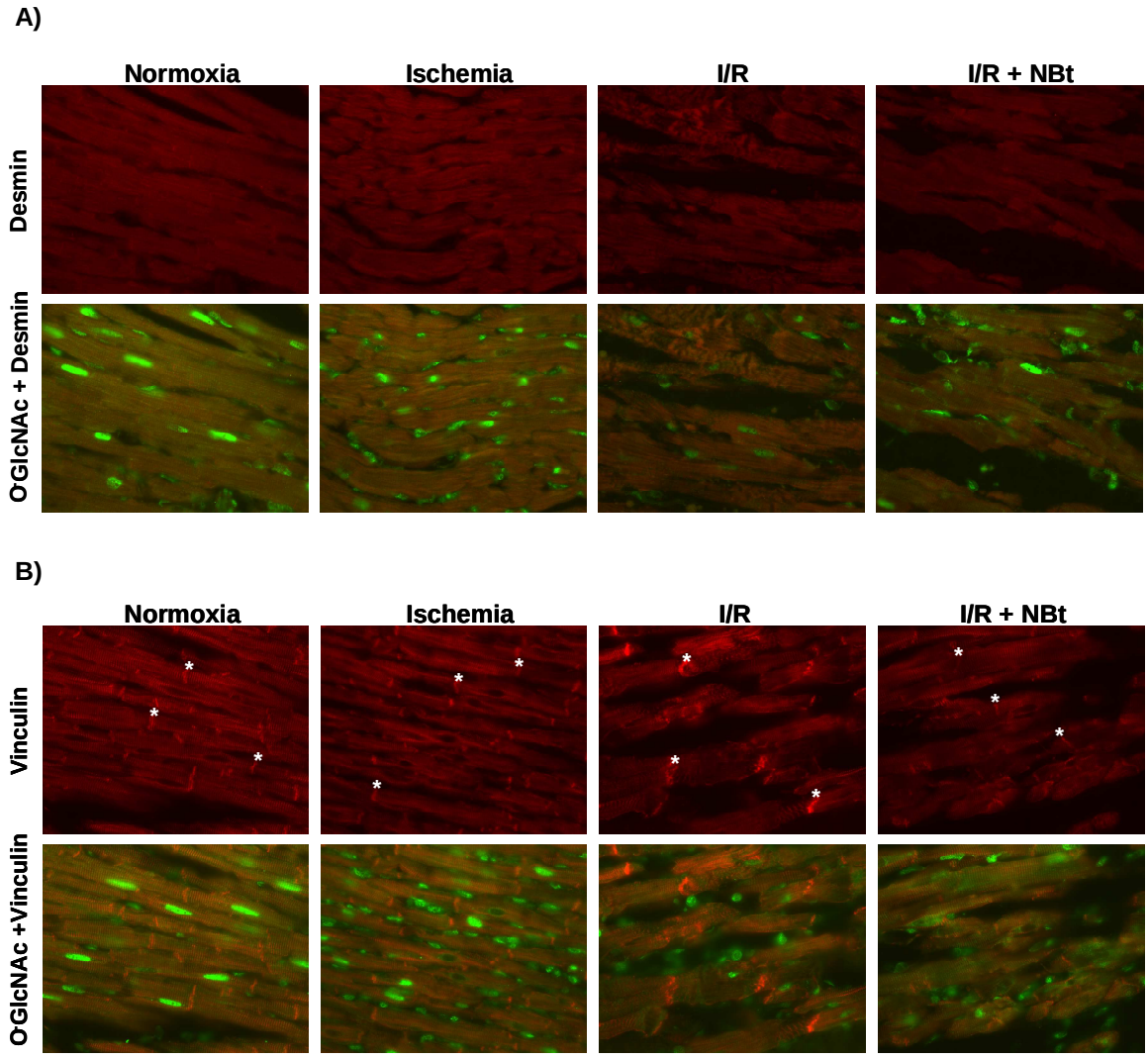

Figure 17. *A) Desmin immunohistochemistry (red) and its co-localization with O-GlcNAc (green) at the Z-line; and B) Vinculin immunohistochemistry (red) and its co-localization with O-GlcNAc (green) at the Z-line, but not the intercalated discs (*) in rat myocardium after normoxic perfusions (Normoxia); after 20 min zero-flow ischemia (Ischemia); and at the end of 60 min reperfusion with no treatment (I/R) and treatment with 50 μM NAG-Bt (I/R+NBt). Note that following ischemia-reperfusion (I/R) there is a loss of structural integrity as well as the co-localization of desmin (A) and vinculin (B) with O-GlcNAc, which was markedly attenuated in NAG-Bt-treated hearts (I/R+NBt).*

Consistent with immunohistochemistry, immunoblot analyses of whole tissue lysates showed that I/R resulted in ~2-fold loss of total desmin (*Fig. 18A*). The decrease in desmin was particularly evident (>2-fold) in the membrane fraction (*Fig. 19C*), both of which were reversed by OGA inhibitors. At the end of reperfusion, there was also a marked loss (>3-fold) of overall O-GlcNAc in the membrane fraction, which was also reversed by OGA inhibitors (*Fig. 19A*).

We found no changes in total tissue levels of vinculin in any of the groups, even in the I/R untreated Control group (*Fig. 18B*). However, OGA inhibitors blunted the I/R-induced increases in vinculin phosphorylation at Tyr(822) (*Fig. 18C*). In contrast, at the end of reperfusion there was a significant loss of total vinculin in the membrane fraction (*Fig. 19B*); however, it was not prevented by OGA inhibitors. While NAG-Bt and NAG-Ae also attenuated Tyr(822) phosphorylation of the membrane-associated vinculin following I/R (*Fig. 19B*). Although vinculin is one of the best characterized interacting proteins of focal adhesion complexes, the physiological role of vinculin phosphorylation in the heart is poorly characterized. In cardiomyocytes, disruption of interacting proteins at focal adhesion complexes has been shown to exacerbate ischemic injury (130). Thus, it is possible that decreased vinculin phosphorylation could contribute to the preservation of focal adhesions thus the structural integrity seen with OGA inhibitors after I/R.

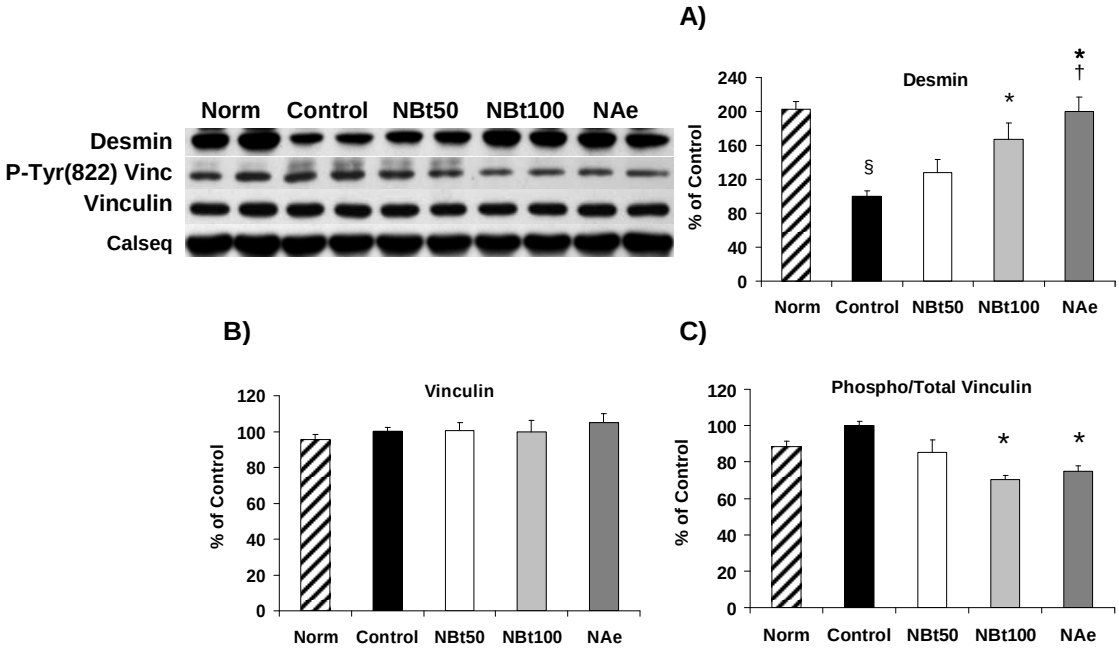

Figure 18. *Immunoblot analyses of A) total desmin, B) total vinculin, and C) phospho-Tyr(822) vinculin levels in cardiac whole tissue lysates (n=3-4 hearts/group) after time-control, normoxic perfusions (Norm) and after ischemia-reperfusion in untreated hearts (Control) and hearts treated with 50 μM NAG-Bt (NBt50), 100 μM NAG-Bt (NBt100) and 50 μM NAG-Ae (NAe). Data are expressed as % of Control group. Results are normalized to calsequestrin levels and are expressed as % of Control group.*
*§ p<0.05 vs. Norm, * p<0.05 vs. Control; † p<0.05 vs. NBt50 (one-way ANOVA; Bonferroni)*

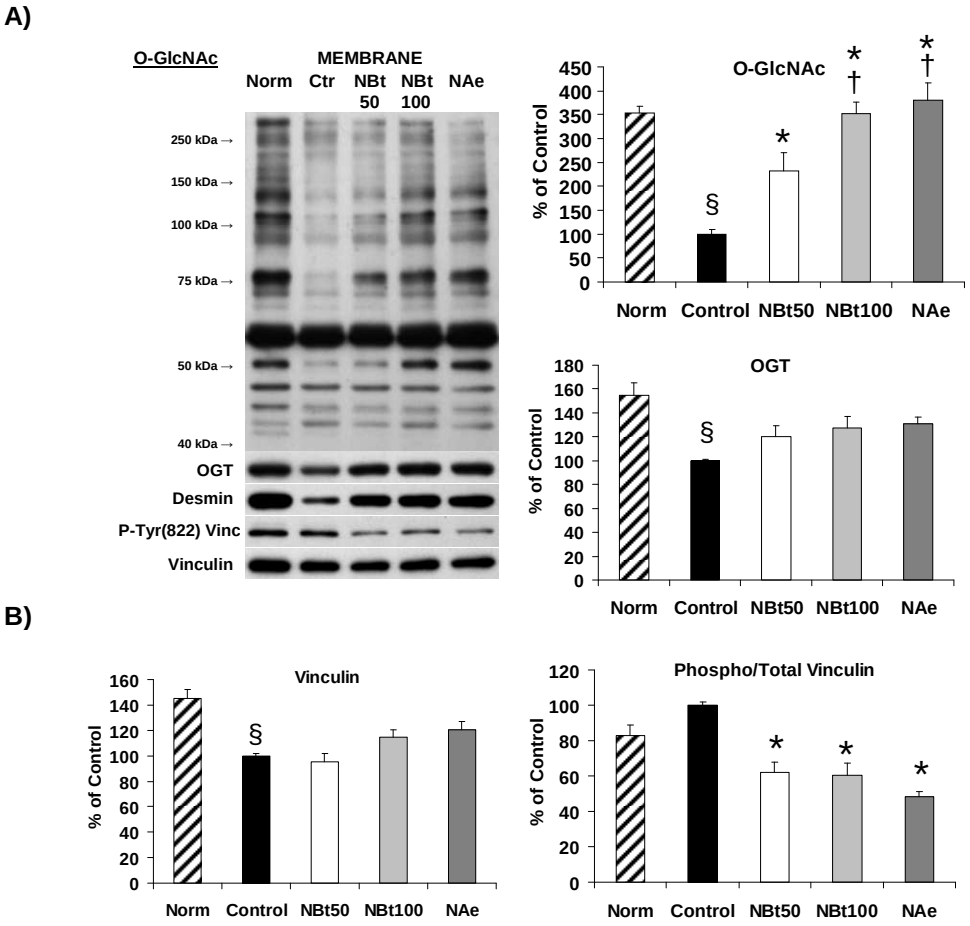

Figure 19. *Immunoblot analyses of A) O-GlcNAc, OGT; B) phospho-Tyr(822) vinculin, total vinculin; and C) desmin in the membrane fraction (n=3 hearts/group) of time-control, normoxic hearts (Norm), and hearts after ischemia-reperfusion in the untreated (Control) and NAG-thiazoline-treated groups (NBt50, NBt100, NAe). Data are expressed as % of Control group.*

*§ p<0.05 vs. Norm; * p<0.05 vs. Control; † p<0.05 vs. NBt50 (one-way ANOVA; Bonferroni)*

2.4. Effects of ischemia, ischemia-reperfusion and selective OGA inhibitor treatments on specific cardiac proteins targeted by O-GlcNAc modification

We purposed to determine whether ischemia and/or reperfusion resulted in changes in O-GlcNAc levels on specific cardiac proteins and whether altered proteins were potential targets for O-GlcNAc modification. Before ischemia, there were no significant differences in baseline cardiac functions between any of the groups (data not shown). We found that ischemia, after as little as 10 min, significantly increased

overall O-GlcNAc (~60%) compared to time-matched normoxic hearts (*Fig. 20*). This increase in O-GlcNAc during ischemia was accompanied by a significant loss in ATP and increase in UDP-HexNAc levels (*Figs. 21A, B*), consistent with earlier reports (46).

At the end of 60 min reperfusion, there was a significant decrease in overall cardiac O-GlcNAc compared to the ischemic (non-reperfused) hearts (*Fig. 20*), similarly to that after longer ischemia as shown by immunohistochemistry (*Fig. 14*). The I/R-induced mitigated O-GlcNAcylation was associated with suppressed UDP-HexNAc levels compared to the ischemic hearts, and ATP levels were not restored compared to the normoxic hearts (*Fig. 21*).

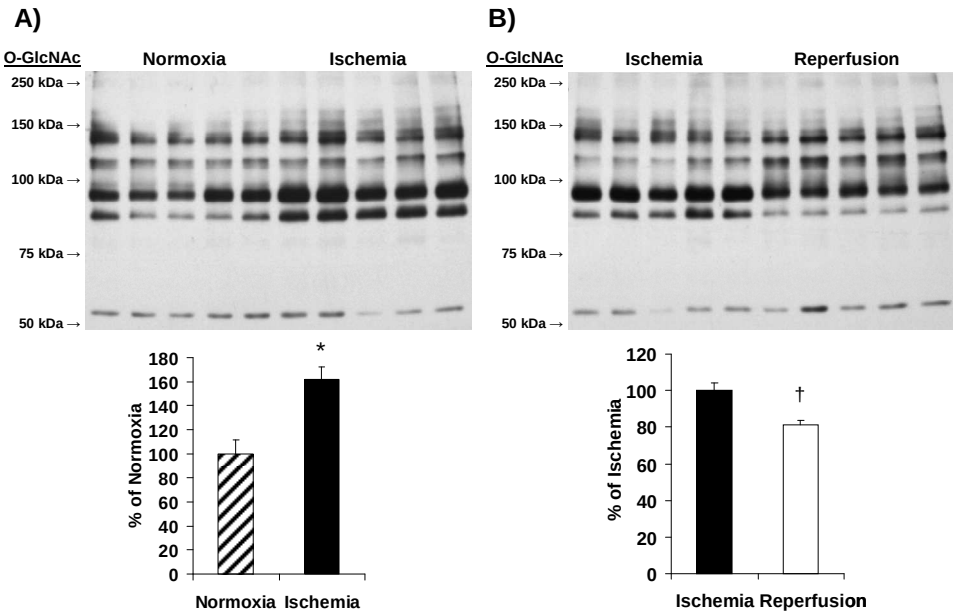

Figure 20. *Effects of A) ischemia and B) ischemia-reperfusion on overall cardiac O-GlcNAc levels. After 30 min stabilization, isolated hearts were either perfused as time-matched controls for a total of 40 min normoxic perfusion (Normoxia) or subjected to 10 min no-flow ischemia (Ischemia), or 10 min no-flow ischemia followed by 60 min reperfusion (Reperfusion). Data were analyzed for the entire lane of O-GlcNAc (n=5-5 hearts/group). Note that there is a differential response of individual bands, suggesting that O-GlcNAc-signaling targets different protein populations during ischemia and reperfusion.*
** p<0.05 vs. Normoxia; † p<0.05 vs. Ischemia (unpaired t-test)*

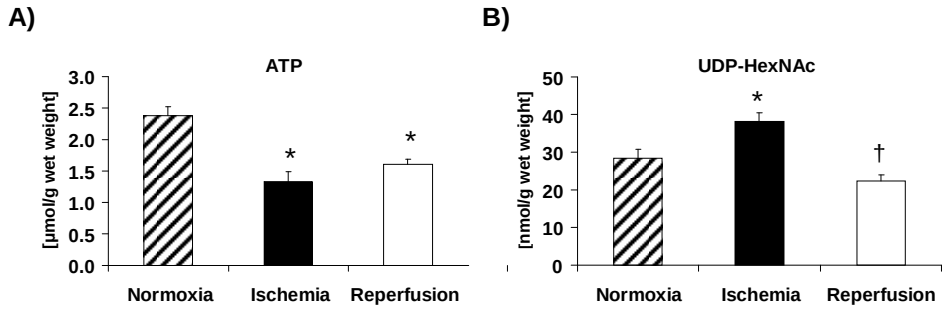

Figure 21. *Effects of ischemia and ischemia-reperfusion on A) ATP and B) UDP-HexNAc levels in time-matched normoxic hearts (Normoxia, n=5); and hearts subjected to 10 min no-flow ischemia (Ischemia, n=7); and 60 min reperfusion after 10 min ischemia (Reperfusion, n=5).*
** p<0.05 vs. Normoxia; † p<0.05 vs. Ischemia (unpaired t-test)*

As shown in *Fig. 22*, densitometric analyses of individual O-GlcNAc immunoreactive protein bands (i.e. I-VIII lanes) revealed that after ischemia there were significant increases in O-GlcNAc of protein bands between 75-100 kDa at VI and VII lanes compared to normoxia (*Fig. 22A*), both of which were subsequently decreased following reperfusion (*Fig. 22B*). At the end of reperfusion, a protein band (V lane) between 100 kDa-150 kDa showed significantly higher O-GlcNAc compared to ischemia (*Fig. 22B*). Identification of these groups of proteins exhibiting altered O-GlcNAc levels in response to ischemia and/or reperfusion were analyzed by MALDI-TOF Mass Spectrometry. MASCOT database search of *in-gel* digested peptide sequences resulted in several potential protein identifications (*Fig. 22C*); however, three cardiac proteins showed relatively high coverage, certainty hit and correct molecular weights. Interestingly, one of these proteins observed in the O-GlcNAc band that increased only with reperfusion and was elevated compared to both ischemia and normoxia (V lane) was identified as the Z-line protein Vinculin (X1, *Fig. 22C*). The proteins of O-GlcNAc positive bands that were significantly increased during ischemia and decreased following reperfusion (VI and VII lanes) were identified as Glycogen phosphorylase b (X2) and mitochondrial Aconitase (X3) (*Fig. 22C*).

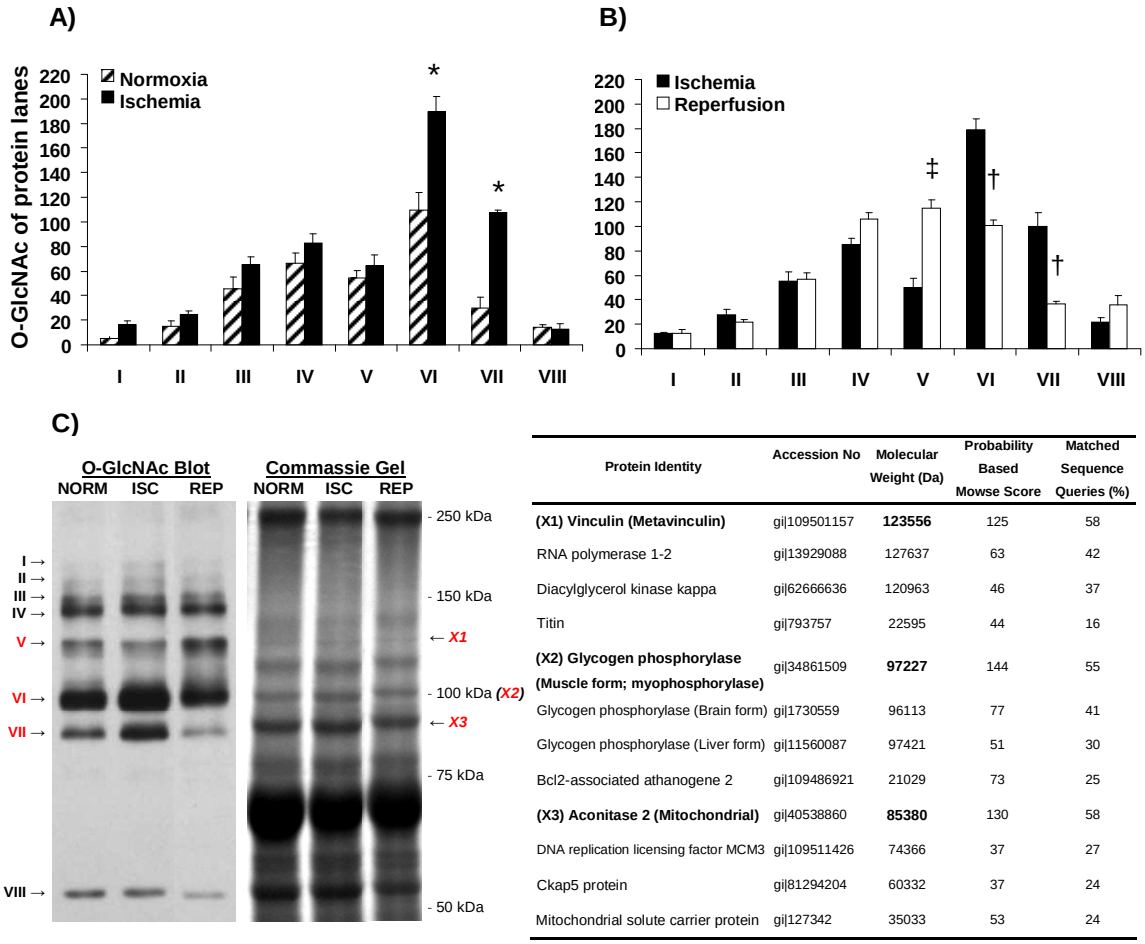

Protein Identity	Accession No	Molecular Weight (Da)	Probability Based Mowse Score	Matched Sequence Queries (%)
(X1) Vinculin (Metavinculin)	gi|109501157	**123556**	125	58
RNA polymerase 1-2	gi|13929088	127637	63	42
Diacylglycerol kinase kappa	gi|62666636	120963	46	37
Titin	gi|793757	22595	44	16
(X2) Glycogen phosphorylase (Muscle form; myophosphorylase)	gi|34861509	**97227**	144	55
Glycogen phosphorylase (Brain form)	gi|1730559	96113	77	41
Glycogen phosphorylase (Liver form)	gi|11560087	97421	51	30
Bcl2-associated athanogene 2	gi|109486921	21029	73	25
(X3) Aconitase 2 (Mitochondrial)	gi|40538860	**85380**	130	58
DNA replication licensing factor MCM3	gi|109511426	74366	37	27
Ckap5 protein	gi|81294204	60332	37	24
Mitochondrial solute carrier protein	gi|127342	35033	53	24

Figure 22. *Effects of A) ischemia and B) ischemia-reperfusion on individual O-GlcNAc protein bands at I-VIII lanes in time-matched normoxic hearts (NORM); and in hearts after 10 min no-flow ischemia (ISC), and at the end of 60 min reperfusion after 10 min no-flow ischemia (REP). Densitometric data are expressed as arbitrary units (n=5-5 hearts/groups). C) Representative anti-O-GlcNAc immunoblot and the Commassie gel demonstrate corresponding protein bands in I-VIII lanes. Those proteins bands that were significantly altered by ischemia and reperfusion (lanes V, VI, VII) were subjected to MALDI-TOF protein identifications. Results of X1, X2 and X3 protein annotations and identities are listed in the table.*
** p<0.05 vs. Normoxia; † p<0.05 vs. Ischemia (unpaired t-test)*

Total protein contents of Vinculin (Vinc), Glycogen phosphorylase b (GP), and mitochondrial Aconitase (ACO2) did not differ in response to ischemia or reperfusion (*Fig. 23A*). Vinc, GP, and ACO2 were subsequently immunoprecipitated and all three proteins were positive with anti-O-GlcNAc antibody (*Fig. 23B*), suggesting that these identified proteins are potential targets for O-GlcNAc modification. Moreover, immunoprecipitated Vinc, GP, and ACO2 showed consistent changes in O-GlcNAc levels with stress conditions, as we found increased O-GlcNAc of Vinc only after

reperfusion, while both GP and ACO2 showed increased O-GlcNAc with ischemia and decreased O-GlcNAc with reperfusion (*Fig. 23B*).

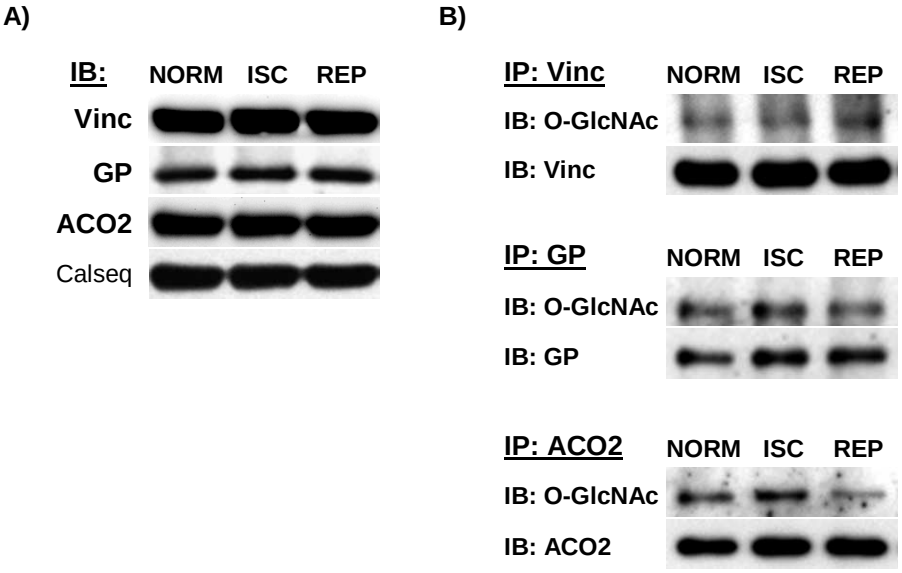

Figure 23. *A) Representative immunoblots show total protein contents of Vinculin (Vinc), Glycogen phosphorylase (GP), and Aconitase 2 (ACO2) in whole cardiac tissue lysates of normoxic hearts (NORM); and hearts after 10 min no-flow ischemia (ISC) and following 60 min reperfusion after 10 min no-flow ischemia (REP). Calsequestrin (Calseq) is shown as the loading control. B) Subsequent immunoprecipitations of these identified proteins followed by O-GlcNAc immunoblots.*

We next determined whether OGA inhibition, which we showed to reverse the I/R-induced loss of overall O-GlcNAc, could also augment the O-GlcNAc levels on these identified proteins and whether these proteins were co-immunoprecipitated with OGT. We found no differences in total protein levels of Vinc, GP or ACO2 in whole tissue lysates after I/R or the OGA inhibitor treatments with NAG-Bt and NAG-Ae (*Fig. 24A*). OGT was markedly decreased with I/R which was reversed with OGA inhibitors (*Fig. 24A*), similar that seen earlier in the nuclear and cytsolic fractions (*Fig. 15*).

As shown in *Fig. 24B*, despite equal protein amounts of immunoprecipitated Vinc, GP, and ACO2, there was an I/R-induced loss of O-GlcNAc on all three proteins and OGA inhibitors prevented this loss of O-GlcNAcylation of Vinc, GP, and ACO2. In addition, incubation with β-N-acetylglucosamine completely competed away the anti-O-GlcNAc antibody, indicating that Vinc, GP and ACO2 are most likely subjects to O-GlcNAc modification.

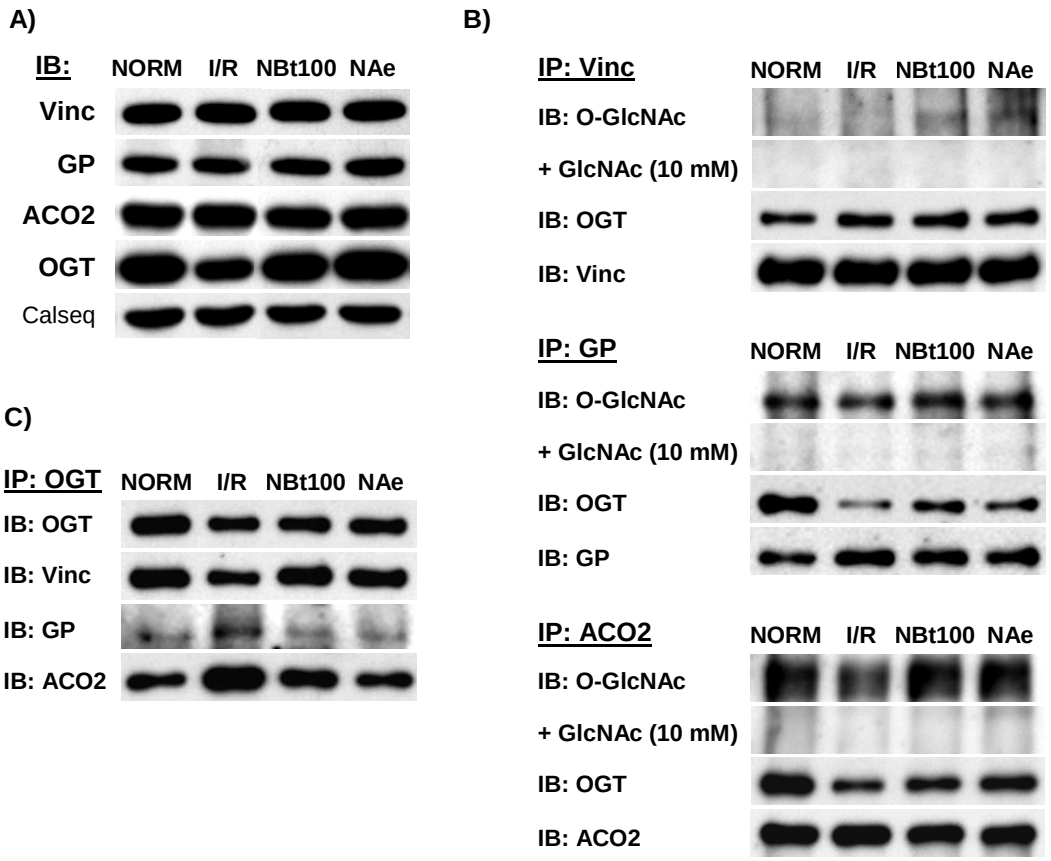

Figure 24. *A) Representative immunoblot on total protein levels of Vinculin (Vinc), Glycogen phosphorylase (GP), Aconitase 2 (ACO2) and OGT in whole cardiac tissue lysates of hearts after time-control (110 min) normoxic perfusions (NORM), and hearts after 20 min ischemia followed by 60 min reperfusion (I/R) and treated with 100μM NAG-Bt (NBt100) and 50μM NAe (NBt50) during 60 min reperfusion. Calsequestrin (Calseq) is shown as the loading control. B) Immunoprecipitation of identified proteins followed by O-GlcNAc and OGT immunoblots. Specificity of O-GlcNAc antibody was confirmed by co-incubation with 10 mM β-N-acetylglucosamine (GlcNAc). C) Immunoprecipitation of OGT followed by Vinc, GP and ACO2 immunoblots.*

Furthermore, Vinc, GP, and ACO2 were all co-immunoprecipitated with OGT (*Fig. 24B*). While, there were no differences in immunoprecipitated protein contents of Vinc, GP, and ACO2 after I/R or OGA inhibitor treatments, we found that lower amounts of OGT could be pulled down with GP and ACO2 after I/R, but not with vinculin. This is consistent with the loss of OGT following I/R and could contribute to decreased O-GlcNAcylation; however, we do not have readout on OGT activity. Strikingly, these results were recapitulated by showing that immunoprecipitation of OGT resulted in associations with Vinc, GP, and ACO2, and that higher levels of GP and ACO2 could be pulled down with OGT following I/R (Fig. *24C*).

To determine whether I/R and OGA inhibitors had impact on ACO2 enzyme, which is known to be sensitively inactivated by ROS, we analyzed the mitochondrial changes of ACO2 protein levels and assayed its activity (*Fig. 25*). We found that both ACO2 and OGT decreased with I/R in the mitochondrial fraction, both of which could be prevented by OGA inhibitors. While changes were alike in OGT levels in the post-mitochondrial fraction after I/R, there was a redistribution of ACO2 leading to increased levels in the post-mitochondrial fraction, which was largely attenuated by OGA inhibitor treatments (*Fig. 25A*).

At the end of I/R, aconitase activity significantly decreased in the myocardial tissue lysates from untreated Control hearts compared to time-control normoxic hearts, while treatments with both NAG-Bt and NAG-Ae prevented the I/R-induced loss of aconitase activity (*Fig. 25B*).

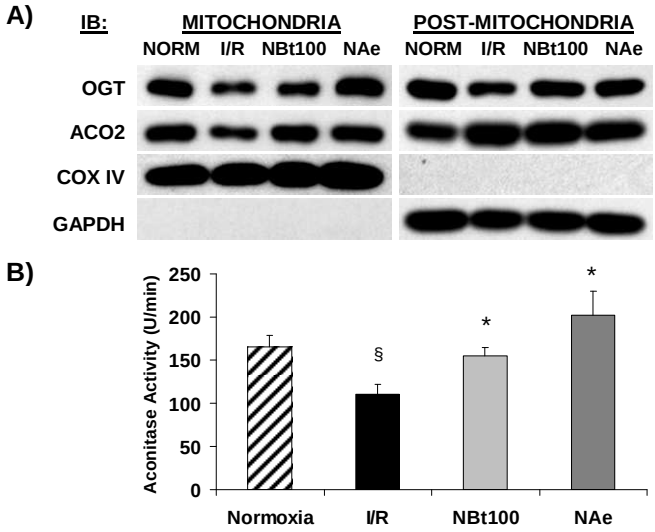

Figure 25. *A) Representative immunoblots show Aconitase 2 (ACO2) and OGT protein levels in the mitochondrial and post-mitochondrial (microsomal and cytosolic) fractions of cardiac tissue lysates from hearts after time-control (110 min) normoxic perfusions (NORM), and after 20 min ischemia followed by 60 min reperfusion with no treatment (I/R) or treatments with 100μM NAG-Bt (NBt100) and 50μM NAe (NBt50) during 60 min of reperfusion. GAPDH and COXIV are shown as purity controls. B) Aconitase enzyme activity was measured in cardiac tissue lysates (15 μg protein) by the conversion of citrate to α-ketoglutarate coupled to the reduction of NADP and was detected spectrophotometrically (340 nm) where the initial linear change was recorded.*
*§ p<0.05 vs. Normoxia; * p<0.05 vs. I/R (Dunnett)*

3. Investigations on the role of increased HBP flux and protein O-GlcNAcylation, micro-inflammatory state and oxidative stress as contributing factors to the pathogenesis of diabetes-related complications and chronic kidney disease.

3.1. *Ex vivo* experiments on the effects of increased HBP flux and protein O-GlcNAcylation on the regulation of cardiac metabolism.

Diabetes is known to increase protein O-GlcNAcylation in several tissue types, including kidney, cardiac tissue. An early consequence of diabetes on the heart is the imbalance of increased fatty acid oxidation and suppressed glucose metabolism, which contributes to the development of cardiac dysfunctions (e.g. diabetic cardiomyopathy). Activation of the HBP and protein O-GlcNAcylation with glucosamine has been shown to mimic some of the diabetes induced adverse changes on the heart; however, the effect on cardiac metabolism is unknown. Therefore, our goal was to determine whether glucosamine by increasing the HBP flux and O-GlcNAc levels resulted in metabolic dysregulation that characteristic of the diabetic heart. We subsequently examined the role of AMPK, ACC, and fatty acid transporter (FAT)/CD36 in the background of increased in fatty acid oxidation seen with glucosamine and that whether increased membrane-associated FAT/CD36 could be a direct result of O-GlcNAc modification.

Materials and methods:

Materials: Chemicals were obtained from Sigma (St. Louis, MO), unless otherwise noted. ^{13}C-labeled substrates were obtained from Cambridge Isotope Laboratories.

Animals: Non-fasted, 300-350 g Sprague Dawley male rats (Charles Rivers Laboratories) were used.

Isolated heart perfusions and experimental groups: After anesthesia (100 mg/kg ketamine hydrochloride i.p., Lloyd Laboratories) animals were sacrified, hearts were rapidly removed and perfused retrogradely under standard perfusion conditions as described in *Chapter 2*. The perfusion KHB buffer contained (in mM) glucose 5.0, lactate 1.0, pyruvate 0.1, palmitate 0.32, glutamine 0.5, and was supplemented with

3% BSA (fatty acid free; Serologicals Proteins Inc.), and 50 μU/mL insulin (NovoNordisk). All hearts were paced at 320 beats/min rate during the whole experiment. Hearts were assigned to one of six groups and perfused for 60 min under normoxic conditions with: 1) 0 mM glucosamine (n=8); 2) 0.05 mM glucosamine (n=5); 3) 0.1 mM glucosamine (n=8); 4) 1.0 mM glucosamine (n=4); 5) 5.0 mM glucosamine (n=8); and 6) 10.0 mM glucosamine (n=7).

^{13}C-isotopomer analyses: Hearts were perfused with [U-^{13}C]-palmitate, [3-^{13}C]-lactate, and [2-^{13}C]-pyruvate for the final 40 min of protocol. At the end of perfusions, hearts were freeze-clamped, acid extracted and ^{13}C-NMR isotopomer analyses were performed, as previously described (71), in order to determine the relative contribution of substrates to total acetyl-CoA entering the tricarboxylic acid (TCA) cycle; as this fraction originates from unlabeled, [1,2 ^{13}C]-, [2-^{13}C]- and [1-^{13}C]-acetyl-CoA originating from unlabeled glucose, [U-^{13}C]-palmitate, [3-^{13}C]-lactate, and [2-^{13}C]-pyruvate respectively. Chatham et al. (24) previously showed that under these perfusion conditions in the isolated rat heart, there is negligible contribution from endogenous triglycerides to unlabeled acetyl-CoA formation.

Determination of lactate efflux and uptake rates: ^{1}H-NMR spectroscopy was used to determine the ratio of unlabeled lactate formed by the exogenous glucose or endogenous glycogen and [3-^{13}C]-lactate added to the perfusate. These data, multiplied by the total lactate concentration in the effluent and coronary flow, were used to determine the rates of exogenous [3-^{13}C]-lactate uptake and unlabeled endogenously produced lactate efflux as described in detail elsewhere (71).

Immunoblot analyses: Frozen heart tissue powder was homogenized in T-PER (Pierce) as previously described for O-GlcNAc in *Chapter 2*. For ACC and AMPK detection, lysis buffer containing (in mM) Tris (pH: 7.4) 50.0, mannitol 250.0, EDTA 1.0, EGTA 1.0, 10 (w/v)% glycerol, DTT 1.0, NaF 1.0, Na-pyrophosphate 5.0, and 2.5 (v/v)% PIC was used, and homogenates were centrifuged at 9,000 g, for 5 min, at 4ºC. Proteins were separated by SDS-PAGE and transferred onto PVDF membrane (Pall). Membranes were probed for O-GlcNAc (1:2500; CTD110.6, UAB), phospho-Ser(79) ACC and total ACC, phospho-Thr(172) AMPK-α and total AMPK-α (1:1000; Cell

Signaling). After incubation with appropriate secondary antibodies blots were visualized by ECL method (Pierce).

Membrane associated FAT/CD36 levels: The preparation of cardiac membrane fraction and Western blot of proteins by protocols described in *Chapter 2* were used. Blots were immunostained with antibodies against FAT/CD36 (1:1000; Cascade Biosciences), and pan-cadherin (1:1000; Abcam) as the loading and purity control for the membrane fraction.

Immunoprecipitation: Frozen heart tissue was homogenized to obtain whole tissue or membrane fraction lysates, as described in *Chapter 2*. Immunoprecipitation as detailed in *Chapter 2* was performed using anti-CD36 antibody (sc-9154, Santa Cruz). Immunoblots were probed with CTD 110.6 (1:1000), anti-CD36 (1:500), and anti-OGT (DM-17; 1:1000, Sigma) antibodies, followed by incubation with HRP-conjugated secondary antibodies and ECL visualization. The specificity of the O-GlcNAc antibody was confirmed by co-incubation with 10 mM β-N-acetylglucosamine (29).

HPLC analysis: ATP and UDP-HexNAc levels were determined by HPLC method, as described in *Chapter 2*.

Statistical analysis: Data are presented as means ± SE. Differences between experimental groups were evaluated with one-way ANOVA (Dunnett`s posthoc test) or unpaired t-test using SPSS 13.0 (SPSS Inc). Statistically significant differences between groups were defined as $p < 0.05$.

Results:

3.1.1. Acute effects of glucosamine on the HBP flux and O-GlcNAc levels, ATP levels and cardiac substrate utilization

Glucosamine had no adverse effects on cardiac function: Addition of 0.05, 0.1, 1.0, 5.0 or 10.0 mM glucosamine at the time of 60 min normoxic perfusion did not alter cardiac functions assessed by RPP, ± dp/dt or coronary flow compared to the control hearts perfused without glucosamine (0 mM) (*Table 2*).

Table 2. Cardiac performance of isolated rat hearts perfused in the absence (0 mM) and presence of 0.05, 0.1, 1, 5, 10 mM glucosamine

Groups (N)	**0 mM** *(8)*	**0.05 mM** *(5)*	**0.1 mM** *(10)*	**1 mM** *(4)*	**5 mM** *(8)*	**10 mM** *(4)*
Coronary Flow (mL/min)	11.5 ± 0.8	12.2 ± 0.6	11.1 ± 0.4	11.5 ± 0.7	12.5 ± 0.6	13.5 ± 0.9
+ dP/dt (mmHg/s)	4,125 ± 225	4,101 ± 323	3,515 ± 149	4,021 ± 357	3,626 ± 231	3,595 ± 205
- dP/dt (mmHg/s)	2,054 ± 140	2,222 ± 191	1,846 ± 85	1,998 ± 177	1,882 ± 91	2,076 ± 295
RPP (mmHg/min)	29,058 ± 1,042	33,165 ± 2,256	28,033 ± 1,101	29,826 ± 2,443	28,692 ± 1,525	31,142 ± 1,303

Glucosamine had no effect on cardiac functions (means ± SE) of isolated rat hearts perfused with 0.05 (n=5), 0.1 (n=10), 1 (n=4), 5 (n=8) and 10 mM (n=7) glucosamine for 60 min compared to the untreated control hearts (0 mM; n=8).
N, number of hearts; ± dP/dt, maximum and minimum rate of left ventricular developed pressure; RPP, rate pressure product (left ventricular developed pressure x heart rate); (NS: one-way ANOVA; Dunnett)

Glucosamine augmented cardiac O-GlcNAc and UDP-GlcNAc levels and had no impact on ATP levels: Immunoblot analyses indicated a clear dose response with glucosamine treatments on augmented O-GlcNAc levels (*Figs. 26A, B*). Perfusion with as low as 0.1 mM glucosamine resulted in ~50% increase in O-GlcNAc and maximal increase (~2-fold) was at 5 mM glucosamine concentration. UDP-HexNAc levels showed similar response to glucosamine perfusions as O-GlcNAc levels (*Fig. 26C*). There was a significant increase in UDP-HexNAc with as little as 0.1 mM glucosamine and maximal increase (~2-fold) was seen with 1 mM glucosamine, indicating increased flux through the HBP. While others in cell culture studies reported that high doses of glucosamine led to decreased ATP levels (76), here in the isolated perfused heart we found no effect of glucosamine on ATP levels at any concentration (*Fig. 26D*).

Glucosamine significantly increased palmitate oxidation and decreased lactate oxidation: Using ^{13}C-isotopomer analyses we found that glucosamine significantly increased palmitate oxidation at all concentrations compared to the control hearts perfused without glucosamine (0 mM) (*Fig. 27A*), and this was accompanied by a concomitant decrease in total carbohydrate oxidation (*Fig. 27A*). Even the lowest glucosamine concentration (0.05 mM) significantly increased palmitate oxidation and decreased total carbohydrate oxidation that reached a maximal response at 0.1 mM glucosamine (*Fig. 27A*).

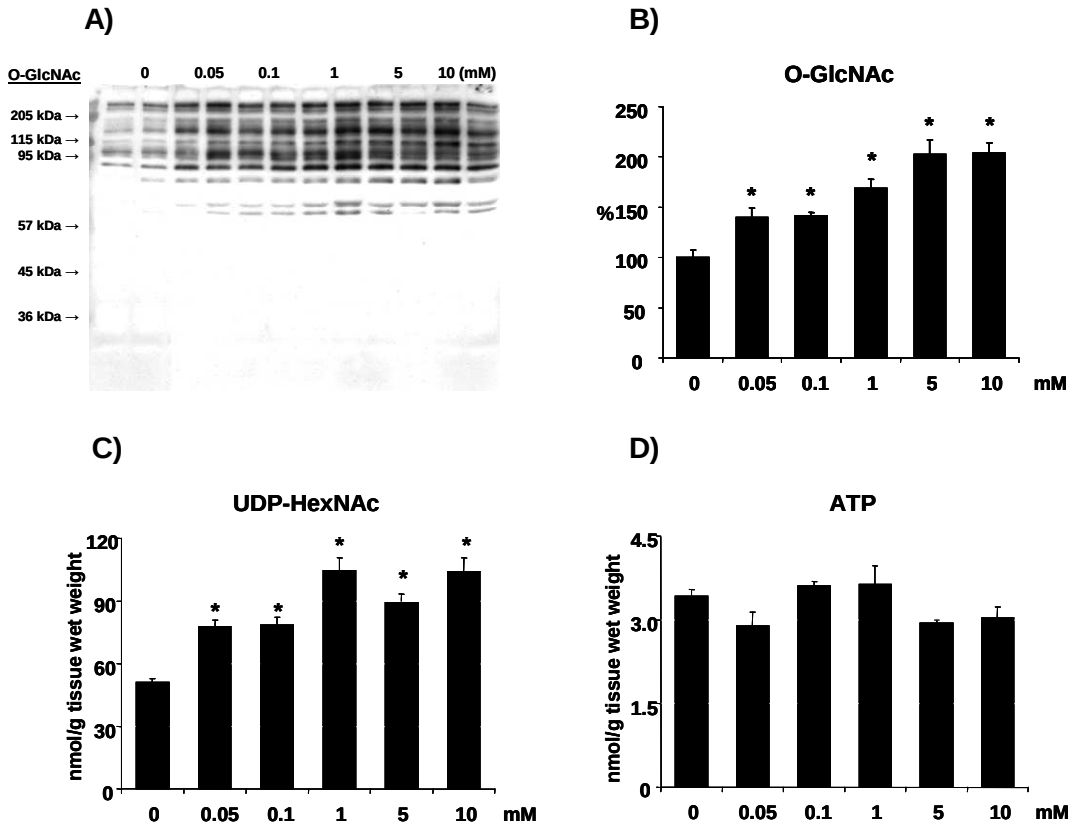

Figure 26. *Effects of glucosamine on A-B) overall cardiac O-GlcNAc levels, C) UDP-HexNAc levels, and D) ATP concentrations. [Immunoblot: 0 mM (n=8), 0.05 mM (n=5), 0.1 mM (n=9), 1 mM (n=4), 5 mM (n=8), 10 mM (n=7); HPLC: 0 mM (n=4), 0.05 mM (n=5), 0.1 mM (n=5), 1 mM (n=4), 5 mM (n=3), 10 mM (n=3)*]
** p<0.05 vs 0 mM (one-way ANOVA; Dunnett)*

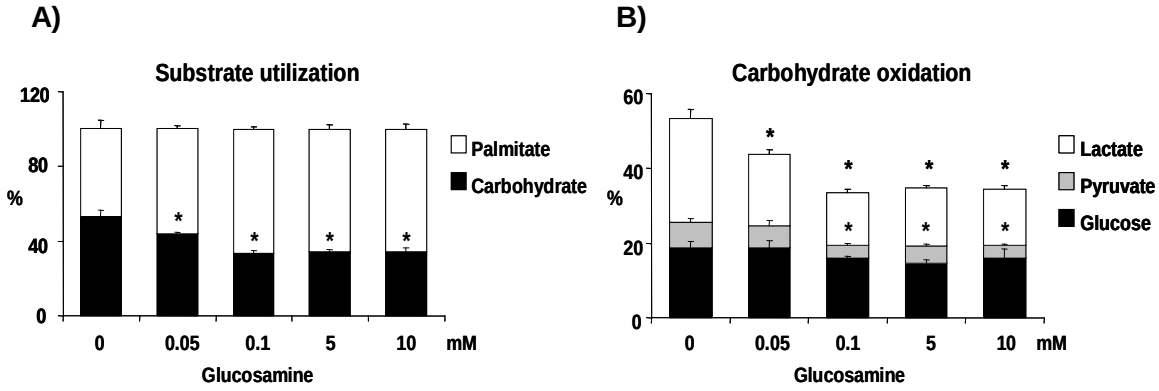

Figure 27. *A) Glucosamine treatment for 60 min significantly increased palmitate oxidation and decreased total carbohydrate utilization at all concentrations compared to the untreated control hearts. There was no further increase in fatty acid utilization with higher (> 0.1 mM) glucosamine concentrations in treated hearts. B) The overall decrease in carbohydrate oxidation was a result of decreased lactate (0.05, 0.1, 5, 10 mM) and decreased pyruvate (0.1, 5, 10 mM) oxidation compared to untreated hearts. Glucosamine had no effect on glucose oxidation at any concentration. [0 mM (n=6), 0.05 mM (n=4), 0.1 mM (n=5), 5 mM (n=5), 10 mM (n=4)]*
** p<0.05 vs 0 mM (one-way ANOVA; Dunnett)*

Since hearts were perfused with [3-^{13}C]-lactate, [2-^{13}C]-pyruvate, and unlabeled glucose, we were able to evaluate their relative contributions to total pyruvate oxidation. Under these experimental conditions, the contribution of glucose to pyruvate oxidation is determined from the fraction of unlabeled acetyl-CoA. We found that glucosamine had no effect on glucose oxidation that remained unaltered at all glucosamine concentrations (*Fig. 27B*). The decrease in total carbohydrate oxidation (*Fig. 27A*) was largely due to significantly reduced lactate oxidation (at 0.05, 0.1, 5, 10 mM glucosamine) and a lesser degree to decreased pyruvate oxidation (at 0.1, 5, 10 mM gucosamine) (*Fig. 27B*).

Glucosamine significantly decreased lactate uptake, but it had no effect on glycolytic lactate efflux: ^{1}H-NMR analyses of perfusate effluents from the hearts enabled us to determine the rates of exogenous ^{13}C-labeled lactate uptake and unlabeled/glycolytic lactate efflux. We found that lactate uptake rates were reduced by ~2-fold with 0.1 mM glucosamine, consistent with the ~2-fold decrease in lactate oxidation (*Fig. 28A*), and with previous studies showing that the rate of exogenous lactate uptake was tracked with lactate oxidation (71). Glucosamine had no effect on the rate of glycolytic lactate efflux (*Fig. 28B*).

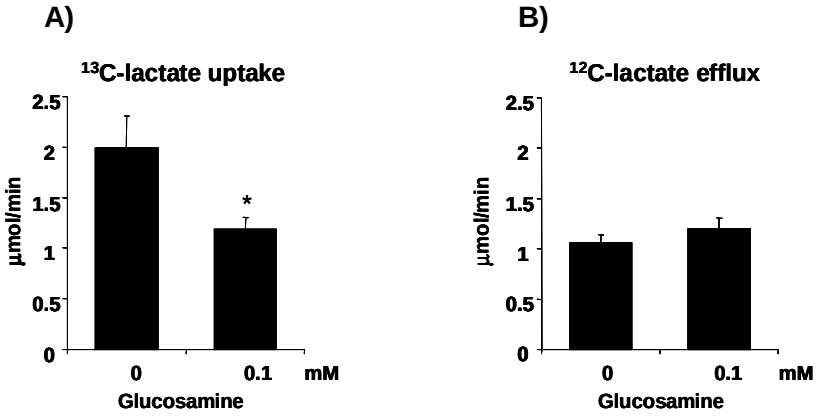

Figure 28. *0.1 mM glucosamine significantly decreased A) exogenous [3-^{13}C]-lactate uptake, but B) did not alter unlabeled/glycolytic lactate efflux [0 mM (n=4), 0.1 mM (n=5)]*
** p<0.05 vs 0 mM (unpaired t-test)*

3.1.2. Acute effects of glucosamine on the activation of AMPK, ACC, and FAT/CD36 levels

Glucosamine had no effect on AMPK or ACC phosphorylation in cardiac tissue: Luo et al. (73) reported that in 3T3L1 adipocytes glucosamine increased AMPK and ACC phosphorylation leading to increased fatty acid oxidation. Glucosamine in the heart no effect on AMPK and ACC phosphorylation at any concentrations (data not shown), not even at 0.1 mM glucosamine concentration (*Fig. 29*), at which palmitate oxidation was markedly enhanced (*Fig. 27A*).

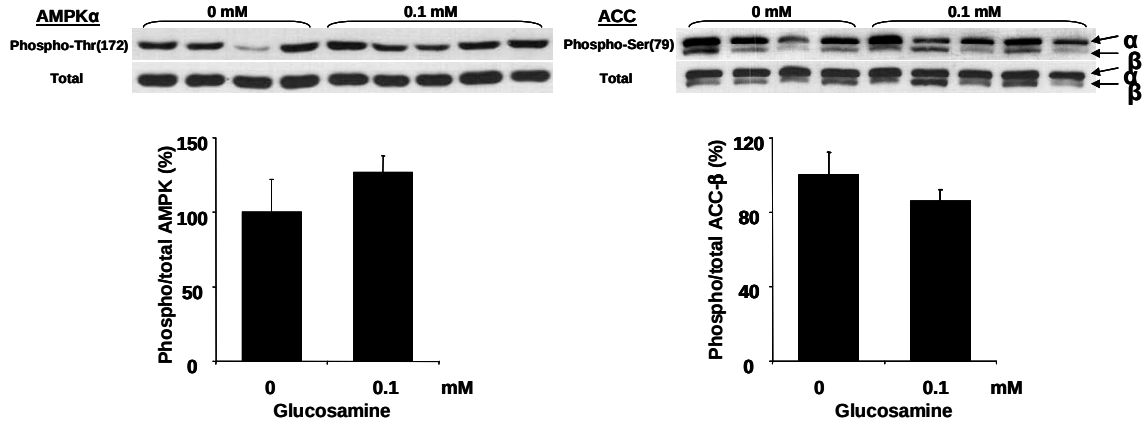

Figure 29. *Glucosamine had no effect on AMP-activated protein kinase (AMPK) and acetyl-CoA carboxylase (ACC) phosphorylation in the heart after 60 min perfusion with 0.1 mM glucosamine (NS, unpaired t-test). [0 mM (n=4), 0.1 mM (n=5)]*

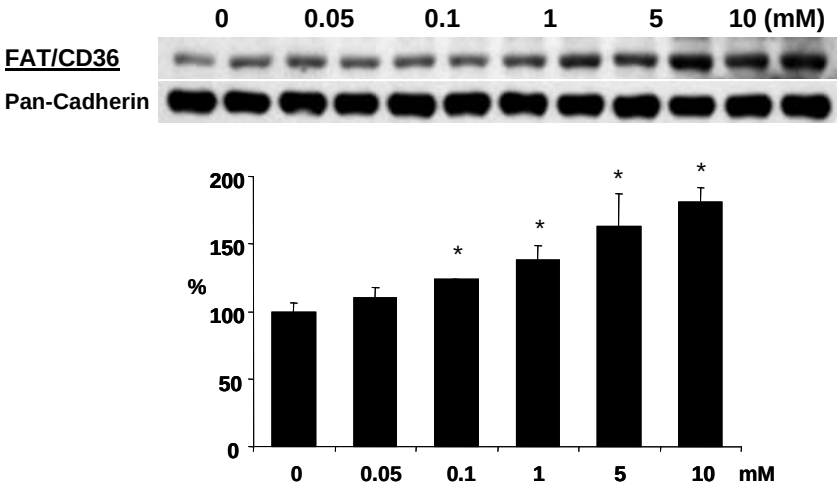

Figure 30. *Representative immunoblot [n=2 in each group] and densitometric results show that FAT/CD36 levels in the membrane fraction significantly increased following 60 min perfusion with 0, 0.05, 0.1, 1, 5 and 10 mM glucosamine in a concentration dependent manner (* p<0.05 vs 0 mM; one-way ANOVA; Dunnett). FAT/CD36 levels are normalized to pan-cadherin shown as the plasma membrane marker, and are expressed as % of untreated controls (i.e. 0 mM glucosamine).*

Glucosamine significantly increased membrane-associated FAT/CD36 levels: Fatty acid transport into the heart is also regulated by FAT/CD36 (15). Therefore, we assessed the effects of glucosamine on the membrane levels of FAT/CD36. As shown in *Fig. 30*, glucosamine treatments (0.1, 1.0, 5.0 and 10.0 mM) markedly increased membrane-associated FAT/CD36 levels in a dose-dependent manner.

3.1.3. FAT/CD36 is a potential target for O-GlcNAcylation

Membrane-associated FAT/CD36 is targeted by O-GlcNAc and co-immunoprecipitates with OGT: FAT/CD36 was immunoprecipitated in whole tissue and membrane fraction of cardiac lysates. Since O-GlcNAcylation is known to be a relatively low abundance modification, these studies were performed on hearts where overall O-GlcNAc was increased ~3 fold by 60 min-perfusion with a combination of glucosamine and NAG-Bt (data not shown). As shown in *Fig. 31*, there is evidence of O-GlcNAc modification of FAT/CD36 in both fractions; however, this is particularly apparent in the membrane fraction. The lack of signal with the co-incubation of 10 mM β-N-acetylglucosamine indicates that positive O-GlcNAc staining is a result specific binding of the O-GlcNAc antibody (29). We also found that OGT, which is responsible for O-GlcNAcylating the proteins co-immunoprecipitated with FAT/CD36.

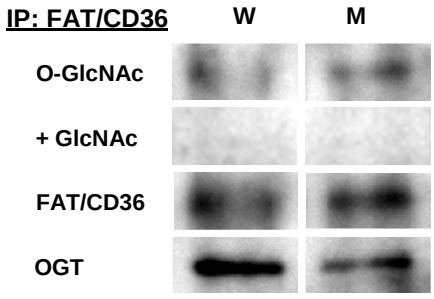

Figure 31. *Immunoprecipitation of FAT/CD36 from whole tissue (W) and plasma membrane (M) lysates followed by O-GlcNAc and OGT immunoblots. Specificity of O-GlcNAc antibody was confirmed by co-incubation with 10 mM β-N-acetylglucosamine (GlcNAc).*

3.2. *Clinical study* to investigate effectiveness of the anti-inflammatory pentoxifylline and pentosan polysulfate combination therapy on diabetic neuropathy and albuminuria in type 2 diabetic patients.

The mechanisms underlying microangiopathy in diabetes are multiple; however, particularly in T2DM, the oxidative stress and chronic inflammation are important pathogenic factors. Both pentoxifylline (PF) and pentosan polysulfate (PPS) have been shown to possess significant pro-circulatory, anti-inflammatory, and anti-proteinuric effects, thus these drugs could offer symptomatic and in part, causal approaches to attenuate microvascular complications. We purposed to determine the beneficial effects of combined PF and PPS infusion therapy on cardiovascular autonomic and peripheral sensory functions (as regard with neuropathy), and the urinary albumin excretion (as regard with nephropathy) in T2DM patients.

Subjects, materials and methods:

Study protocol and participants: Studied groups were: 1) treated patients (*Verum group*; n=77), who daily received a combination of pentoxifylline (100 mg, Trental®, Biogal) and pentosan polysulfate (100 mg, SP54®, Bene-Arzneimittel GmbH) dissolved in saline infusions (500 mL) for 5 days; and 2) untreated, control subjects (*Placebo group*; n=12) were given only saline infusions (500 mL) in the same regimen. Due to the facts that absorption of orally taken PPS is low (1-2%) and relatively high doses of PF were found ineffective to improve sensory symptoms of neuropathy in diabetics (26, 27, 67), we administered PF-PPS intravenously by infusions at reasonably lower doses (100-100 mg). Inclusion criteria were T2DM (≥ 1 year duration) and symptoms of distal peripheral sensory neuropathy (e.g. positive signs of paresthesias: numbness, tickling, itchy, or negative signs of hypasthesias/analgesias: decreased perceptions of pain, temperature, position, vibration). Controls were matched for age, gender, hemoglobin A1c, and renal function. ACE-I and/or ARB, statin, or anti-platelet therapy did not differ between the groups. Taken ethical considerations, we included lower number of participants in the Placebo group, since untreated patients suffered from severe symptoms of distal sensory neuropathy.

Exclusion criteria were as follows: neuropathies with other etiology, advanced liver disease, heart failure, arrhythmia, blood pressure >160 mmHg, serum creatinine >200 μmol/L, advanced diabetic retinopathy, bleeding disorder, disability, incompliance. Examinations (case history, physical examinations, ECG, blood pressure) for in-patients were performed at hospitalization, tests for neuropathies and albuminuria were assessed on the 1st day (before therapy) and 5th day (after therapy) during hospitalization. Current medications were unchanged throughout the study (diet, oral hypoglycemics, insulins, antihypertensive, lipid-lowering drugs). All incidental and adverse effects were recorded. The study was approved by the Ethical Committee of Medical Faculty, University of Pécs. All patients gave written informed consent. Clinical characteristics of study participants are shown in *Table 3*.

Assessment of cardiovascular autonomic neuropathy, vibration perception and albuminuria: CA-N was assessed with five reflex tests described by Ewing (38). These standardized, non-invasive tests are well-established physiologic maneuvers, reproducible and reliable, thus valuable tools for evaluating the progression of CA-N (14). Those reflexes that evaluate changes in heart rate are primarily markers of the parasympathetic nerve function (i.e. heart rate variability to deep breath test [expiration/inspiration ratio]; to Valsalva maneuver [Valsalva ratio]; and to standing up [30/15 ratio]. Reflexes assessing the blood pressure responses are indicators of the sympathetic nerve function (i.e. postural systolic blood pressure fall, and diastolic blood pressure rise upon handgrip test) (38). Results of individual tests were generated in age-matched categories (normal, borderline, abnormal) by Innobase 3.1 software attached to ECG (Innomed Medical), as well as the summarized score of all five tests (i.e. autonomic score) that expresses the overall severity of CA-N in four categories: none (0–1), mild (2–3), explicit (4–6), severe (≥ 7).

Vibration perception using a 128 Hz Riedel-Seiffer calibrated tuning fork was assessed to evaluate somatic neuropathy. Vibration threshold values (pallesthesia: normal: 6–8; abnormal: < 5) were measured three times at the lower limbs (at the tip of hallux, dorsal side of first metatarsus, medial malleolus) and mean data were used.

Urinary albumin excretion was assessed from single urine samples (Verum: n=67; Placebo: n=11) by nephelometry and albumin/creatinine ratio (ACR) were calculated.

Statistical analysis: Accordingly to variable distribution by Kolmogorov-Smirnov test, non-parametric (Wilcoxon, Mann–Whitney U) or parametric tests (unpaired- and paired t-test), and X^2-test, Spearman's correlation were used (SPSS 10.0, SPSS Inc). Data are expressed as means ± SE and $p < 0.05$ was defined as statistically significant.

Table 3. *C*linical characteristics of type 2 diabetic patients (means ± SE)

	VERUM	**PLACEBO**
Age (years)	62±1	61±2
Gender (male/female)	32/45	4/8
T2DM duration (years)	14±1	14±3
Body Mass Index (kg/m^2)	32±1	29±2
Fasting Plasma Glucose (mmol/L)	9.4±0.4 *	7.3±0.8
Hemoglobin A1c (%)	7.75±0.24	7.32±0.93
Fructosamine (µmol/L)	315±9	401±59
Serum Creatinine (µmol/L)	101±4	91±8
GFR (mL/min)	76±4	84±8
Systolic BP (mmHg)	135±2 *	125±4
Diastolic BP (mmHg)	76±1	74±1
ACE-I and/or ARB (yes/no)	59/18	12/0
Statin (yes/no)	46/31	10/2
Aspirin (yes/no)	45/32	10/2
Diabetic Nephropathy	16/61	1/11
Diabetic Retinopathy	22/55	4/8
Coronary Artery Disease	22/55	6/6
Cerebrovascular Disease	7/70	2/10
Peripheral Artery Disease	4/73	0/12

T2DM, type 2 diabetes mellitus; GFR, glomerular filtration rate; BP, blood pressure; ACE-I, angiotensin converting enzyme inhibitor; ARB, angiotensin receptor blocker;
** p<0.05 Verum vs Placebo group (unpaired t-test)*

Results:

3.2.1. Effects of pentoxifylline and pentosan polysulfate infusion therapy on cardiovascular autonomic and peripheral sensory neuropathy in type 2 diabetic patients

For all studied patients we found a significant positive correlation between T2DM duration and overall CA-N severity assessed by autonomic score (r=0.270, *p<0.05*; *Fig. 32A*). Vibration threshold values were inversely correlated with fructosamine levels (r= -0.317, *p<0.05*) for all studied patients (*Fig. 32B*). Vibration threshold values were

also inversely correlated with autonomic score (r= -0.195, p<0.05), but not with hemoglobin A1c (r= -0.179, p=.172) or T2DM duration (r= -0.027, p=0.330) (data not shown).

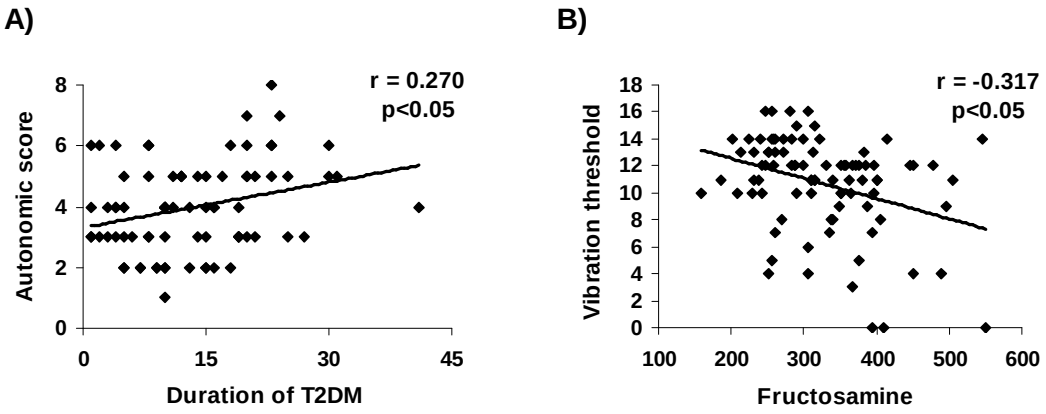

Figure 32. *Significant relationships of A) autonomic score and type 2 diabetes (T2DM) duration; and B) vibration threshold values and fructosamine levels for all patients participated in the study (p<0.05; Spearman's correlation)*

PF-PPS infusions significantly improved cardiovascular autonomic neuropathy: PF-PPS infusions were well-tolerated and adverse effects or infusions-related complications were not recorded. Results of cardiovascular autonomic reflexes before and after therapy are summarized in *Table 4*. PF-PPS infusions significantly decreased autonomic score values in Verum group (*p<0.001*) indicating an overall improvement in cardiovascular autonomic responses. The number of those patients that showed mild, explicit or severe dysfunctions prior to therapy markedly decreased after PF-PPS infusions, and autonomic score became normalized in 20 patients (none category) in Verum group (*p<0.001; Fig. 33*).

PF-PPS infusions significantly increased heart rate variability to deep breath test in Verum group (*p<0.001; Table 4*). The number of patients with abnormal heart rate variability (n=47) was decreased by 23.3 % after therapy (n=29) in Verum group (*Fig. 34A*). PF-PPS infusions significantly increased the diastolic blood pressure rise to handgrip test in Verum group (*p<0.001; Table 4*). The number of patients showing abnormal response to handgrip before therapy (n=48) was decreased by 29.9% after therapy (n=25) in Verum group (*Fig. 34B*). Other CA-N tests (Valsalva, 30/15 ratio, postural blood pressure fall) remained unaltered after PF-PPS infusions (*Table 4*).

Table 4. Results of standard cardiovascular autonomic tests (means ± SE)

	VERUM		PLACEBO	
	Before therapy	After therapy	Before therapy	After therapy
- Resting heart rate (beat/min)	72±1	72±1	69±2	64±2
- Heart rate variability in response to deep breath (beat/min)	13.87±1.53	18.22±1.70 [a]	14.67±4.76	13.00±3.96
- Valsalva ratio	1.69±0.09	1.71±0.09	1.84±0.29	1.59±0.22
- 30/15 ratio	1.56±0.18	1.38±0.12	1.25±0.06	1.30±0.13
- Postural systolic BP fall in response to standing (mmHg)	16±1	14±1	19±3	19±3
- Diastolic BP rise in response to handgrip (mmHg)	10±1	14±1 [a]	12±1	11±1
Autonomic Score	3.79±0.17	2.79±0.19 [a b]	3.92±0.48	4.50±0.45

[a] *p<0.001 after vs before therapy in Verum group (Wilcoxon)*
[b] *p<0.001 Verum vs Placebo after therapy (Mann-Whitney U)*

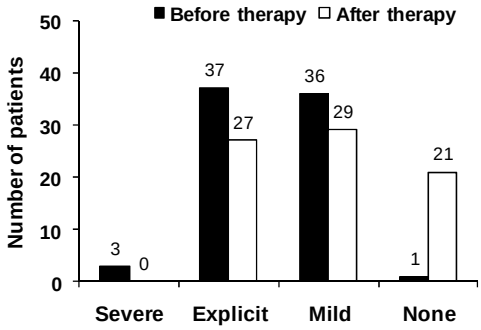

Figure 33. *The number of patients showing mild, explicit or severe CA-N by autonomic score was clearly decreased after therapy in Verum group (p<0.001; X^2 test)*

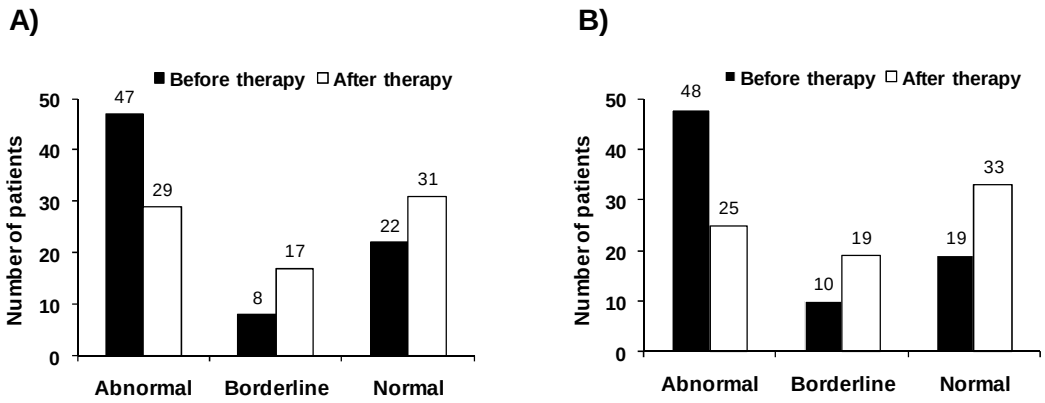

Figure 34. *The number of patients showing A) abnormal heart rate variability to deep breath test, and B) abnormal diastolic blood pressure rise to handgrip test was significantly decreased after therapy in Verum group (p<0.001; X^2 test)*

In Placebo group there were no changes in any of the autonomic responses after sham-infusions (*Table 4*). Before infusions, there were no differences in patient

distributions showing abnormal tests between the groups [(Verum/Placebo) deep breath test: 47/9; Valsalva ratio: 5/1; 30/15 ratio: 1/0; postural BP: 9/3; handgrip test: 48/4]. Neither were differences between the groups before (pB) or after (pA) therapy in heart rate variability (pB=0.543; pA=0.063), Valsalva ratio (pB=0.805; pA=0.227), 30/15 ratio (pB=0.339; pA=0.718), postural hypotension (pB=0.199; pA=0.052), diastolic blood pressure rise to handgrip (pB=0.227; pA=0.087). While before therapy autonomic score did not differ between the groups (pB=0.673), after therapy it was significantly lower in the Verum group (*pA<0.05 vs. Placebo group*).

PF-PPS infusions significantly improved vibration perception: PF-PPS infusions significantly increased vibration threshold values in the Verum group (*p<0.001*; *Fig. 35*). There were no changes in the Placebo group after sham-infusions (11.58±1.15 vs. 10.67±1.23). There were no differences between the two groups before or after therapy at either lower limbs (right: pB=0.157, pA=0.571; left: pB=0.272, pA=0.671).

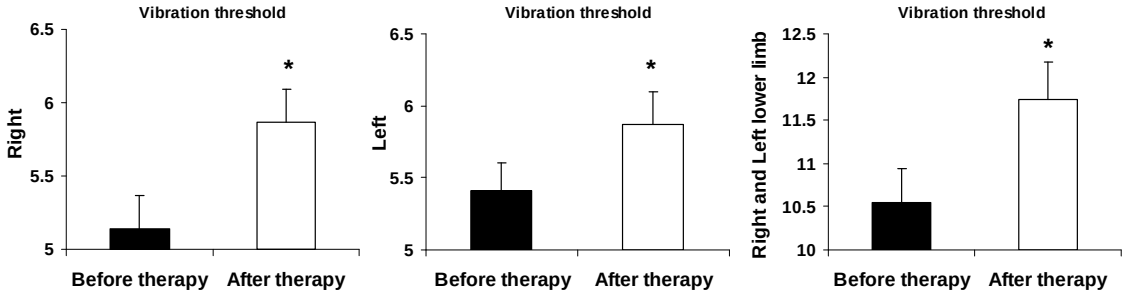

Figure 35. *Vibration threshold values of lower limbs were significantly increased in Verum group after therapy (* p<0.001; Wilcoxon)*

3.2.2. Effects of pentoxifylline and pentosan polysulfate infusion therapy on urinary albumin excretion in type 2 diabetic patients

PF-PPS infusions had no effect on albuminuria: The majority of patients had normalbuminuria in both studied groups (Verum: n=47; 70% and Placebo: n=9; 82%). We did not find difference in ACR (mg/mM) in Verum group after therapy (3.47±1.36 vs. 4.34±1.31; p=0.364). There were also no changes in ACR in the Placebo group after sham-infusions (6.39±4.71 vs. 9.34±8.22; p=0.436). Neither were differences between the two groups before or after therapy (pB=0.449, pA=0.278).

3.3. *Clinical study* to investigate erythropoietin resistance and the effects of the anti-inflammatory acetylsalicylic acid on anemia correction in type 2 diabetes mellitus and chronic kidney disease

Anemia, a frequent complication of T2DM and CKD, has been mostly attributed to decreased EPO synthesis; however, unresponsiveness to EPO has been also advanced. Increased pro-inflammatory state and oxidative stress, both of which are characteristic features of T2DM and CKD have been proposed to contribute to the absolute lack and ineffectiveness of EPO. While replacement therapy with exogenous EPO has been widely used for improving the availability of EPO and anemia, it is not known whether administration of an anti-inflammatory and free radical scavenger agent was capable of abrogating the adverse effects of T2DM and CKD on serum EPO levels and erythropoiesis. Our aims were to determine the presence of EPO resistance in patients with T2DM and CKD, and whether patients with both conditions (i.e. diabetic nephropathy) had higher degree of anemia and unresponsiveness to endogenous EPO; and whether treatment with a single, high-dose of ASA, a potent anti-inflammatory and hydroxyl free radical scavenger had benefits on low EPO levels and anemia correction in a subgroup of patients with T2DM and CKD.

Subjects, materials and methods:

The cross-section study protocol and participants: In a cross-section study we examined the presence of EPO resistance by comparing four groups: 1) T2DM patients with normal glomerular function (DM, n=15); 2) T2DM patients with nephropathy (DM+CKD; n=15); 3) non-diabetic patients with CKD (CKD; n=15); and 4) healthy individuals matched for age and gender (CONTR; n=10). T2DM was diagnosed by the American Diabetes Association criteria. Normal glomerular function was defined as serum creatinine: 60–120 μmol/L and glomerular filtration rate (GFR): 90–120 mL/min. Patients with comparable serum EPO levels were recruited in order to determine the contributions of T2DM and/or CKD to the development of anemia by comparing the study cohorts. There were no differences in glycemic control between the DM and DM+CKD groups measured by hemoglobin A1c, fructosamine, and

plasma glucose. Renal function measured by serum creatinine and GFR did not differ between the CONTR and DM groups, or the DM+CKD and CKD groups. In the CKD group etiologies of kidney diseases were as follows: hypertensive nephropathy (n=9), chronic pyelonephritis (n=3), analgesic nephropathy (n=1), chronic glomerulonephritis (n=1), and polycystic kidney disease (n=1). Anemic patients with etiology of malignancy, autoimmune disease, or deficiencies were excluded. Clinical characteristics of study participants are summarized in *Table 5*. The severity of anemia was assessed by hematocrit and hemoglobin, the nature of anemia was evaluated by red blood cell properties, including mean cell volume, mean cell hemoglobin, and mean cell hemoglobin concentration. All parameters were measured by standard laboratory methods.

The intervention study protocol and participants: In a subsequent intervention study, a subgroup of anemic patients (DM: n=3; DM+CKD: n=4; CKD: n=3) with low serum EPO levels were included and received per os 1 gram ASA (2x500 mg, Aspirin®, Bayer). Exclusion criteria were smoking, hyperacidity, gastric/duodenal ulcer, gastrointestinal bleeding, malignancy, chronic pulmonary disease. Fasting blood samples were collected at baseline and after ASA administration at the 4^{th}, 8^{th}, 24^{th}, and 48^{th} hour. Serum EPO, reticulocyte count and ratio, red blood cell count, hematocrit, hemoglobin, and lactate dehydrogenase (LDH) were measured by standard laboratory methods. After ASA treatment, patients were fasting and were given infusions (Ringer, 500 mL) to avoid dehydration during the initial four hours. Vital parameters were closely monitored to prevent hypoglycemia and other adverse events. The study was approved by the Ethical Committee of Medical Faculty, University of Pécs. All patients gave signed informed consent.

Statistical analysis: All variables showed normal distribution by Kolmogorov-Smirnov test. Differences between experimental groups were evaluated by one-way ANOVA (Bonferroni`s posthoc test), $X^2$-test, Pearson`s correlations, unpaired- and paired t-test using SPSS 10.0 (SPSS Inc.). Data are expressed as means ± SE and $p < 0.05$ was defined as statistically significant.

Results:

3.3.1. Results of the cross-section study on the presence of erythropoietin resistance in type 2 diabetes mellitus and chronic kidney disease

As shown in *Table 5*, due to intentional recruitment of patients, there were no differences in EPO levels (p=1.000), gender, age, lipid profile, and systolic blood pressure between any of the study groups. There was no difference in renal impairment between the DM+CKD and CKD groups (serum creatinine: p=0.795; GFR: p=0.820). There was also no difference in glycemic parameters between the DM and DM+CKD, the two diabetic groups (fructosamine: p=0.797; hemoglobin A1c: p=0.298). T2DM duration was higher in the DM+CKD group than in the DM group (*p≤0.05*). ACE-I drugs were equally applied in all patients groups (i.e. DM, DM+CKD, and CKD).

Table 5. Clinical characteristics of study participants (means ± SE)

	CONTR	DM	DM+CKD	CKD
Gender (female/male)	5/5	7/8	7/8	7/8
Age (years)	63±2	64±3	65±3	61±4
T2DM duration (years)	-	13±2 [a]	20±3	-
Body Mass Index (Kg/m^2)	30±1	28±1	33±5	27±1[a]
Hemoglobin A1$_C$ (%)	-	6.7±0.3	6.7±0.3	-
Fructosamine (μmol/L)	-	299±15	317±15	-
Glucose (mmol/L)	5.0±0.2	7.9±0.8	8.9±1.0[b]	5.3±0.3[a]
Cholesterol (mmol/L)	5.4±0.4	5.1±0.2	5.8±0.4	5.7±0.5
Triglyceride (mmol/L)	1.7±0.3	2.2±0.4	2.4±0.3	2.4±0.4
HDL cholesterol (mmol/L)	1.3±0.1	1.2±0.1	1.3±0.1	1.3±0.1
Serum Creatinine (μmol/L)	85±7	72±3	254±29[b c]	223±23[b c]
GFR (mL/min)	92.1±9.5	93.9±10.3	31.4±3.4[b c]	32.4±2.9[b c]
Serum. EPO level (U/L)	11.9±1.7	11.0±0.8	11.1±1.0	9.7±1.0
ACEI therapy (yes/no)	4/6	12/3[b]	13/2[b]	10/5
Systolic BP (mmHg)	133±6	135±4	137±4	130±4

T2DM, type 2 diabetes mellitus; GFR, glomerular filtration rate; EPO, erythropoietin; ACE-I, angiotensin converting enzyme inhibitor; BP, blood pressure;
[a] p≤0.05 vs DM+CKD group
[b] p≤0.05 vs CONTR group
[c] p≤0.05 vs DM group (one-way ANOVA; Bonferroni)
Statistically non-significant differences analyzed by adequate tests (one-way ANOVA, unpaired t-test, X^2 test) are not indicated

Despite comparable serum EPO levels, hematocrit values were significantly lower in the DM, DM+CKD, and CKD groups compared to the CONTR group, indicating a loss of responsiveness to endogenous EPO (*Fig. 36A*). In addition, patients in the DM+CKD group had significantly lower hematocrit values compared to the DM and DM+CKD groups (*Fig. 36A*). Hemoglobin levels closely mirrored those seen with hematocrit values (*Fig. 36B*). Hemoglobin levels were significantly lower in the DM+CKD group compared to the DM group that was matched for glucose metabolism and the CKD group that was matched for renal failure (*Fig. 36B*). Red blood cell parameters were in the normal range showing no differences between any of the studied groups (*Table 6*).

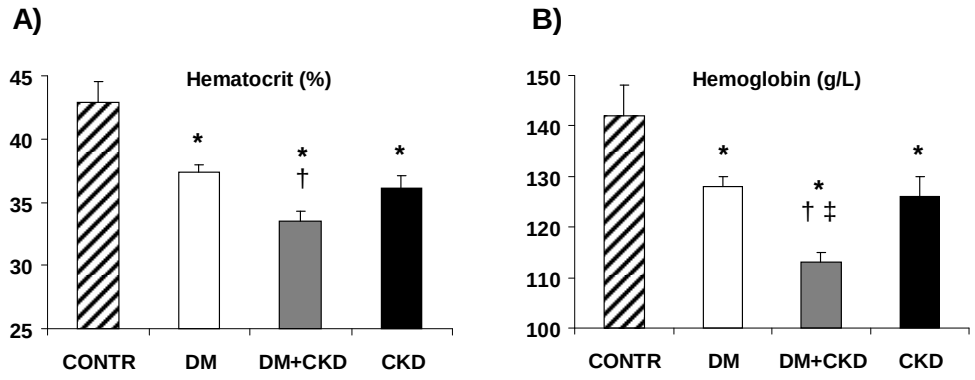

Figure 36. *Both A) hematocrit and B) hemoglobin values were the lowest in patients of the DM+CKD group*
** p≤0.05 vs CONTR; † p≤0.05 vs DM; ‡ p≤0.05 vs CKD (one-way ANOVA; Bonferroni)*

Table 6. Red blood cell properties (means ± SE)

	CONTR	DM	DM+CKD	CKD	NORMAL RANGE
MCV (fl)	91.0±1.2	87.3±1.0	89.8±1.3	88.9±1.0	80-97
MCH (pg)	30.1±0.7	29.5±0.5	30.9±0.5	30.8±0.3	27-31,2
MCHC (g/L)	330±5	338±4	342±3	347±3	318-354

Red blood cell properties (MCV: mean cell volume; MCH: mean cell hemoglobin; MCHC: mean cell hemoglobin concentration) were within normal range with no differences between any of the groups (NS: one-way ANOVA; Bonferroni)

Correlation analyses showed that there were no significant relationships between serum EPO levels and hematocrit values in any of the patient groups [DM: R^2=0.025, p=0.575; DM+CKD: R^2=0.106, p=0.236; and CKD: R^2=0.000, p=0.949] (*Fig. 37*). Similarly, we did not find positive correlations between serum EPO levels and hemoglobin values in any of the patient groups [DM: R^2=0.000, p=0.956; DM+CKD: R^2=0.100, p=0.316; and CKD: R^2=0.000, p=0.960] (data not shown). In correction analyses, evaluation of different variables revealed no significant relationships between EPO levels and hematocrit values for age, serum creatinine, hemoglobin A1c, fructosamine, serum glucose, total cholesterol, HDL cholesterol, or systolic blood pressure in any of the patient groups. In the DM group, however, serum EPO levels correlated with hematocrit values only after corrections for body mass index (R^2=0.410, *p<0.05*) and triglyceride levels (R^2=0.285, *p<0.05*).

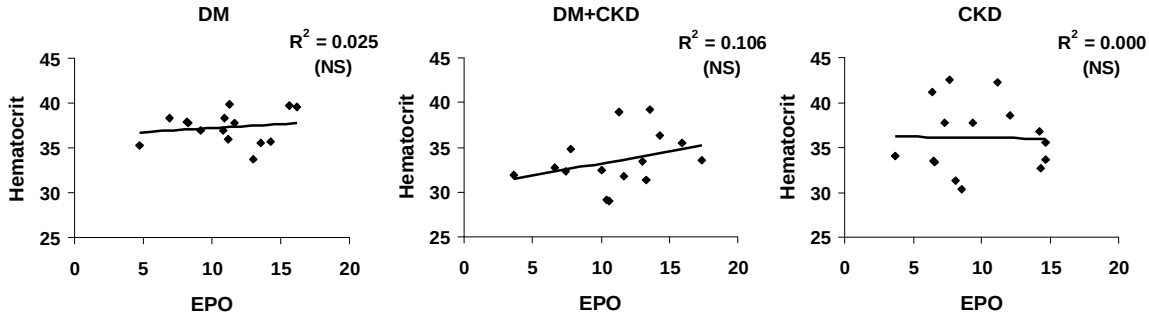

Figure 37. *Correlations between serum EPO levels and hematocrit values in the DM, DM+CKD, and CKD groups (NS: Pearson`s test)*

3.3.2. Effects of the anti-inflammatory acetylsalicylic acid on erythropoietin levels and anemia correction in type 2 diabetes mellitus and/or chronic kidney disease

Results of the intervention study involving a subgroup of anemic patients with low baseline EPO levels are summarized in *Table 7*. Administration of 1 gram ASA significantly increased serum EPO levels by 59%, the reticulocyte count by 33%, the reticulocyte ratio by 14%, the red blood cell count by 7%, the hemoglobin levels by 6%, and the hematocrit values by 8%. At the same time, it significantly decreased serum LDH activity by 12% (*Table 7*). No adverse effects of ASA were noticed.

Table 7. Effects of acetylsalicylic acid on erythropoiesis in a subgroup of anemic patients with low baseline EPO levels (means ± SE)

	Before therapy	After therapy
Serum EPO level (U/L)	7.71±5.41	12.26±8.73 *
Red blood cell count (T/L)	3.75±0.26	4.01±0.29 *
Reticulocyte count (G/L)	42±12	56±16 *
Reticulocyte ratio (%)	0.81±0.49	0.92±0.68 *
Hemoglobin (g/dL)	111.1± 7.6	118.3±8.6 *
Hematocrit (%)	33.0±2.6	35.8±2.6 *
Serum LDH activity (U/L)	319±36	280±35 *

EPO, erythropoietin; LDH, lactate dehydrogenase;
** p<0.01 vs before therapy (paired t-test)*

As shown in *Fig. 38*, ASA treatment resulted in acute increases of the red blood cell count in a time-dependent manner.

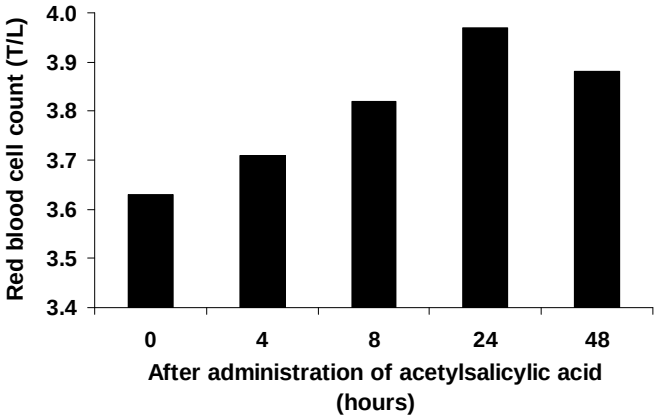

Figure 38. *Representative graph illustrates the time-dependent changes of red blood cell count after acetylsalicylic acid treatment in an anemic patient.*

DISCUSSION

1. Oxidative stress and endothelial dysfunction: *In vitro* experiments on the cigarette smoke induced alterations in endothelial cells.

Over the last decade accumulating evidence suggested that cigarette smoke leads to endothelial dysfunction by disturbing the integrity of L-arginine–eNOS–cGMP–NO pathway, resulting in decreased NO availability. Consistently, Su et al. (121) showed that incubation of endothelial cells with cigarette smoke extract for 24 hours resulted in decreased mRNA level and protein expression of eNOS. In addition, decreased eNOS activity and NO production were found in endothelial cells treated for 12 hours with sera from cigarette smokers, although it was accompanied by increased eNOS protein expression (7). Short-term exposure (60 min) of endothelial cells to cigarette smoke also inhibited eNOS activity with a concomitant reduction in NO production; however, eNOS expression was unaltered (144). Although previous reports have demonstrated that there is an overall reduced NO bioavailability in endothelial cells after cigarette smoke exposure; most of these studies focused on the cigarette smoke induced alterations in eNOS expression and/or NO production providing scarce data on other regulatory changes. In addition, our earlier studies showing that cigarette smoke rapidly and dose-dependently decreased the agonist-induced calcium signaling and cGMP production in porcine aortic endothelial cells (78, 87) suggested the role of posttranslational eNOS modifications in mediating more promptly the cigarette smoke induced inhibitory effects. Therefore, we examined eNOS phosphorylations and dimerization after a short-term application of cigarette smoke buffer (CSB; ≤ 30 min) in endothelial cells.

We found that acute CSB treatment of endothelial cells dose- and time-dependently increased eNOS phosphorylations at both Ser(1177) and Ther(495) sites, as well as the dissociation of the catalytically active eNOS dimers; whereas it had no impact on total eNOS protein content. Although the posttranslational regulation of eNOS activity is relatively complex, it is coordinated mainly at two well-described phosphorylation sites, of which Ser(1177) is considered as an activating (36); whereas

Thr(495) is known as an inhibitory residue (43). We showed that CSB-induced phosphorylation of Thr(495) was higher than that of Ser(1177), supporting the notion that this inhibitory shift could contribute to decreased eNOS activity and NO production associated with cigarette smoke induced endothelial dysfunction. As noted, CSB increased eNOS phosphorylations at both the activating Ser(1177) and inhibitory Thr(495) residues, which seems contrary to a common concept that there is a simultaneous reciprocal phosphorylation-dephosphorylation reaction at these two sites (55, 77, 83). Alternatively, it suggests that there may be independent regulatory responses to CSB leading to increased eNOS phosphorylations of both sites, due probably to oxidant stress caused by the excessive amount of ROS.

The role of oxidant stress in altering eNOS phosphorylations was confirmed by showing that GSH markedly diminished the CSB-induced increases in eNOS phosphorylations at both Ser(1177) and Thr(495) sites, which was more pronounced at the inhibitory Thr(495) site. In addition, GSH prevented eNOS dimers from destabilization by preventing the CSB-induced eNOS disruption into an inactive monomeric form. Conclusively, GSH significantly attenuated the inactivating eNOS modifications to the CSB-induced oxidative stress thus it could contribute to preserved eNOS activity and NO production. We previously reported that antioxidant actions of superoxide dismutase, catalase, and desferrioxamine were ineffective to abolish the CSB-induced inhibitory effects on eNOS-cGMP-NO pathway (78, 87), suggesting that superoxide, hydroxyl free radical, or lipid peroxidation are not involved in this process. In contrast, GSH protected the endothelial cells against the adverse effects of the water-soluble, gas phase cigarette smoke (i.e. CSB) by neutralizing the aldehydes, especially the formaldehyde, which is abundant in CSB (78). Interestingly, N-acetylcysteine blunted the decreased eNOS activity and NO production in endothelial cells after CSB, whereas dithiol-oxidizing agents mimicked the CSB-induced changes (144). Moreover, GSH and captopril, both of which possess sulfhydryl moiety have been shown to attenuate impaired endothelium-dependent vasorelaxation in rabbit aortas after CSB (93). Therefore, it is highly likely that beneficial effects of GSH are related to its aldehyde scavenger action to prevent eNOS dysregulation in response to CSB. The fact that GSH markedly decreased eNOS phosphorylations after CSB also

suggests that aldehydes may have regulatory role in mediating the CSB-induced acute oxidant stress leading to increased eNOS phosphorylations found here.

As shown, CSB reduced the ratio of dimer/monomer eNOS levels, which was reversed by GSH. The ratio of dimer/monomer eNOS is a useful redox state marker of the enzyme; eNOS catalytic activity requires the homodimeric structure, whereas the monomeric form is less active and produces superoxide free radicals (108). Additionally, thiredoxin/thioreductase system prevented the loss of dimeric eNOS structure, implicating the role of tetrathiolate cysteine residues in the stability thus the activity of homodimeric eNOS (99). Anionic oxidants, such as peroxynitrite or superoxide, may oxidize thiols by releasing zinc and forming disulfide bonds, resulting in eNOS uncoupling (137). Therefore; eNOS very likely exists in uncoupled state in response to CSB, thus it produces mainly superoxide instead of NO. Superoxide reacting with NO forms peroxynitrite, which further aggravates the oxidative stress. Nevertheless, GSH conserved the dimeric eNOS structure, at least in part, by eliminating the CSB-induced oxidative damage of critical thiol groups within eNOS.

Several protein kinases have been identified to regulate eNOS activity in response to different stimuli. The Ser/Thr kinase PKB/Akt, which mediates signaling events in cell survival and insulin pathways, plays an essential role in activating eNOS via Ser(1177) phosphorylation (47). However, CSB concentration- and time-dependently inactivated PKB/Akt and there were dissimilar changes between decreased phospho-Ser(473)-Akt and increased phospho-Ser(1177)-eNOS levels, suggesting that PKB/Akt may not phosphorylate directly eNOS at Ser(1177) in response to CSB. Because Akt mediates many downstream events controlled by PI3-K, we also tested effects of the selective PI3-K inhibitor (LY-294002), which we showed to further enhance the Ser(1177) phosphorylations after CSB treatment. These findings indicate that the PI3-K/Akt pathway is unlikely being responsible for the increased Ser(1177) phosphorylations seen with CSB. In addition to PKB/Akt, the PKA pathway plays also a key role in phosphorylating eNOS at Ser(1177) under physiological conditions (e.g. shear stress, bradykinin) leading to increased eNOS activity and NO production (6, 12). However, the selective PKA inhibitor (H-89) had no impact on CSB-induced eNOS phosphorylations at either site. On the contrary, by blocking PKC pathway with

selective PKC inhibitor (Ro-318425) we found that phospho-Thr(495) eNOS levels were concentration-dependently suppressed, indicating the involvement of PKC in phosphorylating eNOS at Thr(495) after CSB treatment. However, to date, PKC has been shown to maintain eNOS phosphorylation at Thr(495) only in unstimulated endothelial cells leading to decreased NO production (43, 77). Our finding is also in agreement with the notion that cigarette smoke could activate the PKC pathway (82). In endothelial cells, peroxynitrite increased the AMPK-dependent eNOS phosphorylation at Ser(1177), and MEK/Erk pathway is also known to alter eNOS activity (147, 20). As to, whether these protein kinases that are involved in regulating Ca^{2+}- and ischemia-related signaling events, may also phosphorylate eNOS at Ser(1177) in response to CSB has yet to be determined.

The ubiquitous PKC superfamily has a wide range of actions in signal transduction. Activation of the PKC pathway, in particular PKCβII, has been linked to diabetes-associated vascular dysfunctions, including endothelial hyperplasia, increased vascular permeability, and neovascularization (129). Whereas the isoform specific PKCßII-inhibitor, ruboxistaurin prevented vascular dysfunction by preserving the endothelium-dependent vasodilation (8). PKCβII-inhibitor also attenuated the diabetic nephropathy-related abnormalities *in vivo* animal models by decreasing TGF-β1, type IV collagen, and fibronectin mRNA levels, by reducing glomerular-mesangial expansion, and albuminuria (17). Given that PKCβII activation has been implicated in mediating the adverse effects of diabetes on vascular-endothelial function and that ruboxistaurin prevented the endothelium-dependent vasodilation, we subsequently tested whether ruboxistaurin could recapitulate the effects seen with the selective PKC inhibitor. Ruboxistaurin markedly attenuated the CSB-induced phospho-Thr(495) eNOS levels in a concentration-dependent manner, indicating that PKCβII pathway has a definitive role in mediating the CSB-induced eNOS phosphorylation at Thr(495).

In summary, we showed that acute exposure of endothelial cells to cigarette smoke altered eNOS phosphorylations resulting in shift to an inhibitory state and that it increased the disruption of the enzimatically active eNOS dimers, both of which could contribute to decreased eNOS activity and NO production. These findings support the notion that cigarette smoke reduces NO bioavailability, which is an important factor in

the development and progression of vascular diseases. GSH, a potent free radical and aldehyde scavenger salvaged eNOS from inactivating modifications in response to cigarette smoke by preventing its inhibitory phosphorylation and the disruption of homodimeric eNOS into an inactive monomeric form. Acute effects of cigarette smoke on eNOS phosphorylations seemed to be independently regulated of both the PKA and PI3-K/Akt pathways. The PKC pathway, more specifically PKCβII appears to play a key role in mediating the cigarette smoke induced changes in eNOS phosphorylations by increasing its inhibitory phosphorylation at Thr(495), rather than its activating phosphorylation at Ser(1177). PKCßII inhibition with ruboxistaurin could be a promising strategy to prevent the cigarette smoke induced deleterious effects.

2. Oxidative stress and cardiac dysfunction: *Ex vivo* experiments on the role of protein O-GlcNAcylation in mediating cardioprotection against ischemia-reperfusion injury in the isolated perfused rat heart.

Protein O-GlcNAcylation is emerging as a novel signaling mechanism regulating diverse cellular functions, and in particular, plays a critical role in modulating the responses of cells to pathophysiological stress conditions, such as the I/R injury (66, 90). Our goals were to determine whether OGA inhibition with the novel, highly selective NAG-thiazolines, NAG-Bt and NAG-Ae at the time of reperfusion attenuated I/R injury in the isolated perfused heart, and the effects of ischemia, reperfusion and OGA inhibitors on O-GlcNAcylation in the heart, as well as potential mechanisms by which O-GlcNAc could contribute to myocardial preservation.

As expected, I/R significantly suppressed cardiac contractile functions (3-fold), ATP levels, and increased tissue injury compared to time-matched normoxic hearts; however, it also resulted in a ~50% loss of overall protein O-GlcNAcylation. OGA inhibitors during reperfusion significantly increased O-GlcNAc in a drug- and dose-dependent manner; both NAG-Bt and NAG-Ae not only prevented the I/R-induced loss in O-GlcNAc, but even increased above that seen in the normoxic time-control group. At the end of reperfusion, 50 µM NAG-Ae treated hearts showed ~50% increase in O-

GlcNAc compared to 50 µM NAG-Bt, which is consistent with NAG-Ae being a more effective OGA inhibitor (50, 140).

Importantly, while there were no differences in baseline cardiac functions, NAG-thiazolines significantly improved functional recovery following I/R in a drug- and dose-dependent manner. At the end of reperfusion, RPP, LVDP and max dP/dt were all significantly higher in the NBt and NAe groups compared to untreated controls; and were higher in the NAe group compared to both NBt50 and NBt100 groups. Moreover, decreases in tissue injury were also directly proportional to the effectiveness of NAG-thiazolines at increasing O-GlcNAc; cTnI release was lower in the NAe group compared to both NBt50 and NBt100 groups. Overall, 100 µM NAG-Bt exhibited a greater degree of protection that 50 µM NAG-Bt; and 50 µM NAG-Ae approximately doubled the functional recovery, and reduced cTnI release by ~50% compared to 50 µM NAG-Bt. In addition, NAG-thiazolines attenuated the post-ischemic arrhythmic activity; VT and/or VF upon reperfusion did not occur in hearts of the NBt100 and NAe groups. The significant correlations between O-GlcNAc, functional recovery, and tissue injury further support the notion that OGA inhibition at the time of reperfusion exerts cardioprotective effects via increased protein O-GlcNAcylation, and as noted, with the more effective OGA inhibition the greater degree of protection could be observed.

While OGA inhibitors clearly attenuated tissue injury and improved functional recovery, they had no effect on ATP levels. Predictably, since OGA inhibitors were administered at reperfusion, and the majority of ATP depletion occurs during ischemia; furthermore, the majority of ATP breakdown products are lost on reperfusion, thus preventing any substantial re-synthesis of ATP (63). Thus, the protection observed with OGA inhibitors cannot be attributed to an ATP sparing effect or an increased ATP salvage on reperfusion. There were no significant differences in UDP-HexNAc between any of the I/R groups regardless of treatment indicating that OGA inhibitors during reperfusion had no upstream effects on precursors for O-GlcNAc synthesis.

Taken together, NAG-thiazolines, which compared to PUGNAc have markedly higher selectivity for OGA, protected the heart against I/R injury as indicated by increased functional recovery, and decreased tissue injury and arrhythmogenesis. The degree of protection was related to both specificity of the OGA inhibitor (i.e. NAG-Ae >

NAG-Bt at equivalent concentrations) and overall protein O-GlcNAcylation. Moreover, cardioprotective effects were evident even though NAG-thiazolines were administered only at the time of reperfusion; and improved functional recovery was evident after as early as 5 min of reperfusion. This might be of potential clinical relevance; since extensive efforts have been made for developing novel strategies to attenuate cardiomyocyte death with restoration of blood flow, and many promising therapeutic agents which are effective before ischemia are often ineffective when used only during reperfusion (11, 86). These data provide further support for the notion that increasing cardiac O-GlcNAc by inhibiting OGA may be a valuable approach for cardioprotection following I/R, although there are limitations in extrapolating to potential success in an *in vivo* milleu (i.e. *ex vivo* isovolumic perfused heart model was used, infarct size was not measured). Further studies are warranted to assess whether there would be additional benefit by inhibiting OGA prior to and during reperfusion; if so this might indicate potential utility in clinical settings where pre- and very early revascularization treatment protocols are practical.

Although we showed that ischemia alone, even after 10 min, increased overall O-GlcNAc, there was a marked loss in O-GlcNAcylation after reperfusion, which appears contrary to earlier studies indicating that increasing cellular O-GlcNAc was an endogenous response to stress (143). However, Fülöp et al. (46) reported that O-GlcNAc levels of the perfused heart increased during ischemia followed by a decline during reperfusion. Nőt et al. (91) observed similar phenomenon *in vivo* following hemorrhagic shock, where the loss of tissue O-GlcNAcylation was sustained for up to 24 hours following resuscitation. The mechanisms underlying this loss of O-GlcNAc following I/R have not been previously identified. Jones et al. (64) showed that H_2O_2 treatment of cardiomyocytes resulted in loss of O-GlcNAcylation, which was attenuated by OGA inhibition with PUGNAc. This suggests that oxidative stress, which is a key component of reperfusion injury, could be a contributing factor to decreased O-GlcNAc that occurs during reperfusion.

To obtain better insights into the effects of ischemia and I/R on O-GlcNAc, we used immunohistochemistry and examined O-GlcNAc distribution of cardiac tissue. In normoxic hearts, we found higher levels of O-GlcNAc staining in the nucleus,

consistent with other systems (2, 34, 102), as well as a cross-striated pattern throughout the cytosol, indicating O-GlcNAc-enrichment at the Z-lines in cardiomyocytes that has not been previously described. Ischemia alone had relatively little effect on overall O-GlcNAc, and structured association of O-GlcNAc with the Z-lines was maintained. However, there was a striking loss of O-GlcNAc within the nuclei with the appearance of punctate and perinuclear O-GlcNAc staining, which was not seen in the normoxic hearts. In contrast, I/R resulted in a marked loss of overall O-GlcNAc intensity together with increased number of O-GlcNAc negative nuclei, and loss of structural integrity (e.g. disorganization of myofibrils, loss of striated and manifestation of longitudinal O-GlcNAc staining). While OGA inhibitor increased overall O-GlcNAc and helped to maintain structural integrity (i.e. striated pattern); surprisingly, it did not prevent the loss of nuclear O-GlcNAc, and O-GlcNAc negative nuclei were still readily apparent.

In agreement with the immunohistochemistry, subsequent immunoblot analyses showed that although OGA inhibitors prevented the loss of O-GlcNAc in both nuclear and cytosolic fractions, the relative increases in nuclear O-GlcNAc were consistently lower compared to the cytosolic levels. The fact, that ischemia leads to a marked loss of nuclear O-GlcNAcylation has not been previously reported. However, during ischemia prominent lesions are known to occur within the cardiomyocyte nuclei, such as the disappearance of microtubules in the perinuclear space, peripheral chromatin aggregation (63), both of which are abundantly associated with O-GlcNAc, similarly to the nucleoporins (56). Given the importance of O-GlcNAc in regulating transcription, loss of nuclear O-GlcNAc could have implications for mediating transcriptional events involved in modulating cell survival and repair pathways. The consequences of the ischemia- and I/R-induced changes of nuclear O-GlcNAcylation remain to be determined. As noted, the loss of nuclear O-GlcNAc was not prevented by NAG-Bt treatment; and the recovery of nuclear O-GlcNAc levels lagged behind the cytosolic levels in both NAG-Bt and NAG-Ae treated hearts, which may simply reflect the fact that OGA is predominantly (~90 %) localized in the cytosol (56).

We also found that at the end of reperfusion decreased O-GlcNAc was associated with significantly decreased OGT in whole cardiac tissue, nuclear, mitochondrial, and

in particular, in the cytosolic fraction where high molecular weight OGT immunoreactive bands could be also observed. It is possible that I/R results in covalent modifications to OGT, thereby decreasing the amount of active OGT (110 kDa) thus cytosolic O-GlcNAc levels. These high molecular weight bands could be inactive aggregates or multimers of OGT; however, presence of a band at ~140-150 kDa suggests posttranslational modification (e.g. polyubiquitination). Since mitigated O-GlcNAc seems to be mostly evident under conditions, such as reperfusion, resuscitation, or exposure to H_2O_2, it raises the possibility that high-molecular weight OGT bands are resulting from increased ROS damage of OGT.

As shown, O-GlcNAc exhibited a clear cross-striated pattern in the cytoplasm corresponding to the Z-line regions of cardiomyocytes. This novel finding, that Z-line proteins are enriched in O-GlcNAc was confirmed by demonstrating the co-localization of O-GlcNAc with desmin and vinculin, two proteins well known to be associated with Z-lines (58, 65). Protein O-GlcNAcylation plays a role in altering the activity, function, stability, and subcellular localization of target proteins (142). Given the importance of Z-line proteins in contractile force transmission and regulating cardiomyocyte function by mediating responses to hemodynamic and mechanical stresses (58, 96), augmentation of protein O-GlcNAcylation would be predicted to convey beneficial effects to affect protection in response to I/R.

Although vinculin is one of the best characterized interacting proteins of focal adhesion complexes and is known to be activated by phosphatidylinositol 4,5-bisphosphate (33), its specific role is poorly identified. Previous studies have shown a progressive loss and/or altered subcellular localization of vinculin with ischemia that has been linked to increased cardiomyocyte fragility and the onset of irreversible injury (119, 131). Here, we did not find changes in total tissue vinculin levels, not even in the untreated, control I/R group, which may be due to the relatively short period of ischemia (20 min) compared to 60-90 min used in earlier studies. However, there was a significant decrease in membrane-associated vinculin after reperfusion. Of note, at the end of reperfusion there were some focal alterations in vinculin, such as dislocated Z-lines, higher intensity at intercalated discs due possibly to retraction of sarcomere attachments toward the intercalated discs; however, localization of vinculin to the Z-

lines and intercalated discs remained relatively conserved. Interestingly, OGA inhibitors significantly decreased vinculin phosphorylation in the membrane fraction. The physiological consequences of vinculin phosphorylation in the heart are unclear; however, disruption of interacting proteins at the focal adhesion complex in cardiomyocytes has been shown to exacerbate the ischemic injury (130). Thus, it is possible that decreased vinculin phosphorylation seen with OGA inhibitors could help to prevent the disruption of focal adhesion complexes and attenuate the loss of structural integrity observed following I/R. We found vinculin as a possible O-GlcNAc target, and that association of vinculin with OGT and O-GlcNAc was increased with OGA inhibitors following I/R. As to how O-GlcNAcylation-phosphorylation of vinculin alters the function of the heart in response to I/R injury remains to be determined.

Desmin belongs to the family of intermediate filament proteins connecting the Z-lines of adjacent myofilaments and the Z-lines to the nucleus. Desmin has been implicated in the regulation of mitochondrial metabolism, subcellular organization, and force development (65, 96). In contrast to vinculin, after reperfusion there was an overall decrease in desmin intensity accompanied by the loss of its association with Z-lines, and its reorganization into a longitudinal pattern, which were prevented by NAG-Bt treatment. In immunoblot analyses, the loss of desmin was also evident following reperfusion, which was largely attenuated by OGA inhibitors in both whole cardiac tissue and the membrane fraction. Given the significance of desmin in structural integrity and linking extracellular mechanical stress to the nucleus, protection of desmin seen with OGA inhibitors could be an important contributing factor to the improved functional recovery and decreased tissue injury. Several cytoskeletal proteins are lost during ischemia and reperfusion via increased proteolysis, and desmin is particularly susceptible to calpain-mediated proteolysis (98). Liu et al. (69) showed that increased O-GlcNAc during reperfusion attenuated activation of the Ca^{2+}-activated proteases such as calpain. Jones et al. (64) identified desmin as a potential O-GlcNAc target in the heart; thus it is also possible that O-GlcNAcylation of desmin could decrease its affinity as a calpain substrate, thereby inhibiting or slowing its proteolysis. However, it remains to be determined whether this is a direct effect of O-GlcNAc modification of desmin or secondary to overall increased O-GlcNAc.

Potential mechanisms of cardioprotection associated with NAG-thiazolines and increased O-GlcNAc have yet to be specified. Reperfusion injury involves impaired Ca^{2+}-homeostasis, increased oxidative stress, and mitochondrial dysfunction (138). It is noteworthy that functional recovery was enhanced within the first 5-10 min of reperfusion in the NBt and NAe groups, suggesting that protection resulting from OGA inhibition is likely mediated via transcriptionally independent mechanisms, such as those mentioned above. Reduced post-ischemic arrhythmic activity and improved LVDP during reperfusion seen in NBt- and NAe-treated hearts could be a result of normalized cytosolic and mitochondrial Ca^{2+} levels, respectively (138). Liu et al. (70) showed that glucosamine attenuated the Ca^{2+}-overload of the perfused heart induced by Ca^{2+}-paradox protocol. Augmented O-GlcNAc of the intact heart with PUGNAc and glucosamine decreased the activation of Ca^{2+}-sensitive proteases following I/R (69). Champattanachai et al. (23) showed that in cardiomyocytes NAG-Bt significantly reduced both apoptosis and necrosis following I/R, and attenuated the H_2O_2-induced loss of mitochondrial membrane potential. In addition, increased O-GlcNAcylation of mitochondrial proteins (e.g. voltage-dependent anion channel) protected the cardiomyocytes against lethal ROS damage by increasing mitochondrial stability (64). We found loss of the aconitase activity following reperfusion, coincident with the rapid burst in ROS production, which was prevented by OGA inhibitors. OGA inhibitors also increased the mitochondrial levels of aconitase, as well as its association with O-GlcNAc and OGT. Thus, myocardial preservation seen with OGA inhibitors in response to I/R could be due to reduced Ca^{2+}-overload, decreased oxidative stress or both.

In summary, we showed that administration of novel, selective OGA inhibitors at the time of reperfusion significantly increased cardiac O-GlcNAcylation, improved functional recovery, and attenuated tissue injury following I/R. The degree of functional recovery and reduced tissue injury showed an O-GlcNAc-dependent manner, providing strong support for the notion that increasing O-GlcNAc by inhibiting OGA at the time of reperfusion is an effective cardioprotective strategy. Cardiac proteins at the Z-line regions are highly enriched in O-GlcNAc, which given the potential role of the Z-line in mechano- and signal transduction, could have important implications for protein

O-GlcNAcylation in the heart beyond its cardioprotective effects. There is a loss of overall cardiac O-GlcNAcylation following I/R, and one consequence of ischemia and reperfusion is the redistribution of nuclear and cytoplasmic O-GlcNAc. OGA inhibition significantly attenuated the loss of desmin, a key Z-line protein and the disruption of structural integrity that occurs on reperfusion, but it did not prevent the I/R-induced loss of nuclear O-GlcNAcylation. We showed that ischemia and reperfusion alter the level of O-GlcNAc modification of glycogen phosphorylase, aconitase 2, and vinculin; however, it has yet to be determined whether and how O-GlcNAcylation of either protein could contribute to cardioprotection seen with OGA inhibitors. Links between O-GlcNAcylation and oxidative stress suggest that O-GlcNAc signaling may represent an important redox-sensing pathway that could play integral roles in the ROS-induced cellular responses thus modulating stress tolerance of the heart to I/R injury.

3. Investigations on the role of increased HBP flux and protein O-GlcNAcylation, micro-inflammatory state and oxidative stress as contributing factors to the pathogenesis of diabetes-related complications and chronic kidney disease.

3.1. *Ex vivo* experiments on the effects of increased HBP flux and protein O-GlcNAcylation on the regulation of cardiac metabolism.

An early consequence of diabetes on the heart is increased fatty acid oxidation, which contributes to the pathogenesis of diabetic cardiomyopathy (118). McClain et al. (73) reported that activation of the HBP by exogenous glucosamine and resulting increases in O-GlcNAc increased the fatty acid oxidation in adipocytes. We determined whether in the heart glucosamine induced activation of the HBP and O-GlcNAcylation altered substrate utilization to that diabetic phenotype. As expected, activation of the HBP with short-term glucosamine treatments (60 min) resulted in dose-dependent increases of UDP-GlcNAc and O-GlcNAc in the isolated perfused heart. In contrast to previous studies where high doses of glucosamine caused reduced ATP levels (76), we found no effect of glucosamine on ATP levels at any concentration.

13C-isotopomer analyses showed that glucosamine significantly increased fatty acid oxidation and decreased overall carbohydrate oxidation due primarily to reduced

lactate oxidation and a lesser extent to pyruvate oxidation. The effect of glucosamine on substrate utilization was apparent at a concentration as low as 0.05 mM with a maximal response at 0.1 mM; and even at such low glucosamine concentrations both UDP-GlcNAc and O-GlcNAc levels were significantly increased, suggesting that relatively subtle changes in HBP flux could play an important regulatory role in cardiac metabolism. Even though higher concentrations of glucosamine (1-10 mM) had no further effect on fatty acid or carbohydrate oxidation, there was a progressive increase in both UDP-GlcNAc and O-GlcNAc consistent with the notion that primary pathway for the glucosamine metabolism in the heart is via the HBP. However, glucosamine can be metabolized via other routes (e.g. glucosamine-6-phosphate can be converted to fructose-6-phosphate by the glucosamine-6-phosphate deaminase/isomerase) which could lead to increased glycolytic flux and/or glucose oxidation (28). Although, our results showed that glucosamine had no effect on either glucose oxidation or glucose-derived lactate efflux (i.e. glycolysis) thus, in the heart at least, we found no evidence of glucosamine metabolism via glycolysis and TCA cycle.

Interestingly, glucosamine induced shift in cardiac metabolism is very similar to that Wang et al. (127) previously reported in ZDF-rat hearts perfused under similar conditions. They showed that the onset of T2DM increased fatty acid oxidation and decreased carbohydrate utilization mainly due to decreased lactate oxidation while glucose oxidation was unchanged, and it was also associated with impaired cardiac contractility (127). Although we did not see impaired cardiac performance due probably to such a short-term (60 min) treatment; however, metabolic dysregulation here was very characteristic to that seen in the diabetic ZDF-rat hearts.

Luo at al. (73) reported that increased fatty acid oxidation by exogenous glucosamine was via the activation of AMPK and ACC in cultured adipocytes. They showed that transfecting adipocytes with dominant-negative AMPK blunted the glucosamine-induced effects on palmitate oxidation, and that increased fatty acid oxidation was mediated via O-GlcNAc dependent activation of AMPK. Since the Ser/Thr kinase AMPK plays a crucial role in maintaining cellular energy and metabolic homeostasis in the heart (53), we examined whether glucosamine perfusions increased the phosphorylation of AMPK and and its downstream target ACC that could

account for the increased fatty acid oxidation. In contrast to adipocytes, glucosamine had no effects on AMPK-ACC activation at any concentration, not even at 0.1 mM where increased fatty acid oxidation showed a maximal response. Remarkably, their studies focused on relatively long term glucosamine treatment (24 hours); whereas, we used acute treatments (60 min). In addition, they used 10 mM glucosamine in most of their studies, while we found a maximal response with 0.1 mM glucosamine. This does not exclude the possibility that more sustained elevation of the HBP flux and O-GlcNAcylation in the heart could also lead to O-GlcNAc modification of AMPK and increased ACC phosphorylation. Alternatively, it is conceivable that HBP activation has a tissue specific effect on AMPK regulation therefore the paradox can be explained by differences between the adipose and cardiac tissue.

Another potential mechanism for regulating cardiac fatty acid metabolism is via the plasma membrane levels of fatty acid transporter proteins such as FAT/CD36, which is responsible for ~50-80% of the fatty acid uptake in the heart (15). Typically, upon different stimuli (e.g. insulin, increased cardiac work), FAT/CD36 translocates from the intracellular storage compartments to the plasma membrane, thereby facilitating fatty acid oxidation. In addition, increased myocardial fatty acid oxidation in diabetes has been linked to increased fatty acid transport and plasma membrane FAT/CD36 expression (30). Therefore, we examined FAT/CD36 levels in plasma membrane preparations, and found that glucosamine dose-dependently increased membrane-associated FAT/CD36. Moreover, FAT/CD36 appeared to be targeted by O-GlcNAc, especially in the membrane fraction, and it was also associated with OGT. Thus, the glucosamine induced increase in palmitate oxidation may be due, at least in part, to increased plasma membrane levels of FAT/CD36, possibly as a direct result of increased O-GlcNAc modification of FAT/CD36.

It is worth noting that increased myocardial fatty acid utilization in diabetes has been attributed initially to an increase in circulating lipids contributing to lipotoxicity, mitochondrial dysfunction, and impaired myocardial bioenergetics (5). While we did not measure the rates of fatty acid transport across the plasma membrane, previous studies have demonstrated a close relationship between membrane-associated FAT/CD36 and rates of fatty acid transport (72). Moreover, increased sarcolemmal

abundance of FAT/CD36 has been shown to be a result of impaired recycling between intracellular storage compartments and the sarcolemma (30). Since diabetes is known to increase cardiac O-GlcNAc, it is possible, that in the diabetic heart O-GlcNAcylation of FAT/CD36 may shift the balance towards sarcolemmal localization of FAT/CD36 possibly by inhibiting recycling. Notably, while the increase in fatty acid oxidation was maximal at 0.1 mM glucosamine, FAT/CD36 levels continued to increase up to 5-10 mM glucosamine, similarly the increases in O-GlcNAc. This dissociation between increased FAT/CD36 and fatty acid oxidation is consistent with studies in skeletal muscle from obese rats where excess fatty acid uptake was channeled primarily to esterification rather than oxidation (57). Although, we did not assess the effects of glucosamine on triglyceride levels, it raises the possibility that increased O-GlcNAc of the diabetic heart could be a contributing factor to the accumulation of lipid intermediates involved in lipotoxicity.

Although a definitive cause-effect relationship has not been shown, our results indicate that effects of glucosamine on myocardial substrate utilization (i.e. increased palmitate oxidation) and membrane-associated FAT/CD36 levels are mediated via increased HBP flux and O-GlcNAc levels. These can be supported by novel data showing that in the working rat heart glutamine had similar effect on fatty acid metabolism to that seen with glucosamine and it could be inhibited by azaserine (i.e. GFAT inhibitor). Moreover, glucosamine increased fatty acid oxidation more than glutamine in the normal heart, but it had no effect in SHR/spontaneous hypertensive rat/-hearts which have a mutant/defective FAT/CD36 (personal communications). However, we still cannot rule out the possibility that increases in UDP-GlcNAc or other intermediates in the HBP could influence carbohydrate and fatty acid oxidation via other mechanisms. An ideal approach, would to be to show that inhibition of OGT blocked the effects of glucosamine; however, to date pharmacological approaches for inhibiting OGT in the perfused heart model have been limited to either non-specific (i.e. alloxan) or toxic (TT04) agents.

In summary, we showed that acute activation of the HBP in the isolated perfused rat heart with glucosamine significantly increased fatty acid oxidation and decreased total carbohydrate oxidation at relatively low concentrations, and this was associated

with increased overall cardiac O-GlcNAcylation. We also found that increased fatty acid oxidation appeared to be a consequence of glucosamine-dependent increases in FAT/CD36 protein levels at the plasma membrane rather than alterations in AMPK or ACC activity. Preliminary studies also indicate that FAT/CD36 may be subject to O-GlcNAc modification. In conclusion, HBP flux and O-GlcNAc turnover represent a novel, glucose dependent posttranslational mechanism for the acute regulation of cardiac metabolism. In addition, activation of the HBP flux and O-GlcNAcylation with glucosamine alters cardiac substrate utilization similar to that seen in the diabetic heart. Given that diabetes leads to chronically elevated O-GlcNAc levels, increased HBP flux and O-GlcNAcylation may also be involved in the pathogenesis of diabetic cardiomyopathy.

3.2. *Clinical study* to investigate effectiveness of the anti-inflammatory pentoxifylline and pentosan polysulfate combination therapy on diabetic neuropathy and albuminuria in type 2 diabetic patients.

There is a growing body of data demonstrating that increased oxidative stress and chronic low-grade inflammation are important pathogenic factors in the development and progression of diabetic microvascular complications (110). Based on significant pro-circulatory, anti-inflammatory, and anti-proteinuric actions of PF and PPS, we purposed to determine the therapeutic efficacy of combined PF-PPS infusions on cardiovascular autonomic functions, vibration perception, and albuminuria. This placebo-controlled study involved n=89 patients with T2DM presenting at least one characteristic symptom of distal peripheral sensory neuropathy. The most prevalent signs were burning and spastic pain, numbness, itchy predominantly localized at the lower extremities. There were no significant differences in age, gender, T2DM duration (14 years), body mass index (BMI), and renal function in patients treated with PF-PPS infusions (Verum) compared to those who received sham-infusions (Placebo). There were no significant differences in ACE-I and/or ARB, statin, or anti-platelet therapy between the groups. Although a small number of side effects may occur with PF and

PPS (e.g. flush, nausea, allergy, tachycardia or angina), PF-PPS infusions were well-tolerated, and adverse effects or infusion-related complications were not noticed.

At baseline, there were no differences in CA-N tests, vibration threshold values, and albuminuria between the Verum and Placebo groups. There were significant correlations between autonomic score and T2DM duration and vibration threshold values, consistent with the notion that autonomic neuropathies generally occur after longer duration of diabetes, and that CA-N often coexists with other peripheral neuropathies (125). Before therapy, 53% of study participants exhibited explicit or severe, and 40% mild CA-N as determined by autonomic score, indicating that CA-N is not simply an `all-or-nothing` phenomenon, both mild and severe cases could be present (i.e. ≥ 3 out the six CA-N tests are abnormal). Commonly, reduced heart rate variability is one of the earliest signs of parasympathetic impairment in CA-N, while resting tachycardia is usually a late finding in diabetic patients (125). Before therapy, 35% of all studied patients had impaired vibration threshold values. There was a significant inverse relationship between vibration threshold values and fructosamine levels, indicating a stronger association between large sensory nerve dysfunction and the adverse effects of `brief` hyperglycemic episodes (21).

Importantly, PF-PPS infusions significantly decreased the autonomic score in the Verum group, indicating an overall improvement of the cardiovascular autonomic responses. Consistently, there was increasing number of patients in the Verum group showing mild abnormalities or normal CA-N tests after the therapy. In contrast, there were no changes in any of the responses or the autonomic score in the Placebo group. Of the CA-N tests, we found that PF-PPS significantly improved the response to deep breath test as reflected by increased heart rate variability, as well as the response to handgrip test as indicated by increased diastolic blood pressure rise upon isometric exercise. While other CA-N tests remained unaltered with PF-PPS infusions, and there were also no changes in the resting heart rate that stayed normal. It is noteworthy that before therapy a larger proportion of the Verum group patients exhibited abnormal responses to both deep breath (61%) and handgrip (62%) tests, and only a small number of patients showed abnormal Valsalva test (7%), 30/15 ratio (1%), and postural blood pressure fall (12%). Consequently, these parameters due to low

prevalence could not have been substantially influenced by PF-PPS therapy. It can be also seen that most of the Verum group patients showed mixed parasympathetic (i.e. reduced heart rate variability) and sympathetic impairment (i.e. abnormal handgrip test), both of which were improved by PF-PPS therapy.

PF-PPS infusions significantly increased vibration threshold values in the Verum group, while there were no changes in the Placebo group after sham-infusions. This seems contrary to earlier reports showing that PF although reduced certain symptoms of the distal sensory peripheral neuropathy (e.g. pain, paresthesias), it had no significant effect when compared to placebo (26, 27, 67). However, in these studies PF was administered orally and for longer periods (3-12 months). In addition to different study protocols, we used PF in combination with PPS, which has not been examined in the management of peripheral neuropathy, and this could also explain the disparate findings.

It should be noted that there is a considerable `placebo effect` during treatment of any, if not all, forms of neuropathies, which should be taken into account, especially when `curative infusions` are applied (14). Although, visual analog scale has not been conducted, upon surveys the Verum group patients reported significant improvements of their symptoms, such as burning pain and numbness, while these remained unaltered by sham-infusions in patients of the Placebo group. Nevertheless, we found that PF-PPS infusions significantly improved both autonomic score and vibration threshold values as assessed by objective and reproducible tests. It is also acknowledged that specific mechanisms by which PF-PPS improved CA-N and vibration perception have not been examined. However, we believe that both pro-circulatory and anti-inflammatory effects of PF-PPS contributed to the amended CA-N and vibration perception found here.

Albuminuria is a surrogate marker of chronic inflammation and endothelial dysfunction in CKD, including the diabetic kidney disease (120). While we found that most of the study participants (93%) showed impaired CA-N tests and in a lesser degree impaired vibration perception (35%), the majority of patients had normalbuminuria in both groups (Verum: n=47; 70% and Placebo: n=9; 82%). Diabetic neuropathy, and above all the autonomic dysfunctions may be isolated preceding the

manifestation of other diabetic microangiopathy (i.e. nephropathy) (134). However, the majority of all studied patients (Verum: n=59; 80% and Placebo: n=12; 100%) was on RAS-inhibitors which are evidently renoprotective by preventing the progression of albuminuria (107), and this could explain the higher incidence of CA-N that of increased albuminuria seen here. It also suggests that protective effects of RAS-inhibitors may be minor to delay the manifestation and progression of diabetic neuropathy that of nephropathy, at least in these study cohorts.

Our results showed that PF-PPS infusions had no effect on albuminuria, not even on microalbuminuria found in a small number of patients in the Verum group (n=8). Several reports in T2DM nephropathy demonstrated significant anti-proteinuric effects of PF when added on to ACE-I and/or ARB therapy or when administered alone (54, 109, 115). However, in most of these studies PF reduced the albuminuria after long-term administration at relatively high doses (400-1200 mg), and only in cases of more advanced nephropathy (i.e. micro- and macroalbuminuria). Therefore, as found here, it is likely that anti-proteinuric effect of PF could be afforded within the normal range. On the other hand, short duration (5 days) and/or low dose of PF (100 mg) may be also insufficient to convey reduction in albuminuria. Clearly, randomised, well-designed, multicentre studies are warranted to better characterize the benefits and provide evidenced-based recommendation for PF and PPS in the management of diabetic microangiopathy.

In summary, short-time infusion therapy with PF-PPS, two pro-circulatory and anti-inflammatory drugs, significantly improved CA-N and vibration perception in T2DM patients. In this study cohort, majority of patients exhibited CA-N affecting both parasympathetic and sympathetic functions, of which impaired heart rate variability and handgrip test were significantly improved by PF-PPS therapy. Cardiovascular autonomic dysfunctions correlated with both T2DM duration and impaired vibration perception, which showed stronger relationship with increased fructosamine levels. Majority of studied patients had normalbuminuria possibly due to a higher rate of RAS-inhibitor treatment. Although combination of PF-PPS attenuated both autonomic and sensory neuropathy, it had no effect on urinary albumin excretion within the normal range. Conclusively, short-term administration of PF-PPS (5 days iv.) in regular

intervals may be a cost-effective, complementary therapeutic strategy to improve CA-N and peripheral sensory neuropathy, predominantly among hospitalized T2DM patients.

3.3. *Clinical study* to investigate erythropoietin resistance and the effects of the anti-inflammatory acetylsalicylic acid on anemia correction in type 2 diabetes mellitus and chronic kidney disease.

EPO resistance was investigated in a cross-section study by comparing four groups of subjects with T2DM (DM), chronic kidney disease (CKD) or both (DM+CKD), and healthy individuals (CONTR group). There were no differences between any of the groups in age, gender, and serum EPO that was measured in the mornings to avoid circadian changes. Despite comparable endogenous EPO levels, we found that all three patient groups (DM, CKD, and DM+CKD) had more severe anemia as indicated by lower hematocrit and hemoglobin values compared to the CONTR group. The DM+CKD group had the highest degree of anemia exhibiting lower hematocrit and hemoglobin values compared to both DM and CKD groups that were matched for glucose metabolism and renal failure, respectively. Thus, patients suffering from both conditions, T2DM and CKD (i.e. diabetic nephropathy) showed the highest degree of EPO resistance. This is consistent with the notion that anemia occurs earlier and it is more severe in diabetic CKD than in non-diabetic CKD (88) contributing to the higher risk of ischemic organ damage thus the progression of CKD and cardiovascular disease in this patient population (107). Red blood cell properties were in the normal range in all patient groups and the CONTR group, and there were no significant differences between any of the groups. These data indicate that anemia of the patient groups (DM, DM+CKD, and CKD) was normocyter in nature and was unrelated to deficiencies (e.g. iron, folic acid, vitamin B_{12}).

We found no significant correlations between serum EPO and hematocrit- and hemoglobin values in any of the patient groups (DM, DM+CKD, and CKD) indicating indeed the presence EPO resistance in these study cohorts. It is worth noting that two groups of patients with renal failure (DM+CKD and CKD) exhibited comparable serum creatinine levels suggesting that these patients were similarly over-hydrated due to

water retention associated with CKD; thus differences in the fluid overload were unlikely to account for the discrepancy in hematocrit values seen here. In fact, diabetic patients are very often dehydrated due to osmotic diuresis, which would rather lead to increases than decreases in hematocrit and hemoglobin values. Nevertheless, hematocrit and hemoglobin levels were significantly lower in the DM+CKD group compared to the CKD group. Patients in the DM+CKD group had longer diabetes duration compared to the DM group (20±3 vs. 13±2 years), consistent with the notion that diabetic nephropathy is a late onset microangiopathy in the course of T2DM. There were no differences in glycemia and glycation parameters between the two diabetic groups (DM, DM+CKD), thus it seems unlikely that modification of EPO with glycation substantially contributed to EPO resistance seen in the DM+CKD patients.

In the background of EPO resistance, we also evaluated several parameters (age, serum creatinine, hemoglobin A1c, fructosamine, serum glucose, total cholesterol, HDL cholesterol, systolic blood pressure, BMI, triglyceride) in correction analyses. We did not find significant relationships between serum EPO and hematocrit in any of the groups, except in the DM group, and only after corrections for BMI and triglyceride levels. This is suggesting that somewhat triglycerides and obesity may be involved in inducing EPO resistance in T2DM patients. It is noteworthy that there is a close relationship of increased cytokine production (e.g. TNF-α) and inflammatory markers (e.g. CRP) with insulin resistance and obesity via increased lipolysis and hypertriglyceridemia (110). The pro-inflammatory cytokines have been shown to interfere with EPO-mediated signaling pathways leading to early apoptosis of erythroids and/or dysregulation of transcription factors involved in erythroid differentiation (84). Because BMI and triglyceride levels did not differ in DM and DM+CKD groups, EPO resistance most likely involves additional mechanisms in diabetics with nephropathy (DM+CKD) compared to those without (DM). Although neither insulin resistance nor the levels of inflammatory markers were determined, the effects on EPO resistance might be different in these two diabetic cohorts.

In our intervention study, subgroup of patients with T2DM and/or CKD exhibiting low baseline EPO levels was involved and a single, high-dose (1 gram) of ASA was administered. We found that ASA markedly improved anemia and increased EPO

levels (~59%), supporting the notion that pro-inflammatory processes and oxidative stress most likely contribute to the loss and/or ineffectiveness of EPO. ASA also significantly increased the reticulocyte count by 33%, the reticulocyte ratio by 14%, the red blood cell count by 7%, the hemoglobin levels by 6%, and the hematocrit values by 8%; surprisingly, however, ASA decreased serum LDH activity by 12%.

It is well-recognized that EPO promotes erythropoiesis by directly acting on erythroid progenitors in the bone marrow. However, there is an alternative mechanism, independent of bone marrow, by which EPO could increase red blood cell count and which could also explain the substantial increases in reticulocyte number and ratio found here. Briefly, on high altitude, low oxygen tension leads to increased EPO production, while on return to the sea level there is a rapid decline in EPO levels; this EPO `withdrawal` results in the selective destruction of young erythrocytes (neocytes), a process termed neocytolysis (103). Neocytolysis has been first described in astronauts who had a sudden drop in EPO levels under microgravity accompanied by decreases (~10-15%) in total red blood cell count (103). Neocytolysis has been also noticed in patients with CKD after the withdrawal of EPO therapy (104). Neocytolysis itself is an inflammatory response evoked by a sudden fall in EPO leading to the activation of endothelial cells and macrophages in the spleen, which then phagocyte the young, matured, circulating red blood cells resulting in hemolysis and increased LDH activity (103). Rice et al. (105) demonstrated that administration of low-dose EPO at see level to nine healthy volunteers who were acclimatized to high altitude, prevented the neocytolysis and concomitant increases in LDH activity.

Convincingly, our results raised an intriguing possibility that ASA via its anti-inflammatory effect may inhibit neocytolysis by increasing EPO levels (referred as `neocytosalvation`). This is supported by data showing that ASA significantly increased EPO levels in such a short-term (48 hours), and resultant, time-dependent increases in red blood cell count (7%) lagged behind the increases in reticulocyte number (33%); moreover, this was accompanied by decreased LDH (12%), an opposite to hemolysis. It cannot be ruled out that ASA therapy long-term promotes EPO production as well as the responsiveness to EPO and thus corrects anemia of patients with T2DM and CKD. Chronic ASA therapy (100–325 mg/day) is evidently advantageous in patients with

high cardiovascular risk; further studies would be necessary to investigate whether same ASA dosages as used routinely for cardiovascular prevention could also improve the hematological state of patients with T2DM and CKD.

In summary, we found that both T2DM and CKD can induce EPO resistance, and coexistence of both conditions in patients with diabetic nephropathy shows an additive effect on EPO resistance resulting in higher degree of normocyter anemia. We showed that treatment with the anti-inflammatory and hydroxyl free radical scavenger ASA resulted in significant increases in EPO levels as well as ameliorated anemia, supporting the notion that pro-inflammatory processes and oxidative stress most likely contribute to reduced synthesis and/or ineffectiveness of endogenous EPO, thus anemia in patients with T2DM and/or CKD. We also demonstrated that ASA administration via its anti-inhibitory effect and subsequent acute increases in serum EPO inhibited the rate of neocytolysis and salvaged the young, circulating red blood cells (`neocytosalvation`). These results also indicate that neocytolysis (due to low EPO and increased inflammation) may be an alternative mechanism responsible for the anemia in patients with T2DM and CKD.

Ph.D. THESES

1) Acute effects of cigarette smoke result in endothelial dysfunction via altered posttranslational eNOS modifications in endothelial cells.

- Cigarette smoke in endothelial cells increases the inhibitory eNOS phosphorylation at Thr(495) and the level of catalytically inactive eNOS monomers, both of which could contribute to reduced NO availability and thus the progression of vascular diseases.
- GSH diminishes the cigarette smoke induced pro-oxidant responses on eNOS modifications by preventing its inhibitory phosphorylation and the disruption of homodimeric eNOS, both of which could contribute to preserved NOS activity and NO production.
- Acute increases of eNOS phosphorylations to cigarette smoke appear to be independently regulated by the PI3-K/Akt pathway, whereas PKC/PKCβII pathway seems responsible for the increased inhibitory eNOS phosphorylation at Thr(495). PKCßII inhibition could be a promising strategy to prevent the adverse effects of cigarette smoke.

2) Augmentation of protein O-GlcNAcylation is an effective cardioprotective strategy following ischemia-reperfusion in the isolated heart.

- Selective inhibition of OGA at the time of reperfusion by NAG-thiazolines improves functional recovery and attenuates tissue injury of the isolated heart in an O-GlcNAc dependent manner.
- Reperfusion injury associated with increased oxidative stress decreases overall O-GlcNAcylation of cardiac proteins and the OGT levels, both of which could be prevented by NAG-thiazolines.
- Myocardial proteins within the nuclei and at the Z-line regions are highly enriched in O-GlcNAc, and one consequence of ischemia and I/R is the redistribution of O-GlcNAc-modified proteins and OGT in the heart.
- Selective inhibition of OGA at the time of reperfusion by NAG-thiazolines maintains cardiac structural integrity and attenuates the I/R-induced changes of Z-line proteins in an O-GlcNAc dependent manner.

3) Activation of the HBP and protein O-GlcNAcylation represents a novel mechanism for the regulation of cardiac metabolism.

- Activation of the HBP and protein O-GlcNAcylation with glucosamine in the intact heart results in increased fatty acid utilization and decreased carbohydrate oxidation, similarly to that seen in the diabetic heart.
- Altered substrate utilization with glucosamine in the heart is unrelated to the activation of AMPK and ACC.
- Glucosamine-induced augmentation of fatty acid oxidation appears to be a consequence of increased membrane-associated FAT/CD36 levels, possibly via increased O-GlcNAc modification of FAT/CD36.

4) Combination of pentoxifylline and pentosan polysulfate infusion therapy is an effective approach to improve cardiovascular autonomic and peripheral sensory neuropathy in type 2 diabetic patients.

- Short-time infusion therapy with pentoxifylline and pentosan polysulfate, two pro-circulatory and anti-inflammatory drugs, improves cardiovascular autonomic functions and vibration perception in patients with T2DM.
- Combined pentoxifylline and pentosan polysulfate infusions have no effect on albuminuria within the normal range.

5) Treatment with acetylsalicylic acid increases EPO levels and ameliorates anemia in patients with type 2 diabetes mellitus and chronic kidney disease.

- Both T2DM and CKD cause EPO resistance, and there is a higher degree of EPO resistance and anemia when both conditions are present in diabetic nephropathy.
- Treatment with the anti-inflammatory and hydroxyl free radical scavenger ASA increases EPO levels and corrects anemia in patients with T2DM and CKD, at least in part, by inhibiting the rate of neocytolysis.

REFERENCES

1. United kingdom prospective diabetes study (UKPDS). 13: relative efficacy of randomly allocated diet, sulphonylurea, insulin, or metformin in patients with newly diagnosed non-insulin dependent diabetes followed for three years. *Br Med J* 310: 83-88, 1995.
2. **Akimoto Y, Kawakami H, Yamamoto K, Munetomo E, Hida T, Hirano H.** Elevated expression of O-GlcNAc-modified proteins and O-GlcNAc transferase in corneas of diabetic Goto-Kakizaki rats. *Invest Ophthalmol Vis Sci* 44: 3802-3809, 2003.
3. **Alderton WK, Cooper CE, Knowles RG.** Nitric oxide synthases: structure, function and inhibition. *Biochem J* 357: 593-615, 2001.
4. **Ametov AS, Barinov A, Dyck PJ, Hermann R, Kozlova N, Litchy WJ, Low PA, Nehrdich D, Novosadova M, O'Brien PC, Reljanovic M, Samigullin R, Schuette K, Strokov I, Tritschler HJ, Wessel K, Yakhno N, Ziegler D.** The sensory symptoms of diabetic polyneuropathy are improved with alpha-lipoic acid: the SYDNEY trial. *Diabetes Care* 26: 770-776, 2003.
5. **An D and Rodrigues B.** Role of changes in cardiac metabolism in development of diabetic cardiomyopathy. *Am J Physiol Heart Circ Physiol* 291: H1489-1506, 2006.
6. **Bae SW, Kim HS, Cha YN, Park YS, Jo SA, Jo I.** Rapid increase in endothelial nitric oxide production by bradykinin is mediated by protein kinase A signaling pathway. *Biochem Biophys Res Commun* 306: 981-987, 2003.
7. **Barua RS, Ambrose JA, Srivastava S, DeVoe MC, Eales-Reynolds LJ.** Reactive oxygen species are involved in smoking-induced dysfunction of nitric oxide biosynthesis and upregulation of endothelial nitric oxide synthase: an in vitro demonstration in human coronary artery endothelial cells. *Circulation* 107: 2342-2347, 2003.
8. **Beckman JA, Goldfine AB, Gordon MB, Garrett LA, Creager MA.** Inhibition of protein kinase Cbeta prevents impaired endothelium-dependent vasodilation caused by hyperglycemia in humans. *Circ Res* 90: 107-111, 2002.
9. **Bilous R.** Anaemia--a diabetologist's dilemma? *Acta Diabetol* 39 Suppl 1: S15-19, 2002.
10. **Bobadilla NA, Tack I, Tapia E, Sanchez-Lozada LG, Santamaria J, Jimenez F, Striker LJ, Striker GE, Herrera-Acosta J.** Pentosan polysulfate prevents glomerular hypertension and structural injury despite persisting hypertension in 5/6 nephrectomy rats. *J Am Soc Nephrol* 12: 2080-2087, 2001.
11. **Bolli R, Becker L, Gross G, Mentzer R, Jr., Balshaw D, Lathrop DA.** Myocardial protection at a crossroads: the need for translation into clinical therapy. *Circ Res* 95: 125-134, 2004.
12. **Boo YC and Jo H.** Flow-dependent regulation of endothelial nitric oxide synthase: role of protein kinases. *Am J Physiol Cell Physiol* 285: C499-508, 2003.
13. **Boudina S and Abel ED.** Diabetic cardiomyopathy revisited. *Circulation* 115: 3213-3223, 2007.
14. **Boulton AJ, Vinik AI, Arezzo JC, Bril V, Feldman EL, Freeman R, Malik RA, Maser RE, Sosenko JM, Ziegler D.** Diabetic neuropathies: a statement by the American Diabetes Association. *Diabetes Care* 28: 956-962, 2005.
15. **Brinkmann JF, Abumrad NA, Ibrahimi A, van der Vusse GJ, Glatz JF.** New insights into long-chain fatty acid uptake by heart muscle: a crucial role for fatty acid translocase/CD36. *Biochem J* 367: 561-570, 2002.
16. **Brownlee M.** The pathobiology of diabetic complications: a unifying mechanism. *Diabetes* 54: 1615-1625, 2005.
17. **Budhiraja S and Singh J.** Protein kinase C beta inhibitors: a new therapeutic target for diabetic nephropathy and vascular complications. *Fundam Clin Pharmacol* 22: 231-240, 2008.
18. **Buse MG.** Hexosamines, insulin resistance, and the complications of diabetes: current status. *Am J Physiol Endocrinol Metab* 290: E1-E8, 2006.
19. **Butkinaree C, Park K, Hart GW.** O-linked beta-N-acetylglucosamine (O-GlcNAc): Extensive crosstalk with phosphorylation to regulate signaling and transcription in response to nutrients and stress. *Biochim Biophys Acta* 1800: 96-106, 2010.
20. **Cale JM and Bird IM.** Inhibition of MEK/ERK1/2 signalling alters endothelial nitric oxide synthase activity in an agonist-dependent manner. *Biochem J* 398: 279-288, 2006.
21. **Cameron NE, Eaton SE, Cotter MA, Tesfaye S.** Vascular factors and metabolic interactions in the pathogenesis of diabetic neuropathy. *Diabetologia* 44: 1973-1988, 2001.
22. **Carnevali S, Petruzzelli S, Longoni B, Vanacore R, Barale R, Cipollini M, Scatena F, Paggiaro P, Celi A, Giuntini C.** Cigarette smoke extract induces oxidative stress and apoptosis in human lung fibroblasts. *Am J Physiol Lung Cell Mol Physiol* 284: L955-963, 2003.
23. **Champattanachai V, Marchase RB, Chatham JC.** Glucosamine protects neonatal cardiomyocytes from ischemia-reperfusion injury via increased protein O-GlcNAc and increased mitochondrial Bcl-2. *Am J Physiol Cell Physiol* 294: C1509-1520, 2008.
24. **Chatham JC, Gao Z-P, Forder JR.** The impact of 1 wk of diabetes on the regulation of myocardial carbohydrate and fatty acid oxidation. *Am J Physiol Endocrinol Metab* 277: E342-E351, 1999.
25. **Clark RJ, McDonough PM, Swanson E, Trost SU, Suzuki M, Fukuda M, Dillmann WH.** Diabetes and the accompanying hyperglycemia impairs cardiomyocyte cycling through increased nuclear O-GlcNAcylation. *J Biol Chem* 278: 44230-44237, 2003.
26. **Cohen KL, Lucibello FE, Chomiak M.** Lack of effect of clonidine and pentoxifylline in short-term therapy of diabetic peripheral neuropathy. *Diabetes Care* 13: 1074-1077, 1990.
27. **Cohen SM and Mathews T.** Pentoxifylline in the treatment of distal diabetic neuropathy. *Angiology* 42: 741-746, 1991.
28. **Comb DG and Roseman S.** Glucosamine metabolism. IV. Glucosamine-6-phosphate deaminase. *J Biol Chem* 232: 807-827, 1958.
29. **Comer FI, Vosseller K, Wells L, Accavitti MA, Hart GW.** Characterization of a mouse monoclonal antibody specific for O-linked N-acetylglucosamine. *Anal Biochem* 293: 169-177, 2001.
30. **Coort SL, Bonen A, van der Vusse GJ, Glatz JF, Luiken JJ.** Cardiac substrate uptake and metabolism in obesity and type-2 diabetes: role of sarcolemmal substrate transporters. *Mol Cell Biochem* 299: 5-18, 2007.
31. **Copeland RJ, Bullen JW, Hart GW.** Cross-talk between GlcNAcylation and phosphorylation: roles in insulin resistance and glucose toxicity. *Am J Physiol Endocrinol Metab* 295: E17-28, 2008.
32. **Coppini DV, Wellmer A, Weng C, Young PJ, Anand P, Sonksen PH.** The natural history of diabetic peripheral neuropathy determined by a 12 year prospective study using vibration perception thresholds. *J Clin Neurosci* 8: 520-524, 2001.
33. **Critchley DR.** Cytoskeletal proteins talin and vinculin in integrin-mediated adhesion. *Biochem Soc Trans* 32: 831-836, 2004.
34. **Degrell P, Cseh J, Mohas M, Molnar GA, Pajor L, Chatham JC, Fülöp N, Wittmann I.** Evidence of O-linked N-acetylglucosamine in diabetic nephropathy. *Life Sci* 84: 389-393, 2009.
35. **Del Vecchio L, Cavalli A, Tucci B, Locatelli F.** Chronic kidney disease-associated anemia: new remedies. *Curr Opin Investig Drugs* 11: 1030-1038, 2010.
36. **Dimmeler S, Fleming I, Fisslthaler B, Hermann C, Busse R, Zeiher AM.** Activation of nitric oxide synthase in endothelial cells by Akt-dependent phosphorylation. *Nature* 399: 601-605, 1999.

37. **Du XL, Edelstein D, Dimmeler S, Ju Q, Sui C, Brownlee M.** Hyperglycemia inhibits endothelial nitric oxide synthase activity by posttranslational modification at the Akt site. *J Clin Invest* 108: 1341-1348, 2001.
38. **Ewing DJ, Martyn CN, Young RJ, Clarke BF.** The value of cardiovascular autonomic function tests: 10 years experience in diabetes. *Diabetes Care* 8: 491-498, 1985.
39. **Federici M, Menghini R, Mauriello A, Hribal ML, Ferrelli F, Lauro D, Sbraccia P, Spagnoli LG, Sesti G, Lauro R.** Insulin-dependent activation of endothelial nitric oxide synthase is impaired by O-linked glycosylation modification of signaling proteins in human coronary endothelial cells. *Circulation* 106: 466-472, 2002.
40. **Ferrari E, Fioravanti M, Patti AL, Viola C, Solerte SB.** Effects of long-term treatment (4 years) with pentoxifylline on haemorheological changes and vascular complications in diabetic patients. *Pharmatherapeutica* 5: 26-39, 1987.
41. **Ferrari P, Mallon D, Trinder D, Olynyk JK.** Pentoxifylline improves haemoglobin and interleukin-6 levels in chronic kidney disease. *Nephrology (Carlton)* 15: 344-349, 2010.
42. **Ferreira AC and Macedo FY.** A review of simple, non-invasive means of assessing peripheral arterial disease and implications for medical management. *Ann Med* 42: 139-150, 2010.
43. **Fleming I, Fisslthaler B, Dimmeler S, Kemp BE, Busse R.** Phosphorylation of Thr(495) regulates Ca(2+)/calmodulin-dependent endothelial nitric oxide synthase activity. *Circ Res* 88: E68-75, 2001.
44. **Freyburger G, Larrue F, Manciet G, Lorient-Roudaut MF, Larrue J, Boisseau MR.** Hemorheological changes in elderly subjects--effect of pentosan polysulfate and possible role of leucocyte arachidonic acid metabolism. *Thromb Haemost* 57: 322-325, 1987.
45. **Fülöp N, Mason MM, Dutta K, Wang P, Davidoff AJ, Marchase RB, Chatham JC.** The impact of Type-2 diabetes and aging on cardiomyocyte function and O-Linked N-acetylglucosamine levels in the heart. *Am J Physiol Cell Physiol* 292: C1370-1378, 2007.
46. **Fülöp N, Zhang Z, Marchase RB, Chatham JC.** Glucosamine cardioprotection in perfused rat heart associated with increased O-Linked N-acetylglucosamine protein modification and altered p38 activation. *Am J Physiol Heart Circ Physiol* 292: H2227-2236, 2007.
47. **Fulton D, Gratton JP, McCabe TJ, Fontana J, Fujio Y, Walsh K, Franke TF, Papapetropoulos A, Sessa WC.** Regulation of endothelium-derived nitric oxide production by the protein kinase Akt. *Nature* 399: 597-601, 1999.
48. **Gallucci MT, Lubrano R, Meloni C, Morosetti M, Manca di Villahermosa S, Scoppi P, Palombo G, Castello MA, Casciani CU.** Red blood cell membrane lipid peroxidation and resistance to erythropoietin therapy in hemodialysis patients. *Clin Nephrol* 52: 239-245, 1999.
49. **Gerritsen J, Dekker JM, TenVoorde BJ, Kostense PJ, Heine RJ, Bouter LM, Heethaar RM, Stehouwer CD.** Impaired autonomic function is associated with increased mortality, especially in subjects with diabetes, hypertension, or a history of cardiovascular disease: the Hoorn Study. *Diabetes Care* 24: 1793-1798, 2001.
50. **Gloster TM and Vocadlo DJ.** Mechanism, Structure, and Inhibition of O-GlcNAc Processing Enzymes. *Curr Signal Transduct Ther* 5: 74-91, 2010.
51. **Guan Z, Fuller BS, Yamamoto T, Cook AK, Pollock JS, Inscho EW.** Pentosan Polysulfate Treatment Preserves Renal Autoregulation in Ang II-Infused Hypertensive Rats via Normalization of P2X1 Receptor Activation. *Am J Physiol Renal Physiol* doi:10.1152/ajprenal.00743.2009 2010.
52. **Han KH, Han SY, Kim HS, Kang YS, Cha DR.** Prolonged administration enhances the renoprotective effect of pentoxifylline via anti-inflammatory activity in streptozotocin-induced diabetic nephropathy. *Inflammation* 33: 137-143, 2009.
53. **Hardie DG.** AMPK: a key regulator of energy balance in the single cell and the whole organism. *Int J Obes (Lond)* 32 Suppl 4: S7-12, 2008.
54. **Harmankaya O, Seber S, Yilmaz M.** Combination of pentoxifylline with angiotensin converting enzyme inhibitors produces an additional reduction in microalbuminuria in hypertensive type 2 diabetic patients. *Ren Fail* 25: 465-470, 2003.
55. **Harris MB, Ju H, Venema VJ, Liang H, Zou R, Michell BJ, Chen ZP, Kemp BE, Venema RC.** Reciprocal phosphorylation and regulation of endothelial nitric-oxide synthase in response to bradykinin stimulation. *J Biol Chem* 276: 16587-16591, 2001.
56. **Hart GW, Housley MP, Slawson C.** Cycling of O-linked beta-N-acetylglucosamine on nucleocytoplasmic proteins. *Nature* 446: 1017-1022, 2007.
57. **Holloway GP, Benton CR, Mullen KL, Yoshida Y, Snook LA, Han XX, Glatz JF, Luiken JJ, Lally J, Dyck DJ, Bonen A.** In obese rat muscle transport of palmitate is increased and is channeled to triacylglycerol storage despite an increase in mitochondrial palmitate oxidation. *Am J Physiol Endocrinol Metab* 296: E738-747, 2009.
58. **Hoshijima M.** Mechanical stress-strain sensors embedded in cardiac cytoskeleton: Z disk, titin, and associated structures. *Am J Physiol Heart Circ Physiol* 290: H1313-1325, 2006.
59. **Hu Y, Belke D, Suarez J, Swanson E, Clark R, Hoshijima M, Dillmann WH.** Adenovirus-mediated overexpression of O-GlcNAcase improves contractile function in the diabetic heart. *Circ Res* 96: 1006-1013, 2005.
60. **Huang LE, Arany Z, Livingston DM, Bunn HF.** Activation of hypoxia-inducible transcription factor depends primarily upon redox-sensitive stabilization of its alpha subunit. *J Biol Chem* 271: 32253-32259, 1996.
61. **Huggins CE, Bell JR, Pepe S, Delbridge LM.** Benchmarking ventricular arrhythmias in the mouse--revisiting the 'Lambeth Conventions' 20 years on. *Heart Lung Circ* 17: 445-450, 2008.
62. **James LR, Fantus IG, Goldberg H, Ly H, Scholey JW.** Overexpression of GFAT activates PAI-1 promoter in mesangial cells. *Am J Physiol Renal Physiol* 279: F718-727, 2000.
63. **Jennings RB and Reimer KA.** The cell biology of acute myocardial ischemia. *Annu Rev Med* 42: 225-246, 1991.
64. **Jones SP, Zachara NE, Ngoh GA, Hill BG, Teshima Y, Bhatnagar A, Hart GW, Marban E.** Cardioprotection by N-acetylglucosamine linkage to cellular proteins. *Circulation* 117: 1172-1182, 2008.
65. **Kostin S, Hein S, Arnon E, Scholz D, Schaper J.** The cytoskeleton and related proteins in the human failing heart. *Heart Fail Rev* 5: 271-280, 2000.
66. **Laczy B, Hill BG, Wang K, Paterson AJ, White CR, Xing D, Chen YF, Darley-Usmar V, Oparil S, Chatham JC.** Protein O-GlcNAcylation: a new signaling paradigm for the cardiovascular system. *Am J Physiol Heart Circ Physiol* 296: H13-28, 2009.
67. **Lee Y, Robinson M, Wong N, Chan E, Charles MA.** The effect of pentoxifylline on current perception thresholds in patients with diabetic sensory neuropathy. *J Diabetes Complications* 11: 274-278, 1997.
68. **Li H and Forstermann U.** Nitric oxide in the pathogenesis of vascular disease. *J Pathol* 190: 244-254, 2000.
69. **Liu J, Marchase RB, Chatham JC.** Increased O-GlcNAc levels during reperfusion lead to improved functional recovery and reduced calpain proteolysis. *Am J Physiol Heart Circ Physiol* 293: H1391-1399, 2007.
70. **Liu J, Pang Y, Chang T, Bounelis P, Chatham JC, Marchase RB.** Increased hexosamine biosynthesis and protein *O*-GlcNAc levels associated with myocardial protection against calcium paradox and ischemia. *J Mol Cell Cardiol* 40: 303-312, 2006.
71. **Lloyd SG, Zeng H, Wang PP, Chatham JC.** Lactate isotopomer analysis by ^{1}H-NMR spectroscopy: consideration of long-range nuclear spin-spin interactions. *Magn Reson Med* 51: 1279-1282, 2004.
72. **Luiken JJ, Arumugam Y, Dyck DJ, Bell RC, Pelsers MM, Turcotte LP, Tandon NN, Glatz JF, Bonen A.** Increased rates of fatty acid uptake and plasmalemmal fatty acid transporters in obese Zucker rats. *J Biol Chem* 276: 40567-40573, 2001.

73. **Luo B, Parker GJ, Cooksey RC, Soesanto Y, Evans M, Jones D, McClain DA.** Chronic hexosamine flux stimulates fatty acid oxidation by activating AMP-activated protein kinase in adipocytes. *J Biol Chem* 282: 7172-7180, 2007.
74. **Macauley MS, Whitworth GE, Debowski AW, Chin D, Vocadlo DJ.** O-GlcNAcase uses substrate-assisted catalysis: kinetic analysis and development of highly selective mechanism-inspired inhibitors. *J Biol Chem* 280: 25313-25322, 2005.
75. **Macdougall IC and Cooper AC.** Erythropoietin resistance: the role of inflammation and pro-inflammatory cytokines. *Nephrol Dial Transplant* 17 Suppl 11: 39-43, 2002.
76. **Marshall S, Nadeau O, Yamasaki K.** Dynamic actions of glucose and glucosamine on hexosamine biosynthesis in isolated adipocytes: differential effects on glucosamine 6-phosphate, UDP-N-acetylglucosamine, and ATP levels. *J Biol Chem* 279: 35313-35319, 2004.
77. **Matsubara M, Hayashi N, Jing T, Titani K.** Regulation of endothelial nitric oxide synthase by protein kinase C. *J Biochem* 133: 773-781, 2003.
78. **Mazak I, Wittmann I, Wagner L, Wagner Z, Degrell P, Vas T, Molnar GA, Nagy J.** Cigarette smoke and its formaldehyde component inhibit bradykinin-induced calcium increase in pig aortic endothelial cells. *Endothelium* 9: 103-108, 2002.
79. **McCormick BB, Sydor A, Akbari A, Fergusson D, Doucette S, Knoll G.** The effect of pentoxifylline on proteinuria in diabetic kidney disease: a meta-analysis. *Am J Kidney Dis* 52: 454-463, 2008.
80. **McMillan DE.** The effect of diabetes on blood flow properties. *Diabetes* 32 Suppl 2: 56-63, 1983.
81. **Mercado C and Jaimes EA.** Cigarette smoking as a risk factor for atherosclerosis and renal disease: novel pathogenic insights. *Curr Hypertens Rep* 9: 66-72, 2007.
82. **Michaud SE, Dussault S, Groleau J, Haddad P, Rivard A.** Cigarette smoke exposure impairs VEGF-induced endothelial cell migration: role of NO and reactive oxygen species. *J Mol Cell Cardiol* 41: 275-284, 2006.
83. **Michell BJ, Chen Z, Tiganis T, Stapleton D, Katsis F, Power DA, Sim AT, Kemp BE.** Coordinated control of endothelial nitric-oxide synthase phosphorylation by protein kinase C and the cAMP-dependent protein kinase. *J Biol Chem* 276: 17625-17628, 2001.
84. **Morceau F, Dicato M, Diederich M.** Pro-inflammatory cytokine-mediated anemia: regarding molecular mechanisms of erythropoiesis. *Mediators Inflamm* 2009: 405016, 2009.
85. **Muravyov AV, Tikhomirova IA, Maimistova AA, Bulaeva SV, Zamishlayev AV, Batalova EA.** Crosstalk between adenylyl cyclase signaling pathway and Ca2+ regulatory mechanism under red blood cell microrheological changes. *Clin Hemorheol Microcirc* 45: 337-345, 2010.
86. **Murphy E and Steenbergen C.** Mechanisms underlying acute protection from cardiac ischemia-reperfusion injury. *Physiol Rev* 88: 581-609, 2008.
87. **Nagy J, Demaster EG, Wittmann I, Shultz P, Raij L.** Induction of endothelial cell injury by cigarette smoke. *Endothelium* 5: 251-263, 1997.
88. **Nagy J, Kiss I, Wittmann I.** [Early anemia in diabetic nephropathy]. *Orv Hetil* 146: 397-401, 2005.
89. **Ndiaye M, Chataigneau M, Lobysheva I, Chataigneau T, Schini-Kerth VB.** Red wine polyphenol-induced, endothelium-dependent NO-mediated relaxation is due to the redox-sensitive PI3-kinase/Akt-dependent phosphorylation of endothelial NO-synthase in the isolated porcine coronary artery. *Faseb J* 19: 455-457, 2005.
90. **Ngoh GA and Jones SP.** New insights into metabolic signaling and cell survival: the role of beta-O-linkage of N-acetylglucosamine. *J Pharmacol Exp Ther* 327: 602-609, 2008.
91. **Nőt LG, Brocks CA, Vamhidy L, Marchase RB, Chatham JC.** Increased O-linked beta-N-acetylglucosamine levels on proteins improves survival, reduces inflammation and organ damage 24 hours after trauma-hemorrhage in rats. *Crit Care Med* 38: 562-571, 2010.
92. **Oberg BP, McMenamin E, Lucas FL, McMonagle E, Morrow J, Ikizler TA, Himmelfarb J.** Increased prevalence of oxidant stress and inflammation in patients with moderate to severe chronic kidney disease. *Kidney Int* 65: 1009-1016, 2004.
93. **Ota Y, Kugiyama K, Sugiyama S, Ohgushi M, Matsumura T, Doi H, Ogata N, Oka H, Yasue H.** Impairment of endothelium-dependent relaxation of rabbit aortas by cigarette smoke extract--role of free radicals and attenuation by captopril. *Atherosclerosis* 131: 195-202, 1997.
94. **Pang Y, Bounelis P, Chatham JC, Marchase RB.** The hexosamine pathway is responsible for the inhibition by diabetes of phenylephrine-induced inotropy. *Diabetes* 53: 1074-1081, 2004.
95. **Puranik R and Celermajer DS.** Smoking and endothelial function. *Prog Cardiovasc Dis* 45: 443-458, 2003.
96. **Pyle WG and Solaro RJ.** At the crossroads of myocardial signaling: the role of Z-discs in intracellular signaling and cardiac function. *Circ Res* 94: 296-305, 2004.
97. **Radfar M, Larijani B, Hadjibabaie M, Rajabipour B, Mojtahedi A, Abdollahi M.** Effects of pentoxifylline on oxidative stress and levels of EGF and NO in blood of diabetic type-2 patients; a randomized, double-blind placebo-controlled clinical trial. *Biomed Pharmacother* 59: 302-306, 2005.
98. **Rappaport L.** Ischemia-reperfusion associated myocardial contractile dysfunction may depend on Ca(2+)-activated cytoskeleton protein degradation. *Cardiovasc Res* 45: 810-812, 2000.
99. **Ravi K, Brennan LA, Levic S, Ross PA, Black SM.** S-nitrosylation of endothelial nitric oxide synthase is associated with monomerization and decreased enzyme activity. *Proc Natl Acad Sci U S A* 101: 2619-2624, 2004.
100. **Ren J, Gintant GA, Miller RE, Davidoff AJ.** High extracellular glucose impairs cardiac E-C coupling in a glycosylation-dependent manner. *Am J Physiol Heart Circ Physiol* 273: H2876-H2883, 1997.
101. **Renke M, Tylicki L, Rutkowski P, Knap N, Zietkiewicz M, Neuwelt A, Aleksandrowicz E, Lysiak-Szydlowska W, Wozniak M, Rutkowski B.** Effect of pentoxifylline on proteinuria, markers of tubular injury and oxidative stress in non-diabetic patients with chronic kidney disease - placebo controlled, randomized, cross-over study. *Acta Biochim Pol* 57: 119-123, 2010.
102. **Rex-Mathes M, Werner S, Strutas D, Griffith LS, Viebahn C, Thelen K, Schmitz B.** O-GlcNAc expression in developing and ageing mouse brain. *Biochimie* 83: 583-590, 2001.
103. **Rice L and Alfrey CP.** The negative regulation of red cell mass by neocytolysis: physiologic and pathophysiologic manifestations. *Cell Physiol Biochem* 15: 245-250, 2005.
104. **Rice L, Alfrey CP, Driscoll T, Whitley CE, Hachey DL, Suki W.** Neocytolysis contributes to the anemia of renal disease. *Am J Kidney Dis* 33: 59-62, 1999.
105. **Rice L, Ruiz W, Driscoll T, Whitley CE, Tapia R, Hachey DL, Gonzales GF, Alfrey CP.** Neocytolysis on descent from altitude: a newly recognized mechanism for the control of red cell mass. *Ann Intern Med* 134: 652-656, 2001.
106. **Ritz E.** Advances in nephrology: successes and lessons learnt from diabetes mellitus. *Nephrol Dial Transplant* 16 Suppl 7: 46-50, 2001.
107. **Ritz E.** Diabetic nephropathy. *Saudi J Kidney Dis Transpl* 17: 481-490, 2006.
108. **Rodriguez-Crespo I, Gerber NC, Ortiz de Montellano PR.** Endothelial nitric-oxide synthase. Expression in Escherichia coli, spectroscopic characterization, and role of tetrahydrobiopterin in dimer formation. *J Biol Chem* 271: 11462-11467, 1996.
109. **Rodriguez-Moran M, Gonzalez-Gonzalez G, Bermudez-Barba MV, Medina de la Garza CE, Tamez-Perez HE, Martinez-Martinez FJ, Guerrero-Romero F.** Effects of pentoxifylline on the urinary protein excretion profile of type 2 diabetic patients with microproteinuria: a double-blind, placebo-controlled randomized trial. *Clin Nephrol* 66: 3-10, 2006.

110. **Schalkwijk CG and Stehouwer CD.** Vascular complications in diabetes mellitus: the role of endothelial dysfunction. *Clin Sci (Lond)* 109: 143-159, 2005.
111. **Schmieder RE, Schrader J, Zidek W, Tebbe U, Paar WD, Bramlage P, Pittrow D, Bohm M.** Low-grade albuminuria and cardiovascular risk : what is the evidence? *Clin Res Cardiol* 96: 247-257, 2007.
112. **Smith CJ and Fischer TH.** Particulate and vapor phase constituents of cigarette mainstream smoke and risk of myocardial infarction. *Atherosclerosis* 158: 257-267, 2001.
113. **Smulders YM, Jager A, Gerritsen J, Dekker JM, Nijpels G, Heine RJ, Bouter LM, Stehouwer CD.** Cardiovascular autonomic function is associated with (micro-)albuminuria in elderly Caucasian sujects with impaired glucose tolerance or type 2 diabetes: the Hoorn Study. *Diabetes Care* 23: 1369-1374, 2000.
114. **Solerte SB and Fioravanti M.** Hemodynamic alterations in long-term insulin-dependent diabetic patients with overt nephropathy: role of blood hyperviscosity and plasma protein changes. *Clin Nephrol* 28: 138-143, 1987.
115. **Solerte SB, Fioravanti M, Bozzetti A, Schifino N, Patti AL, Fedele P, Viola C, Ferrari E.** Pentoxifylline, albumin excretion rate and proteinuria in type I and type II diabetic patients with microproteinuria. Results of a short-term randomized study. *Acta Diabetol Lat* 23: 171-177, 1986.
116. **Spallone V, Maiello MR, Kurukulasuriya N, Barini A, Lovecchio M, Tartaglione R, Mennuni G, Menzinger G.** Does autonomic neuropathy play a role in erythropoietin regulation in non-proteinuric Type 2 diabetic patients? *Diabet Med* 21: 1174-1180, 2004.
117. **Stanley P.** A method to the madness of N-glycan complexity? *Cell* 129: 27-29, 2007.
118. **Stanley WC, Lopaschuk GD, McCormack JG.** Regulation of energy substrate metabolism in the diabetic heart. *Cardiovasc Res* 34: 25-33, 1997.
119. **Steenbergen C, Hill ML, Jennings RB.** Cytoskeletal damage during myocardial ischemia: changes in vinculin immunofluorescence staining during total in vitro ischemia in canine heart. *Circ Res* 60: 478-486, 1987.
120. **Stehouwer CD, Gall MA, Twisk JW, Knudsen E, Emeis JJ, Parving HH.** Increased urinary albumin excretion, endothelial dysfunction, and chronic low-grade inflammation in type 2 diabetes: progressive, interrelated, and independently associated with risk of death. *Diabetes* 51: 1157-1165, 2002.
121. **Su Y, Han W, Giraldo C, De Li Y, Block ER.** Effect of cigarette smoke extract on nitric oxide synthase in pulmonary artery endothelial cells. *Am J Respir Cell Mol Biol* 19: 819-825, 1998.
122. **Thomas SR, Chen K, Keaney JF, Jr.** Hydrogen peroxide activates endothelial nitric-oxide synthase through coordinated phosphorylation and dephosphorylation via a phosphoinositide 3-kinase-dependent signaling pathway. *J Biol Chem* 277: 6017-6024, 2002.
123. **Turgut F, Bolton WK.** Potential new therapeutic agents for diabetic kidney disease. *Am J Kidney Dis* 55: 928-40, 2010.
124. **Vinik A, Ullal J, Parson HK, Casellini CM.** Diabetic neuropathies: clinical manifestations and current treatment options. *Nat Clin Pract Endocrinol Metab* 2: 269-281, 2006.
125. **Vinik AI and Ziegler D.** Diabetic cardiovascular autonomic neuropathy. *Circulation* 115: 387-397, 2007.
126. **Wagner L Wittmann I, Katai J, Melegh B, Nagy J.** Does cigarette smoke affect the protein components of endothelial cells? *Nephrology, Dialysis, Transplantation,* 14, A10., 1999.
127. **Wang P, Lloyd SG, Zeng H, Bonen A, Chatham JC.** The impact of altered substrate utilization on cardiac function in isolated hearts from Zucker diabetic fatty rats. *Am J Physiol Heart Circ Physiol* 288: 2102-2110, 2005.
128. **Wardle EN.** Heparins for proliferative nephritides? Short review on an advancing topic. *Nephron* 73: 515-519, 1996.
129. **Way KJ, Katai N, King GL.** Protein kinase C and the development of diabetic vascular complications. *Diabet Med* 18: 945-959, 2001.
130. **Wei H, Campbell W, Vander Heide RS.** Heat shock-induced cardioprotection activates cytoskeletal-based cell survival pathways. *Am J Physiol Heart Circ Physiol* 291: H638-647, 2006.
131. **Wei H, L'Ecuyer T, Vander Heide RS.** Effect of increased expression of cytoskeletal protein vinculin on ischemia-reperfusion injury in ventricular myocytes. *Am J Physiol Heart Circ Physiol* 284: H911-918, 2003.
132. **Wild S, Roglic G, Green A, Sicree R, King H.** Global prevalence of diabetes: estimates for the year 2000 and projections for 2030. *Diabetes Care* 27: 1047-1053, 2004.
133. **Winer N and Sowers JR.** Epidemiology of diabetes. *J Clin Pharmacol* 44: 397-405, 2004.
134. **Wirta OR, Pasternack AI, Mustonen JT, Laippala PJ, Reinikainen PM.** Urinary albumin excretion rate is independently related to autonomic neuropathy in type 2 diabetes mellitus. *J Intern Med* 245: 329-335, 1999.
135. **Wittmann I, Molnar GA, Degrell P, Wagner Z, Tamasko M, Laczy B, Brasnyo P, Wagner L, Nagy J.** Prevention and treatment of diabetic nephropathy. *Diabetes Res Clin Pract* 68 Suppl1: S36-42, 2005.
136. **Wyska E.** Pharmacokinetic-pharmacodynamic modeling of methylxanthine derivatives in mice challenged with high-dose lipopolysaccharide. *Pharmacology* 85: 264-271, 2010.
137. **Xu J, Xie Z, Reece R, Pimental D, Zou MH.** Uncoupling of endothelial nitric oxidase synthase by hypochlorous acid: role of NAD(P)H oxidase-derived superoxide and peroxynitrite. *Arterioscler Thromb Vasc Biol* 26: 2688-2695, 2006.
138. **Yellon DM and Hausenloy DJ.** Myocardial reperfusion injury. *N Engl J Med* 357: 1121-1135, 2007.
139. **Young MJ, Bennett JL, Liderth SA, Veves A, Boulton AJ, Douglas JT.** Rheological and microvascular parameters in diabetic peripheral neuropathy. *Clin Sci (Lond)* 90: 183-187, 1996.
140. **Yuzwa SA, Macauley MS, Heinonen JE, Shan X, Dennis RJ, He Y, Whitworth GE, Stubbs KA, McEachern EJ, Davies GJ, Vocadlo DJ.** A potent mechanism-inspired O-GlcNAcase inhibitor that blocks phosphorylation of tau in vivo. *Nat Chem Biol* 4: 483-490, 2008.
141. **Zachara NE.** Detecting the "O-GlcNAc-ome"; detection, purification, and analysis of O-GlcNAc modified proteins. *Methods Mol Biol* 534: 251-279, 2009.
142. **Zachara NE and Hart GW.** Cell signaling, the essential role of O-GlcNAc! *Biochim Biophys Acta* 1761: 599-617, 2006.
143. **Zachara NE, O'Donnell N, Cheung WD, Mercer JJ, Marth JD, Hart GW.** Dynamic O-GlcNAc modification of nucleocytoplasmic proteins in response to stress. A survival response of mammalian cells. *J Biol Chem* 279: 30133-33142, 2004.
144. **Zhang WZ, Venardos K, Chin-Dusting J, Kaye DM.** Adverse effects of cigarette smoke on NO bioavailability: role of arginine metabolism and oxidative stress. *Hypertension* 48: 278-285, 2006.
145. **Ziegler D and Gries FA.** Alpha-lipoic acid in the treatment of diabetic peripheral and cardiac autonomic neuropathy. *Diabetes* 46 Suppl 2: S62-66, 1997.
146. **Ziegler D, Schatz H, Conrad F, Gries FA, Ulrich H, Reichel G.** Effects of treatment with the antioxidant alpha-lipoic acid on cardiac autonomic neuropathy in NIDDM patients. A 4-month randomized controlled multicenter trial (DEKAN Study). Deutsche Kardiale Autonome Neuropathie. *Diabetes Care* 20: 369-373, 1997.
147. **Zou MH, Hou XY, Shi CM, Nagata D, Walsh K, Cohen RA.** Modulation by peroxynitrite of Akt- and AMP-activated kinase-dependent Ser1179 phosphorylation of endothelial nitric oxide synthase. *J Biol Chem* 277: 32552-32557, 2002.

PUBLICATIONS RELATED TO THE Ph.D. THESIS

1. Wittmann I., Molnár G.A., Degrell P., Wagner Z., Tamaskó M., **Laczy B.**, Brasnyó P., Wagner L., Nagy J.: Prevention and treatment of diabetic nephropathy. *Diabetes Research and Clinical Practice 68(S1): S36-42 (2005)* **IF: 1.236 [citation: 4]**

2. Wittmann I., Molnár G.A., Wagner L., Kőszegi T., Wagner Z., **Laczy B.**, Tamaskó M., Markó L., Mohás M., Nagy J.: Single dose of acetylsalicylic acid in patients with Type 2 diabetes mellitus and/or chronic renal failure ameliorates anaemia by decreasing the rate of neocytolysis. *Acta Physiologia Hungarica 94(1-2): 159-166 (2007)* **IF: 0.453**

3. **Laczy B.***, Wagner L.*, Tamaskó, M. Mazák I., Markó L., Molnár G.A., Wagner Z., Mohás M., Cseh J., Fekete A., Wittmann I.: Cigarette smoke-induced alterations in endothelial nitric oxide synthase phosphorylation: Role of protein kinase C. *Endothelium 14(4): 245-255 (2007)* **IF: 1.740 [citation: 6]**

4. **Laczy B.**, Cseh J., Mohás M., Markó L., Tamaskó M., Kőszegi T., Molnár G.A., Wagner Z., Wagner L., Wittmann I.: Effects of pentoxifylline and pentosan polysulphate combination therapy on diabetic neuropathy in type 2 diabetes mellitus. *Acta Diabetologica 46(2): 105-111 (2009)* **IF: 1.549 [citation: 1]**

5. **Laczy B.**, Hill B.G., Wang K., Paterson A.J., White C.R., Darley-Usmar V., Oparil S., Chatham J.C.: Protein O-GlcNAcylation: A new signaling paradigm for the cardiovascular system. *Am J Physiol Heart Circ Physiol 296(1): H13-28 (2009)* **IF: 3.712 [citation: 29]**

6. **Laczy B.**, Marsh S.A., Brocks C.A., Wittmann I., Chatham J.C.: Inhibition of O-GlcNAcase in perfused rat hearts by NAG-thiazolines at the time of reperfusion is cardioprotective in an O-GlcNAc dependent manner. *Am J Physiol Heart Circ Physiol 299: H1715-H1727 (2010)* **IF: 3.712** (in 2009) **[citation: 1]**

7. **Laczy B.***, Fülöp N.*, Onay-Besikci A., Des Rosiers C., Marchase R.B., Chatham J.C.: Acute regulation of cardiac metabolism by the hexosamine biosynthesis pathway and protein O-GlcNAcylation. *PLoS One 6(4): e18417 (2011)* **IF: 4.351** (in 2009)

8. **Laczy B.**, Molnár G.A., Kőszegi T., Wagner L., Wagner Z., Tamaskó M., Markó L., Mohás M., Wittmann I.: Az acetil-szalicilsav egyszeri, nagy dózisban javítja az anaemiát 2-es típusú diabetes mellitusban és krónikus veseelégtelenségben a neocytolysis gátlásán keresztül. *Magyar Belorvosi Archivum 61: 274-280 (2006)*

9. Wittmann I., Molnár G.A., Tamaskó M., **Laczy B.**, Markó L., Mohás M., Cseh J., Wagner Z., Wagner L.: A protein kináz C β szelektív gátlásának jelentôsége a diabéteszes mikrovaszkuláris szövôdmények kezelésében. *Diabetologia Hungarica 14(S4):13-18 (2006)*

10. **Laczy B.**, Markó L., Tamaskó M., Cseh J., Kőszegi T., Wagner L., Wagner Z., Molnár G.A., Mohás M., Wittmann I.: A pentoxifylline és pentosan polysulphate kombinációs kezelés hatása a diabéteszes neuropathiára és az albuminuriára 2-es típusú diabetes mellitusban. *Diabetologia Hungarica 15(1): 21-29 (2007)*

11. **Laczy B.***, Wagner L.*, Cseh J., Tamaskó M., Mazák I., Markó L., Molnár G.A., Wagner Z., Mohás M., Fekete A., Wittmann I.: Cigarettafüst okozta elváltozások az endothélsejtekben. *Hypertonia es Nephrologia 14(3): 153-58 (2010)*

SELECTED ABSTRACTS

1. Tamaskó M., Molnár G.A., **Laczy B.**, Wagner Z., Wagner L., Kőszegi T., Kocsis B., Mazák I., Nagy J., Wittmann I.: Anemia caused by oxidative stress in type 2 diabetes mellitus and azotemia might be decreased by the free radical scavenger acetylsalicylic acid. *Nephrology Dialysis Transplantation 20 (S4): iv267 (2005)* **IF: 2.976**; XLII ERA-EDTA Congress, Istanbul, Turkey, June 2005

2. **Laczy B.***, Wagner L.*, Tamaskó M., Mazák I., Markó L., Molnár G., Wagner Z., Mohás M., Cseh J., Fekete A., Wittmann I.: The effect of cigarette smoke on the phosphorylation of endothelial nitric oxide synthase: role of protein kinase C. *Nephrology Dialysis and Transplantation 22 (S6): 243-244 (2007)* **IF: 3.167**; XLIV ERA-EDTA Congress, Barcelona, Spain, June 2007

3. **Laczy B.**, Wilson L., Brocks C.A., Marchase R.B., Chatham J.C.: Effect of ischemia-reperfusion on O-GlcNAcylation of specific proteins in isolated rat hearts. *FASEB J (22): 750.16 (2008)* **IF: 6.721**; Experimental Biology, San Diego, CA, April 2008

4. **Laczy B.**, Marsh S.A., Brocks C.A., Marchase R.B., Chatham J.C.: Inhibition of O-GlcNAcase in perfused rat hearts by NAG-thiazolines at the time of reperfusion is cardioprotective in an O-GlcNAc dependent manner. *FASEB J (23): 793.14 (2009)* **IF: 6.791**; Experimental Biology, New Orleans, LA, April 2009

5. **Laczy B.**, Marsh S.A., Marchase R.B., Chatham J.C.: O-linked-β-N-acetylglucosamine (O-GlcNAc) mediated ischemic cardioprotection associated with increased O-GlcNAcylation of cytoskeletal Z-line proteins. *Circulation Research 105: e10-53 (2009)* **IF: 9.214**; Basic Cardiovascular Sciences Conference, Lake Las Vegas, NV, July 2009

6. Chatham J.C., Zou L., Nőt L.G., **Laczy B.**, Marchase R.B.: Protein O-GlcNAcylation: A critical regulator of the cellular response to stress. *Glycobiology 19(11): 1300 (2009)* **IF: 3.929**; Annual Conference of the Society for Glycobiology, San Diego, CA, November 2009

7. Fülöp N.*, **Laczy B.***, Onay-Besikci A., Des Rosiers C., Marchase R.B., Chatham J.C.: Glucosamine increases hexosamine biosynthesis and O-linked N-acetylglucosamine in the heart, and leads to metabolic alterations similar to those seen in diabetic cardiomyopathy. *Diabetologia 52 (Supp1): S15 (2009)* **IF: 6.551**; 45th EASD Annual Meeting, Vienna, Austria, September 2009

(* authors contributed equally to works)

Cumulative impact factor of listed publications related to the Ph.D. thesis: 16.753; cumulative impact factor of all publications (without abstracts): 33.782

Cumulative impact factor of listed abstracts related to the Ph.D. thesis: 39.349; cumulative impact factor of all abstracts (without publications): 78.866

ACKNOWLEDGEMENTS

I would like to express my appreciation to **Prof. Dr. István Wittmann** and **Prof. Dr. Judit Nagy** for providing me the opportunity to be a member of a great scientific research group and clinicians at the 2nd Department of Internal Medicine and Nephrological Center, and for supporting my scientific carrier and clinical work since I had graduated. Without their excellent leadership and encouragement I would not have been able to finish my Ph.D.

I am very grateful to **Prof. Dr. John C. Chatham** for giving me the chance to work at the Division of Cardiovascular Disease at UAB in a very pleasant environment, for helping me in my scientific progress and I do appreciate his exceptional enthusiasm, productive and inspiring suggestions that advanced my scientific thinking and carrier.

I am very thankful to **Dr. László Wagner**, **Dr. István Mazák**, **Dr. Zoltán Wagner** for their continued suggestions during my postdoc years and support in my work.

Special thanks to **Dr. Gergő A. Molnár**, who helped a lot when I was a 'beginner', and thanks to my former postdoc-mates **Dr. Mónika Tamaskó**, **Dr. Lajos Markó**, **Dr. Judit Cseh**, **Dr. Márton Mohás** for their contributions to common projects, for sharing joyful moments and successes in the lab.

I am very thankful to **Anikó L. Heitmanné** and **Ilona V. Sámikné**, for teaching me first the basic rules around a lab and how to work precisely, for their excellent technical assistance and for their great, 'mother-like' friendship.

I am very pleased to have friends and colleagues like **Enikő Bodor** and **Zsuzsanna Rumszauer**, who have been always kindly helping me out in anything that seems `mission impossible`, many thanks for their administrative and organizing contributions to my official affairs.

I am especially thankful to **Charlye A. Brocks**, who showed me first what Southern hospitality is all about, for making my professional life smooth and my private life so enjoyable in Birmingham, she has been always a true and caring friend to me. Certainly, I would not have been able to manage my works without her exceptional technical assistance and amity.

I am also thankful to my friends and co-authors **Dr. Sue A. Marsh** for her constructive suggestions and critics, and for her valuable contributions to my works, to **Dr. Norbert Fülöp** for teaching me heart perfusions and for his thoughtful inputs to my works, to **Dr. László G. Nőt** for having been always there for me in my professional and personal life.

I would like also thank to all my colleagues in the laboratory of **Prof. Dr. Richard B. Marchase** and **Prof. John. C. Chatham**, to **Erica Taylor**, **Xiaoyuan Zhu**, **Luyun Zou**, **Dan Shan**, **Vorarrat Champattanachai**, **Kai He**, **Chris Calderon** for their great support and for being my friends during my stay in Birmingham.

I would like to also thank **Prof. John C. Chatham** for having my work appreciated and for providing me the opportunity to collaborate with principal investigators and members of acclaimed research groups. Here I would like to acknowledge the help of **Prof. Dr. Richard B. Marchase** (President of the Federation of American Societies for Experimental Biology), **Prof. Dr. Suzanne Oparil** (President of the American Society of Hypertension), **Prof. Dr. Victor Darley-Usmar** (President of the Society for Free Radical Biology and Medicine), **Prof. Dr. Christine Des Rosiers** (Montreal Heart Institute, Université de Montréal), **Prof. Martin E. Young D.Phil.** (Division of Cardiovascular Disease, UAB), **Dr**. **James A. Mobley** (Director of Bioanalytical and Mass Spectrometry Facility, UAB), **Prof. Dr. Andrew J Paterson** (Division of Endocrinology, Diabetes and Metabolism, UAB), **Prof. Dr. Roger C. White** (Division of Cardiovascular Disease, UAB) during our grateful collaboration, and the assistance of my co-authors **Elena Ulasova**, **Arzu Onay-Besikci**, **Bradford G. Hill**, **Kai Wang,** and **Landon Wilson**.

I am thankful for **Everyone, Friends and Colleagues** who are not listed here, but had contributed to my accomplishments in my professional or personal life.

And at last but not least I would like to thank my **Family**, without their continous support and compassionate love I would not have been capable of achieving my goals and dreams!